PART I

RADIAL DIFFUSION IN A TURBULENT AIR STREAM

PART II

A. ABSORPTION OF LIGHT BY THE SYSTEM NITRIC ACID-NITROGEN DIOXIDE-WATER

B. IONIZATION IN SOLUTIONS OF NITROGEN DIOXIDE IN NITRIC ACID FROM OPTICAL ABSORBANCE MEASUREMENTS

PART III

KINETICS OF THE DECOMPOSITION OF SODIUM DITHIONITE

PART IV

THE DETERMINATION OF CHROMIUM BY OXIDATION IN THE PRESENCE OF SILVER NITRATE

Thesis by

Scott Lynn

In Partial Fulfillment of the Requirements

For the Degree of

Doctor of Philosophy

California Institute of Technology
Pasadena, California
1954

ACKNOWLEDGEMENTS

The work presented in Part I was done under the supervision of Professor W.H. Corcoran. His help in frequent consultations during the experiment and while preparing the manuscript was of great value and the example he set in directing the work was one to be emulated. Professor Corcoran also assisted in the preparation of the manuscript for Part II B.

The work presented in Parts II, III, and IV was done under the supervision of Dr. D.M. Mason. Dr. Mason also assisted in the preparation of the manuscripts. A large part of the credit for the work presented here belongs to him.

Stanley R. Rawn developed the analytical technique used in the work presented in Part III and also was of great assistance in the preparation of the figures and tables in that section.

Throughout the course of the entire program Professor B.H. Sage took an active interest in the progress of the work being done. His advice and comments on the work presented in Part I were of particular value. He proposed the project initially and suggested several of the design features in addition to his contributions to the discussions of the theoretical aspects of the results.

W. DeWitt and G. Griffith helped in the construction of the equipment; V. Berry and L. Woods helped in the preparation of the tables, and E. Anderson and R. Stampfel did the typing. The assistance of H.H. Reamer in maintaining the equipment is acknowledged.

ABSTRACT

I. The eddy diffusivity and the eddy viscosity near the center of a pipe have been determined for the case of turbulent, cylindrically symmetric, steady, non-uniform flow*. The eddy properties were calculated from measurements of composition and velocity in a test section 36 in. long and 6 in. in diameter. Natural gas was introduced into a turbulent air stream through an annulus section 1/8 in. thick. Experiments were made at Reynolds numbers of 45,000 and 82,300. Both eddy properties were found to vary appreciably with distance downstream from the annulus. The eddy diffusivity varied much more than did the eddy viscosity, being less in some regions and much greater in others. However, there appeared to be no tendency for either eddy property to approach zero at the center of the channel. The results of the experiments are discussed and compared to the data of other workers.

II A. The optical absorbance of the liquid phase of mixtures of nitric acid, nitrogen dioxide**, and water was measured at 32° F at wavelengths of 500 and 425 mμ. At the longer wavelength compositions containing 0.8 or more weight fraction nitric acid were studied. At

---

* Flow is defined as steady when the average velocity, temperature, and other properties of interest at a point do not change with time. Flow is defined as uniform when the derivatives with respect to x, the coordinate in the direction of flow, of velocity, temperature, and other properties of interest are zero. Uniform flow is theoretically unattainable but may be closely approached in practice.

** The term nitrogen dioxide is used to designate equilibrium mixtures of nitrogen dioxide and nitrogen tetroxide.

the shorter wavelength the compositions were limited to a minimum weight fraction nitric acid of 0.93. The results indicate that the absorbance varies linearly with the weight fraction nitrogen dioxide at small concentrations of this component. The optical absorption appears to be a useful intensive property of the liquid phase to be employed as an aid in determining the composition of the ternary system.

II B. Values of the optical absorbance of solutions of nitrogen dioxide in nitric acid were measured at 32° F. and one atmosphere using light at a wave length of 425 mμ. The data obtained were applied in a study of the ionization occurring in the solutions. The numerical solution of simultaneous equations based on equilibrium expressions indicated that in nitric acid solutions containing less than one weight per cent nitrogen dioxide the nitrogen dioxide is about 70 per cent dissociated into nitrosonium (NO^+) and nitrate (NO_3^-) ions whereas the nitric acid is about five per cent dissociated into nitronium (NO_2^+) ions, nitrate ions, and water. Although the uncertainty is high, the order of magnitude of these values is correct.

III. In aqueous solution, $Na_2S_2O_4$, sometimes called sodium hydrosulfite but more correctly sodium dithionite, undergoes irreversible decomposition at a measurable rate to give $NaHSO_3$, sodium bisulfite, and $Na_2S_2O_3$, sodium thiosulfate, as products. Studies of this reaction with initial compositions in the range 0.01 - 0.10 F $Na_2S_2O_4$ were made with the exclusion of air. A solution of $Na_2S_2O_4$ alone decomposes in a fashion suggesting that a degenerate branching chain mechanism is involved. An apparent positive salt effect on the reaction rate results when NaCl is added to the solution. At values of the concentration of H^+ above 10^{-3}

moles per liter this decomposition is extremely rapid. Initial concentrations* of the products of decomposition, $NaHSO_3$ and $Na_2S_2O_3$, less than the initial concentration of $S_2O_4^{=}$ catalyze the decomposition, indicating that it is autocatalytic in nature. Initial concentrations of $S_2O_3^{=}$ up to tenfold that of $S_2O_4^{=}$ markedly catalyze the decomposition.

However, in the presence of initial concentrations of $NaHSO_3$ greater than the initial concentration of $S_2O_4^{=}$ the chain mechanism is overshadowed, and the reaction is first order with respect to both the species $S_2O_4^{=}$ and HSO_3^{-} and is independent of the initial concentration of $SO_3^{=}$ and of the concentration of H^{+} but is slightly dependent on the initial concentration of $S_2O_4^{=}$. With only $SO_3^{=}$ and OH^{-} added the reaction rate is greatly inhibited, and part of this effect may be attributed to the corresponding lowering of the concentration of HSO_3^{-}.

In the presence of initial concentrations of both $Na_2S_2O_3$ and $NaHSO_3$ which are equimolar or greater than the initial concentration of $Na_2S_2O_4$ the reaction appears to be approximately first order with respect to the concentrations of the species $S_2O_4^{=}$, HSO_3^{-}, and $S_2O_3^{=}$. In the presence of both HSO_3^{-} and $S_2O_3^{=}$, however, the reaction rate is dependent on both the initial concentration of the H^{+} and the concentration of $S_2O_4^{=}$. Superposed on these overall first order reactions is an inherent periodicity in the reaction rate. The bulk of the kinetics measurements were made at 60° C, although several measurements were made at 50° and 70° C to obtain the activation energy of the thermal decomposition reaction.

A few measurements were made at 50°, 60°, and 70° C of the rapid oxidation of 0.01 F $Na_2S_2O_4$ in aqueous solution by air. This

---

* Unless otherwise specified, concentrations refer to molar or formal concentrations.

oxidation reaction appears to be first order with respect to the concentration of $S_2O_4^{=}$ and is inhibited in basic solutions. A modified analytical procedure employing methylene blue in a basic aqueous solution of methanol or acetone was used to determine $Na_2S_2O_4$ in the presence of large quantities of other reducing agents.

IV. A method is described for determining amounts of chromium of the order of a few milligrams. Trivalent chromium is oxidized by fuming perchloric acid in the presence of a small amount of silver ion. The dichromate is then determined iodimetrically. For small amounts of chromium the method gives better results than do other methods listed in the literature. The method has not been tried for large amounts of chromium.

TABLE OF CONTENTS

PART I

APPENDIX

PART II A

TABLE OF CONTENTS (cont.)

TABLE OF CONTENTS (cont.)

PART I

RADIAL DIFFUSION IN A TURBULENT AIR STREAM

INTRODUCTION

At a given instant a fluid moving in turbulent flow has at a given point in the stream velocities, u_i, in each of the coordinate directions. These velocities can be considered to be composed of an average velocity, U_i, and a fluctuating velocity, U_i', whose time average is zero[1]. The fluctuating velocities are due to the formation, movement, and decay of turbulent eddies in the flowing stream. In addition to the fluctuating velocities, the eddies produce fluctuations in the temperature at a point when energy is being transported across the stream and fluctuations in the composition at a point when material is being transported across the stream[2]. The fluctuations of a property at a point will be coordinated with the fluctuating velocity in the direction in which a transport process is taking place, so that the value of $\overline{G' U_i'}$ will be different from zero. Thus the transport processes in a turbulent stream are considered to be due to a combination of the transport due to the molecular properties of the fluid and the transport due to the relative movement of the turbulent eddies through the fluid.

Consider, for example, the case of a fluid flowing uniformly through a straight circular conduit, so that the only average velocity is the one in the direction of flow. Reynolds'[3] investigations showed that the shearing stress on a cylindrical surface concentric with the flow channel is given by

$$\tau = \frac{\sigma}{g}\left(\nu \frac{\partial U_x}{\partial r} - \overline{U_x' U_r'}\right) \qquad (1)$$

where

τ = shear stress, lbs/ft^2

σ = specific weight of fluid, lbs/ft^3

g = gravitational acceleration, 32.2 ft/sec^2

ν = kinematic viscosity, ft^2/sec.

In an analogous manner, the transfer of material through a surface by diffusional processes may be expressed as

$$\overset{\circ}{m}_{A_d} = - D \frac{\partial C_A}{\partial r} + \overline{C'_A U'_r} \qquad (2)$$

where

$\overset{\circ}{m}_{A_d}$ = weight of A transported by diffusional processes, lbs/sec ft^2

D = Fick diffusion coefficient, ft^2/sec

C_A = average concentration of A, lbs/ft^3

C'_A = fluctuating component of concentration of A.

The contribution to the shear and to the transport by diffusion of the fluctuations due to the turbulence of the stream can be referred to as the contributions of the eddy viscosity, ε_m, and the eddy diffusivity, ε_D[9]. For ease of manipulation, equations (1) and (2) are frequently written

$$\tau = \frac{\sigma}{g} (\varepsilon_m + \nu) \frac{\partial U_x}{\partial r} \qquad (1a)$$

$$= \frac{\sigma}{g} \varepsilon_m \frac{\partial U_x}{\partial r} \qquad (1b)$$

where

$$\varepsilon_m = - \frac{\partial r}{\partial U_x} \overline{U'_x U'_r} \tag{3}$$

and ε_m is called the total viscosity, and

$$\overset{\circ}{m}_{A_d} = - (\varepsilon_D + D) \frac{\partial C_A}{\partial r} \tag{2a}$$

$$= - \varepsilon_D \frac{\partial C_A}{\partial r} \tag{2b}$$

where

$$\varepsilon_D = - \frac{\partial r}{\partial C_A} \overline{U'_r C'_A} \tag{4}$$

and ε_D is called the total diffusivity. The analogy between the transfers of momentum and energy in a turbulent stream has been recognized since 1874, when Reynolds[3] first proposed that the numerical values of ε_m and ε_c, the eddy conducitivity, were the same. Taylor[4] extended the analogy in his treatment of material transfer in turbulent flow.

Thus, the study of the transfer of material in a turbulently flowing air stream is of interest not only from the standpoint of the empirical design of equipment but also because of the insight into the mechanism of turbulent flow which is provided. The present work is a part of the program which has been initiated by the Chemical Engineering Laboratory of the California Institute of Technology for studying the transfer of energy, momentum, and material in turbulent flow. Corcoran, Page, et al.[5,6] investigated the transfer of energy and momentum in

steady, uniform flow between parallel plates. J.L. Mason[7] studied non-uniform flow between parallel plates, and D.M. Mason and V. J. Berry[8,9] studied the two dimensional wake behind a heated cylinder. Jenkins[10] was unsuccessful in attempting to measure the transfer of material in the parallel-plate test section.

An investigation of the rate of mixing of a stream of gas and an annular stream of air in a circular flow channel by Schlinger[11] was complicated by the tendency of the gas stream to rise in the horizontal test section. In addition, the velocity profile resulting from the effect of having a 1-in. pipe in a 4-in. channel was of a rather specialized nature.

The primary purpose of the present work was to measure the eddy diffusivity near the center of the channel in a stream whose normal velocity profile had been altered as little as possible by the addition of the diffusing material. This was done by measuring the diffusion of an annular stream of natural gas 1/8-in. wide into a stream of air 6 in. in diameter. Composition and velocity were measured as functions of the radius in the channel and the distance downstream from the annulus, and the eddy diffusivity and the eddy viscosity were calculated from formulas which will be derived in the text.

DESCRIPTION OF EQUIPMENT

Flow Channel:

A picture of the flow apparatus is shown in Figure 1, and the structure of the apparatus is indicated diagrammatically in Figure 2. Air at ambient temperature passed from the blower up the 6-in. brass tubing through an orifice plate and into a return section at the ceiling. It then flowed down through the center of a piece of tubing which was mounted concentrically with the flow channel. This piece of tubing formed an annulus with the flow channel through which natural gas flowed. The gas entered the annulus section at ambient temperature at a rate which was measured with a second orifice meter. The annulus was nominally 1/8-in. wide at the end where mixing of the gas and air streams began. The actual width varied between 0.120 in. and 0.130 in. The stream of mixing gases passed through the test section where the concentration and velocity were measured as functions of the radius and the distance downstream from the point of initial mixing. At the outlet of the flow apparatus (outside of the laboratory) the mixed gases passed through a flame holder and were burned.

The flow apparatus had been used in previous diffusion work done in the Chemical Engineering Laboratory[12,13,14] and was known at that time as the Essick apparatus. For the present work it was modified primarily by the addition of the annulus insert and the flame holder for the exhaust gases.

Test Section:

The test section, Figure 3, was a tube of Lucite supported on a brass base which slid through a vertical distance of 5 ft and rotated through an angle of 180°. The sampling probe was mounted on the brass base and moved across the whole diameter of the test section. It served also as a pitot tube and had an opening 0.065 in. in diameter. The static pressure in the test section was determined with a piezometer ring having six openings spaced at regular intervals around the section. The rate of withdrawal of sample was regulated to avoid exceeding the rate of approach of the stream lines at the point of withdrawal. The loose fit of the test section required that it be positioned vertically and laterally after each change of vertical or angular position.

The position of the probe was determined to the nearest 0.01 in. The distance in the direction of flow, x_o, was referred to an arbitrary datum. At $x_o = 0$ the probe opening was 36.5 in. below the exit of the annulus section. The value of x_o was determined to the nearest 0.1 in. The value of θ was determined to the nearest degree.

Method of Analysis:

Point velocities were obtained by using the sampling probe as a pitot tube. A micromanometer with a sensitivity of 0.001 in. of kerosene was used to measure the velocity head. The composition of the sample was determined by a gas-density measurement using the apparatus sketched diagrammatically in Figure 4. One of two glass tubes each of

which had a height of 12 ft was filled with the sample while the other was filled with air taken from the flow channel above the point of entrance of the gas. After both tubes had been thoroughly flushed with their respective gases, the valves to the vacuum pump, the air inlet, and the sample probe were closed. Since the two tubes were connected by a horizontal section at the top, the gases were at the same pressure at that point and the difference in pressure at the bottom of the tubes was due to the difference in density of the sample and air. This pressure difference was measured by means of a high sensitivity micromanometer which is described in Appendix I.

Assuming that mixtures of natural gas and air form ideal solutions, it is easy to show that both the specific weight of a mixture and the concentration of natural gas in a mixture vary directly with the volume per cent of the gas. If it is further assumed that air and natual gas obey the perfect gas laws it is clear that the volume per cent becomes identical to the mole per cent, i.e.,

$$\sigma = \sigma^{\circ}_{air}\,\underline{n}_{air} + \sigma^{\circ}_{gas}\,\underline{n}_{gas}$$

$$= \sigma^{\circ}_{air} - \underline{n}_g(\sigma^{\circ}_{air} - \sigma^{\circ}_{gas})$$

$$\underline{n}_g = \frac{\sigma^{\circ}_{air} - \sigma}{\sigma^{\circ}_{air} - \sigma^{\circ}_{gas}}$$

$$C_g = \underline{n}_g\,\sigma^{\circ}_{gas}$$

σ = specific weight of mixture

σ°_{air} = specific weight of pure air

σ°_{gas} = specific weight of pure gas

$\underline{n}_g$ = volume or mole fraction of gas

C_g = concentration of gas in mixture.

The deviation of the components of natural gas and air from the perfect gas laws is negligible at room temperature and atmospheric pressure. Since the pressure difference at the bottom of the tubes is directly proportional to the difference in density of the two gases in the tubes, it follows that the mole fraction of gas in a sample is equal to the simple ratio $\Delta P_{air-sample}/\Delta P_{air-gas}$ as measured in the analysis apparatus.

The tubes of the analysis apparatus were enclosed in a water jacket, which was wrapped with asbestos, to insure that the gases in the tubes were at the same temperature. The sensitivity of the composition measurements was $\pm$ 0.0003 mole fraction. The sensitivity of the velocity measurements was $\pm$ 0.001 in. of manometer fluid. In both cases the fluctuations due to the turbulence of the air stream outweighed the uncertainties due to the methods of measurement by a considerable margin. In the case of the gas analysis the maximum sensitivity of the apparatus was not used because of this. The analysis apparatus was calibrated each day by a method described in the Appendix. The measurement of $\Delta P_{air-natural\ gas}$ was made at the beginning and end of each run. In general, this value did not vary by more than 0.3 per cent during the course of a run, but the variation from day to day was as much as 6 per cent, indicating a variation in the average molecular weight of the gas of about 3.5 per cent.

The time required to measure the velocity and concentration at a point by the method described above was very short. A traverse consisting of twenty points along a radius could be completed in an

hour and a half under favorable conditions.

The velocity and composition data were smoothed by plotting the points versus the square of the radial position, $\frac{r}{r_o}$. Slopes taken from these curves were then smoothed with respect to $\left(\frac{r}{r_o}\right)^2$ and x. Finally the smoothed slopes were integrated to obtain the recorded values of $\underline{n}_g$ and U_x. The slopes were taken from large scale plots with the aid of a drafting machine. Integrations were done numerically by Simpson's rule[15].

DISCUSSION OF EXPERIMENTS

Re 45,000:

A Reynolds number of 45,000 corresponds to a bulk velocity of 14.4 ft/sec for air and gas flowing through a cylindrical flow channel 6 in. in diameter. The smoothed curves of $\underline{n}_g$ vs. $\frac{r}{r_o}$ are shown in Figure 5 and curves of $\underline{n}_g$ vs. $\left(\frac{r}{r_o}\right)^2$ are shown in Figure 6. The experimental data are given in Table I. The average value of $\underline{n}_g$ was 0.044. The experimental data for two traverses are plotted in Figure 6 to show an example of the scattering. The smooth composition data are listed in Table II. The value of the standard deviation* for the composition data for each traverse is given also in Table II.

---

* The standard deviation is defined here as

$$\sqrt{\frac{\sum_1^n \left(\underline{n}_{g_{exp.}} - \underline{n}_{g_{smoothed}}\right)^2}{n-1}}$$

where $\underline{n}_{g_{exp}}$ and $\underline{n}_{g_{smoothed}}$ are taken at the same value of $\frac{r}{r_o}$.

The velocity profiles are plotted in Figures 7 and 8 against $\frac{r}{r_o}$ and $\left(\frac{r}{r_o}\right)^2$, respectively, and the experimental data are listed in Table III. The experimental data for two traverses are plotted in Figure 8 to show an example of the scattering. The smoothed velocity data are listed in Table IV. The composition and velocity data are plotted versus x_o in Figures 9 and 10 respectively. The value of the standard deviation for the velocity measurements for the first four traverses is given in Table IV. The velocity curve for x_o = 36 in. was raised 0.2 ft/sec above the smooth curve drawn through the experimental points in order to make it agree with the value of $\int_0^1 U_x d\left(\frac{r}{r_o}\right)^2$ obtained for the other four velocity profiles as required by the equations of continuity.

The centers of the velocity and composition profiles corresponded to the geometric center of the channel for the measurements at a Reynolds number of 45,000. However, the values of the integrals $\int_0^1 \underline{n}_g U_x d\left(\frac{r}{r_o}\right)^2$ indicated a constant increase in the fraction of gas flowing in the plane of the traverses, indicating an appreciable tangential diffusion due to the existence of gradients in the coordinate direction normal to the plane of the traverses. The extent of this cylindrical asymmetry is shown in Table V and in Figure 11, a plot of U_x and $\underline{n}_g$ at constant $\frac{r}{r_o}$ vs. θ for the top and bottom planes of the test section. The vertical plane of the traverses was made at $\theta = +30^\circ$.

To approximate the composition profiles which would have existed in the absence of tangential diffusion, a correction was made

in the following manner. The curves of $\underline{n}_g$ vs. (Fig. 6) are, roughly speaking, right parabolas with their vertices at the wall of the channel. A reasonable correction to the composition curves seemed to be one which would leave the general shape of the curves unchanged and which would, furthermore, leave the concentration at the center unchanged. The corrected composition profiles were made to obey the equation of continuity by equating the average concentration at each traverse to that at x_o = 18 in. Expressed analytically,

$$\underline{n}_g^* = \underline{n}_g + \Delta\underline{n}_g$$

$$\Delta\underline{n}_g = K\left(2 - \left[\frac{r}{r_o}\right]^2\right)\left(\frac{r}{r_o}\right)^2$$

$$\int_o^1 \underline{n}_g^* U_x d\left(\frac{r}{r_o}\right)^2 = \int_o^1 \underline{n}_g U_x d\left(\frac{r}{r_o}\right)^2 + \int_o^1 \Delta\underline{n}_g U_x d\left(\frac{r}{r_o}\right)^2$$

$$= \int_o^1 \underline{n}_g U_x d\left(\frac{r}{r_o}\right)^2 \Bigg|_{x_o = 18 \text{ in.}}$$

Therefore

$$K = \frac{\int_o^1 \underline{n}_g U_x d\left(\frac{r}{r_o}\right)^2 \Big|_{x_o} - \int_o^1 \underline{n}_g U_x d\left(\frac{r}{r_o}\right)^2 \Big|_{x_o = 18 \text{ in.}}}{\int_o^1 U_x \left(\frac{r}{r_o}\right)^2 \left(2 - \left[\frac{r}{r_o}\right]^2\right) d\left(\frac{r}{r_o}\right)^2 \Big|_{x=0}} .$$

Values of K and $\Delta\underline{n}_g$ are listed in Table VI. $\underline{n}_g^*$ and $\dfrac{\partial \underline{n}_g^*}{\partial\left(\frac{r}{r_o}\right)^2}$

were used in calculating the eddy diffusivity. The magnitude of the corrections to the composition and to the slopes, $\Delta \underline{n}_g$ and $\partial \Delta \underline{n}_g / \partial \left(\frac{r}{r_o}\right)^2$ did not exceed 7 per cent of the values of $\underline{n}_g$ and $\partial \underline{n}_g / \partial \left(\frac{r}{r_o}\right)^2$, respectively, in the region $\frac{r}{r_o} < 0.7$. The effect of these corrections will be discussed later.

Re 82,300:

The composition data taken at a bulk velocity of 26.4 ft/sec are recorded in Table VII. Curves calculated by integrating the smoothed slopes as before are plotted against $\frac{r}{r_o}$ and $\left(\frac{r}{r_o}\right)^2$ in Figures 12 and 13 respectively. The smoothed composition data are recorded in Table VIII. Experimental and smoothed values of U_x are tabulated in Tables IX and X respectively. The smoothed values are plotted vs. $\frac{r}{r_o}$ and $\left(\frac{r}{r_o}\right)^2$ in Figures 14 and 15 respectively. Velocity and composition are plotted against x_o in Figures 16 and 17. The standard deviations for the velocity and composition traverses are recorded in Tables VIII and IX respectively. Experimental data for two composition traverses and two velocity traverses are plotted in Figures 13 and 15, respectively, to show the scattering.

Random fluctuations in the composition and velocity data taken at a Reynolds' number of 82,300 were initially much greater than for the measurements at a Reynolds number of 45,000. To correct this condition a screen having triangular holes 1/4 in. on a side made of wires 0.1 in. wide was placed in the flow channel 4.0 ft above the annulus exit. The random fluctuations were reduced substantially by the intro-

duction of the screen. It was found, however, that the mean values of the composition curves were essentially unchanged. At this Reynolds number the centers of the velocity and composition profiles (the center is used here to indicate the maximum or minimum of the profile) no longer coincided with the geometric center of the channel but moved away from the center with increasing value of x_o. At x_o = 36 in. this displacement amounted to 0.2 in. This warping of the velocity and concentration profiles is thought to be due primarily to unevenness in the annulus section, but some of the blame should no doubt be placed on the lack of symmetry of the Plexiglas section as well.

Figures 18 and 19 and Table XI show the variations of U_x and $\underline{n}_g$ with θ at x_o = 6 in. and 36 in. respectively. The cylindrical asymmetry is much greater than it was at the lower Reynolds number. The vertical plane of the traverses was again taken at $\theta = +30^o$.

The average value of $\underline{n}_g$ in this case was 0.048 mole fraction. The values of the integral $\int_o^1 \underline{n}_g U_x d\left(\frac{r}{r_o}\right)^2$ again showed an increase with x_o. The method of correction described above was used to obtain an idealized composition, $\underline{n}_g^*$. Values of K and $\Delta\underline{n}_g$ at each traverse are tabulated in Table XII, and are less than the corresponding values for Reynolds number 45,000.

Velocity Data with No Diffusion:

Velocity data taken when no natural gas was flowing through the system were recorded in Table XIII and plotted in Figure 20. They

indicate that the change in the velocity profile for the two diffusion experiments is not due primarily to the diffusion of the natural gas, but rather to the change in cross sectional area at the entrance to the plexiglass section. Other disturbances farther up the channel may also affect the velocities somewhat. The total flow rate was approximately the same as for Reynolds number 45,000, so a direct comparison can be made of Figures 7 and 20. In Figure 7 the change of U_{max} with x amounts overall to about 1.3 ft/sec, or about 7 per cent of U_{max} at $x_o = 0$. This is somewhat greater than the change in U_{max} in Figure 20, but may be within the experimental uncertainty. It should be noted that the change in U_{max} for a Reynolds number of 82,300 amounts to about the same number of ft/sec, but in this case that represents only 4 per cent of U_{max}.

THEORETICAL ANALYSIS OF DATA

Eddy Diffusivity:

Consider an element of volume in cylindrical coordinates situated in a turbulently mixing stream of natural gas and air.

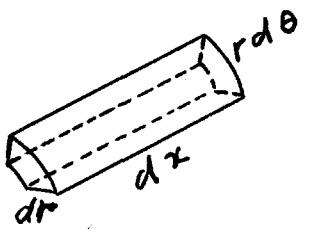

Under steady conditions of turbulent flow the rate of accumulation of gas in the element of volume is zero, and hence the sum of the gradients of the convective flux of gas and the diffusional flux of gas is zero.

Expressed analytically,

$$\frac{\partial C_g}{\partial t} = 0 = \nabla C_g U + \nabla(-\underline{\varepsilon}_D \nabla C_g). \tag{5}$$

Expanding,

$$\frac{\partial}{\partial x}(C_g U_x) + \frac{1}{r}\frac{\partial}{\partial r}(r\, C_g U_r) + \frac{1}{r}\frac{\partial}{\partial \theta}(C_g U_\theta)$$

$$= \frac{\partial}{\partial x}\left(\underline{\varepsilon}_D \frac{\partial C_g}{\partial x}\right) + \frac{1}{r}\left(\frac{\partial}{\partial r}\left[r\, \underline{\varepsilon}_D \frac{\partial C_g}{\partial r}\right]\right) + \frac{1}{r^2}\left(\frac{\partial}{\partial \theta}\left[\underline{\varepsilon}_D \frac{\partial C_g}{\partial \theta}\right]\right) \tag{5a}$$

Implicit in writing the above equation has been the assumption of isotropic turbulence and isotropic eddy diffusivity. However, this assumption is not necessary in the development of the final expression for the eddy diffusivity and is made only to simplify the writing of the equations. Assuming cylindrical symmetry, all derivatives with respect to θ become zero. In addition, it can be shown experimentally that the transport of material by diffusion in the direction of the flow is negligible in comparison to the transport by convection. Equation (5a) then becomes

$$\frac{\partial}{\partial x}(C_g U_x) + \frac{1}{r}\frac{\partial}{\partial r}(r\, C_g U_r) = \frac{1}{r}\frac{\partial}{\partial r}\left(r \underline{\varepsilon}_D \frac{\partial C_g}{\partial r}\right). \tag{5b}$$

Integrating,

$$r\, \underline{\varepsilon}_D \frac{\partial C_g}{\partial r} - r\, C_g U_r = \int_0^r r \frac{\partial}{\partial x}(C_g U_x)\, dr. \tag{6}$$

To evaluate the second term in equation (6), use is made of the equation of continuity for steady flow in a cylindrically symmetric stream

$$\frac{\partial}{\partial x}(\sigma U_x) + \frac{1}{r}\frac{\partial}{\partial r}(r\sigma U_r) = 0 . \tag{7}$$

Integrating,

$$r\sigma U_r = - \int_0^r r \frac{\partial}{\partial x}(\sigma U_x)\, dr. \tag{8}$$

Since the order of integration and differentiation is optional,

$$r\sigma U_r = - \frac{\partial}{\partial x} \int_0^r r\sigma U_x dr . \tag{8a}$$

In the discussion of the method of analysis, the following expressions were developed

$$\sigma = \sigma^{\circ}_{air} - \underline{n}_g(\sigma^{\circ}_{air} - \sigma^{\circ}_g)$$

$$C_g = \underline{n}_g \sigma^{\circ}_g .$$

Thus, equation (6) can be written

$$r\, \underline{\varepsilon}_D \frac{\partial \underline{n}_g}{\partial r} - r\, \underline{n}_g U_r = \frac{\partial}{\partial x} \int_0^r r\, \underline{n}_g U_x dr \tag{6a}$$

clearly,

$$r\, \underline{n}_g U_r = \frac{\underline{n}_g}{\sigma} (r\sigma U_r). \tag{9}$$

Substituting in equation (8a),

$$r\,\underline{n}_g U_r = -\frac{\underline{n}_g}{\sigma}\frac{\partial}{\partial x}\int_o^r r\sigma U_x dr \qquad (9a)$$

$$= -\frac{\underline{n}_g}{\sigma}\frac{\partial}{\partial x}\left[\sigma^o_{air}\int_o^r r\,U_x dr - (\sigma^o_{air} - \sigma^o_{gas})\int_o^r r\,\underline{n}_g U_x dr\right] \qquad (9b)$$

Substituting in equation (6a)

$$r\,\underline{\varepsilon}_D\frac{\partial \underline{n}_g}{\partial r} = \frac{\frac{\partial}{\partial x}\int_o^r r\,\underline{n}_g U_x dr - \underline{n}_g\frac{\partial}{\partial x}\int_o^r r\,U_x dr}{\frac{\sigma}{\sigma^o_{air}}} \qquad (10)$$

The equation is more convenient to handle if the derivatives and integrations are made with respect to $\left(\frac{r}{r_o}\right)^2$, where r_o is the radius of the channel.

Observing that

$$dr = \frac{r_o^2}{2r}\,d\left(\frac{r}{r_o}\right)^2$$

the equation becomes

$$\underline{\varepsilon}_D = \frac{\frac{\partial}{\partial x}\left(\left[\frac{r_o}{r}\right]^2\int_o^{\left[\frac{r}{r_o}\right]^2}\underline{n}_g U_x d\left(\frac{r}{r_o}\right)^2\right) - \underline{n}_g\frac{\partial}{\partial x}\left(\left[\frac{r_o}{r}\right]^2\int_o^{\left[\frac{r}{r_o}\right]^2}U_x d\left(\frac{r}{r_o}\right)^2\right)}{\frac{4}{r_o^2}\frac{\sigma}{\sigma^o_{air}}\frac{\partial \underline{n}_g}{\partial\left(\frac{r}{r_o}\right)^2}} \qquad (10a)$$

The advantages of stating the equations in this form are twofold -- the derivatives of the composition with respect to the square of the radius ratio do not go to zero at the center of the channel, see Figure 6, for example, and also the terms being differentiated with respect to x are seen to be simply the average values of the respective integrands from the center of the channel to the point in question. It follows that

$$\lim_{\left(\frac{r}{r_o}\right)^2 \to 0} \left(\left[\frac{r_o}{r}\right]^2 \int_o^{\left[\frac{r}{r_o}\right]^2} \underline{n}_g U_x d\left(\frac{r}{r_o}\right)^2 \right) = \underline{n}_g U_x \Big|_{\left(\frac{r}{r_o}\right)^2 = 0} \tag{11}$$

Furthermore, $\int_o^1 U_x d\left(\frac{r}{r_o}\right)^2$ is the average (bulk) velocity in the channel, $\bar{U}_x$, a constant, and $\int_o^1 \underline{n}_g U_x d\left(\frac{r}{r_o}\right)^2 / \bar{U}_x$ is the average value of $\underline{n}_g$ in the stream, a constant. The vectorial nature of the eddy diffusivity is sometimes discussed (3), and it should be pointed out that equation (10a) is actually an expression for $\underline{\varepsilon}_{D_r}$, the total diffusivity in the r direction.

Eddy Viscosity:

Consider the forces acting in the x direction on an element of volume in the stream being treated

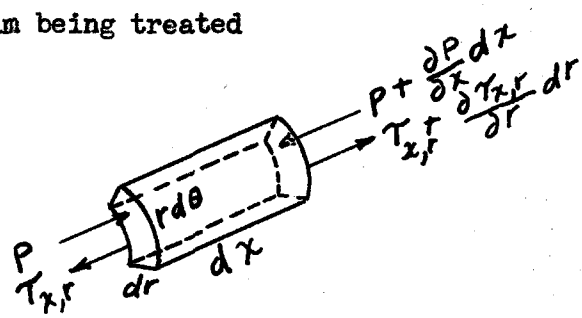

Cylindrical symmetry is assumed, P is assumed independent of r, and the effect of potential fields is neglected. Writing the first law of motion for the element,

$$F_x = \frac{D}{Dt}(\sigma U_x)\, r\, d\,\theta\, dx\, dr = \frac{1}{r}\frac{\partial}{\partial r}(\tau_{r,x} r\, d\,\theta\, dx\, dr) - \frac{\partial}{\partial x}(P\, r\, d\,\theta\, dx\, dr) \tag{12}$$

$$\frac{D}{Dt}(\sigma U_x) = \frac{1}{r}\frac{\partial}{\partial r}(r\,\tau_{r,x}) - \frac{\partial P}{\partial x} \quad . \tag{12a}$$

The relationship between the shear stress on the element and the rate of deformation of the element is

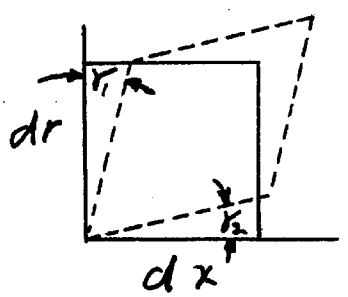

$$\gamma_1\, dr = \frac{dx}{dt}\, dt$$

$$\gamma_2\, dx = \frac{dr}{dt}\, dt$$

$$\tau_{r,x} = \frac{\sigma}{g}\varepsilon_m\left(\frac{\partial \gamma_1}{\partial t} + \frac{\partial \gamma_2}{\partial t}\right) \tag{13}$$

$$= \frac{\sigma}{g}\varepsilon_m\left(\frac{\partial U_x}{\partial r} + \frac{\partial U_r}{\partial x}\right) \tag{13a}$$

$$\frac{D}{Dt} = \frac{\partial}{\partial t} + U_x\frac{\partial}{\partial x} + \frac{U_r}{r}\frac{\partial(r\ -\ )}{\partial r} + U_\theta\frac{\partial}{\partial \theta} \tag{14}$$

Substituting equations (13a) and (14) in (12a) at steady state,

$$U_x\frac{\partial}{\partial x}(\sigma U_x) + \frac{U_r}{r}\frac{\partial}{\partial r}(r\sigma U_r) = \frac{1}{r}\frac{\partial}{\partial r}\left(r\frac{\sigma}{g}\varepsilon_m\frac{\partial U_x}{\partial r}\right)$$

$$+ \frac{1}{r}\frac{\partial}{\partial r}\left(r\frac{\sigma}{g}\varepsilon_m\frac{\partial U_r}{\partial x}\right) - \frac{\partial P}{\partial x} \tag{15}$$

For the present situation the second term on the left hand side of the equation and the second term on the right hand side of the equation were found experimentally to be negligible compared to the other terms in the equation. Thus equation (15) reduces to

$$U_x \frac{\partial \sigma U_x}{\partial x} = \frac{1}{r} \frac{\partial}{\partial r} \left(r \frac{\sigma}{g} \varepsilon_m \frac{\partial U_x}{\partial r} \right) - \frac{\partial P}{\partial x} \qquad (15a)$$

Integrating equation (15a) gives,

$$\varepsilon_m = \frac{\int_o^r r\, U_x \frac{\partial(\sigma U_x)}{\partial x}\, dr + \int_o^r r \frac{\partial P}{\partial x}\, dr}{\frac{\sigma}{g} r \frac{\partial U_x}{\partial r}} \qquad (16)$$

Since the ratio $\frac{\sigma_{air}^o}{\sigma}$ never exceeds 1.03 for the flow conditions studied in these experiments, little uncertainty will result from considering σ to be constant. Using the dimensionless ratio $\left(\frac{r}{r_o}\right)^2$ again, equation (15) becomes

$$\varepsilon_m \cong \frac{r_o^2 \frac{\partial P}{\partial x}}{4\sigma \frac{\partial U_x}{\partial \left(\frac{r}{r_o}\right)^2}} + \frac{1}{8 \frac{\partial U_x}{\partial \left(\frac{r}{r_o}\right)^2}} \frac{\partial}{\partial x} \left(\left[\frac{r_o}{r}\right]^2 \int_o^{\left[\frac{r}{r_o}\right]^2} U_x^2 d \left(\frac{r}{r_o}\right)^2 \right) \qquad (16a)$$

Because the pressure drop along the test section was so small, $\frac{\partial P}{\partial x}$ was estimated from friction-factor data[16].

$$-\frac{\partial P}{\partial x} = \frac{f \sigma (\bar{U}_x)^2}{g r_o}$$

$$f = 0.044\, Re^{-0.2}$$

This expression neglects the effect of the diffusion on the shear at the wall. The expression for ε_m then becomes simply

$$\varepsilon_m \cong \frac{-r_o^2}{4\,\dfrac{\partial U_x}{\partial\left(\dfrac{r}{r_o}\right)^2}} \left[\frac{(\bar{U}_x)^2 f}{r_o} - \frac{1}{2}\frac{\partial}{\partial x}\left(\left[\frac{r_o}{r}\right]^2 \int_o^{\left[\frac{r}{r_o}\right]^2} U_x^2 d\left(\frac{r}{r_o}\right)^2\right)\right] \qquad (16b)$$

The second term in Equation (15b) is the derivative with respect to x of the average value of the square of the velocity from the centerline to the point in question, and becomes zero for uniform flow. The advantage of taking the derivatives of the velocity with respect to $\left(\frac{r}{r_o}\right)^2$ can be appreciated by comparing Figures 7 and 8. It should be noted that the value of $\partial U_x/\partial\left(\frac{r}{r_o}\right)^2$ does not go to zero at the center of the channel.

Discussion of Results:

The total diffusivity and the total viscosity for a Reynolds number of 45,000 are plotted vs. $\frac{r}{r_o}$ in Figure 21. The values are recorded in Tables XIV and XV, respectively. On Figure 22 ε_D and ε_m for a Reynolds number of 82,300 are plotted against $\frac{r}{r_o}$ and are tabulated in Tables XVI and XVII, respectively. The value of D_v for methane in air is 2.0×10^{-4} ft^2/sec[17] and the value of ν is 1.76×10^{-4} ft^2/sec[18]. Thus essentially all of the transfer of momentum and material is due to the eddy terms. The most sensitive function in determining the value of the eddy diffusivity is the rate of change of composition with

distance along the flow channel. In general, therefore, the values of the eddy diffusivity, and also of the eddy viscosity, are less reliable at the extreme traverses. The eddy terms are most reliable for values of $\frac{r}{r_o}$ between 0.3 and 0.6, somewhat less reliable near the center, and least reliable near the wall. The regions of highest uncertainty are indicated by the dotted curves. This gradation is partly the result of the correction which was applied to the composition profiles to adjust for the tangential diffusion and partly a natural consequence of the averaging effect of the integrals in the eddy terms. As was mentioned before the corrections applied to $\underline{n}_g$ and $\Delta\underline{n}_g$ were as high as 7 per cent at the top and bottom traverses. Because the curves of velocity and composition are quite well defined, this correction represents the largest uncertainty in the values of the eddy diffusivities. The values of the eddy viscosity are not affected by the correction for the composition. However, the velocity data show more scatter than do the composition data, and also the value of dP/dx is not well defined. The uncertainty arising from the other steps between the raw data and the final values of $\underline{\varepsilon}_D$ and $\underline{\varepsilon}_m$ is believed to be relatively low, and the final values are believed to be within 12 per cent of the actual values for this particular channel. It is extremely difficult, however, to determine the effect of the particular channel geometry on the values of the eddy properties. Only 8 diameters of straight section precede the exit of the annulus stream, which is not enough to assume the attainment of normal turbulence in the airstream before mixing begins. The value of $\underline{\varepsilon}_m$ for a normal turbulent flow of a Reynolds number

45,000 is 0.020 ft^2/sec at $\frac{r}{r_o} = 0.55$, and for Reynolds number 82,300 it is 0.034 ft^2/sec at $\frac{r}{r_o} = 0.55$, according to the relationships worked out by Connell, Schlinger, and Sage[18], which are based on a velocity-distribution equation and a friction-factor equation. Figures 21 and 22 show that these values of ε_m lie at the lower ends of the ranges found for the two cases studied here. The best agreement was found at the upstream end of the test section.

Changes in the eddy diffusivity with distance downstream were found by Schlinger (loc. cit.) and by Towle and Sherwood[19]. Schlinger found that the eddy diffusivity decreased with increasing distance downstream. His results agree with those reported here in that he found the eddy diffusivity to decrease with decreasing value of $\frac{\partial n_g}{\partial x}$. Schlinger's experimental situations were closer to the one presented here than was Towle's in one important respect. The rate of change of density with distance along the center of the channel in Schlinger's work was also quite appreciable, whereas in Towle's work the change was quite small due to the low concentrations of his diffusing gas. Towle studied the case of a point source at the center of a turbulent cylindrical air stream. His channel had a straight section 70 diameters long before the point of injection. He noted a decrease in ε_D with x at low values of Reynolds number but an increase in ε_D with x at high values of Reynolds number. The change in ε_D with x he ascribed to the disturbing effect of the injector on the normal turbulence structure, but his measurements do not include the eddy viscosity, and hence cannot be checked for the corresponding change in that quantity which would be

expected. In a second series of measurements[20] Towle, Sherwood, and Seder studied the effect of the introduction of a screen grid in their flow channel upstream from the injector. The effect of the grid was to reduce the eddy diffusivity to less than half its original value when the grid was less than 10 diameters from the injector. The variation of ε_D with x was nearly eliminated. The effect of the grid was not lost until it was more than 40 diameters from the injector. At that point the change of ε_D with x was found to be the same as when no grid was in the stream. A plot of ε_D vs. Reynolds number given in Towle's paper gave values about equal to the lowest given at both values of Reynolds number in the present report.

The increase in the eddy viscosity with x observed in the present work would seem to indicate that the level of turbulence in the test section is rising and, as mentioned, the level is above that for uniform flow. It seems quite possible that this change may be due to the effect of the diffusion of the natural gas. The dependence of the values of the eddy diffusivity on the value of $\frac{\partial \underline{n}_g}{\partial x}$ is very strong. The tendency of ε_D to increase with increasing $\frac{\partial \underline{n}_g}{\partial x}$ and to decrease with decreasing $\frac{\partial \underline{n}_g}{\partial x}$ was also found by Schlinger and, at low values of the Reynolds number, by Towle, as was mentioned above. However, at higher values of the Reynolds number, Towle found the reverse to be true. The reason for this last discrepancy is not apparent. However, all of the data mentioned strongly indicate that these eddy properties are influenced by non-uniformity in the composition of a turbulent stream. In addition, the present data also indicate that the eddy diffusivity is to a certain

extent, independent of the eddy viscosity. Thus, the turbulent Schmidt number, $\frac{\varepsilon_m}{\varepsilon_D}$, varies from values greater than 1 to values less than 0.5. This is radically different from the behavior of the turbulent Prandtl number, $\frac{\varepsilon_m}{\varepsilon_c}$, which is found to remain fairly constant, even in non-uniform flow[8,9].

A qualitative explanation of the relative behavior of the eddy quantities can be given on the basis of the defining expressions given before.

$$\varepsilon_D = - \frac{\partial r}{\partial C_g} \overline{U'_r C'_g} \qquad (3)$$

$$= - \frac{\partial r}{\partial \underline{n}_g} \overline{U'_r \underline{n}'_g} \qquad (3a)$$

$$\varepsilon_m = - \frac{\partial r}{\partial U_x} \overline{U'_r U'_x} \qquad (4)$$

The relative change in the value of U_x along the axis of flow near the center of the channel is considerably less than the corresponding change in $\underline{n}_g$. The change of U_x is due primarily to the shape of the channel rather than to the diffusion of the gas, judging by the velocity profiles of Figure 20, wherein no diffusion is taking place. Thus, U'_x might be expected to change much less than $\underline{n}'_g$ along the direction of flow, and $\underline{n}'_g$ can reasonably be expected to go through a maximum when the value of $\underline{n}_g$ is changing most rapidly in the direction of flow.

The definition of eddy diffusivity developed by Taylor (loc. cit.) differs somewhat from that given above. His theory is expressed in terms of a correlation coefficient, R, between the fluctuating velocity U'_i in a specified direction at any instant and its velocity U'_{i_t} an instant

later:

$$R = \overline{U_i'_t \, U_i'} / \overline{U_i'^2} \tag{16}$$

where the bars indicate a time average and $\overline{U_i'^2}$ is the mean square value of U_i'. Taylor thus showed the following relation to exist:

$$\overline{dY^2}/dt = 2\,\overline{U_i'^2} \int_0^t R\,dt \tag{17}$$

where Y is the distance traveled by a particle in the direction i in time t and $\overline{Y^2}$ is the mean square of Y for a large number of particles. If the fluid is moving with an average velocity in the direction x of U_x, then t can be replaced by $\frac{x}{U_x}$.

For large values of x, the correlation coefficient R becomes zero. Then $\frac{1}{U_x} \int_0^x R\,dx$ is a constant and equation (17) can be written

$$\frac{\overline{dY^2}}{dx} = 2\,\overline{U_i'^2} \; \frac{X}{U_x} \tag{18}$$

where $X = \int_0^x R\,dx$ for values of x so large that R = 0. Thus, when the scale of observation is large compared to the scale of the eddies, turbulent diffusion becomes a continuous process, as is molecular diffusion, and an expression for the eddy diffusivity analogous to that for the molecular diffusivity can be written:

$$\varepsilon_D = \frac{U_x}{2} \frac{\overline{dY^2}}{dx} \tag{19}$$

It follows that, by Taylor's theory,

$$\overline{U_i'^2} = \frac{\varepsilon_D U_x}{X} \tag{20}$$

X is really a characteristic of the scale of turbulence in the channel. By association with the eddy viscosity, $\overline{U_i'^2}$ has been assumed to vary comparatively little with x. Thus, in the present situation the scale of turbulence would have to increase remarkably in order for equation (20) to be obeyed. Since this seems unlikely it must be concluded that Taylor's theory does not adequately describe the situation.

Conclusions:

The behavior of the eddy properties found here is not predicted by any of the current theories of turbulent flow. The large variation in the value of the turbulent Schmidt number raises the question of the validity of the assumption of the equality of ε_D and ε_c which is frequently made[19]. A thorough investigation of ε_D for uniform flow, expanding the work of Woertz and Sherwood[21], would perhaps be of greatest interest because of the large amount of careful work which has been done in determining the eddy conductivity in uniform flow. An investigation of the transfer of energy in a non-uniform, steady state situation analogous to the one studied here would be equally valuable.

NOMENCLATURE

Latin Letters:

C_A Concentration of A, lbs/ft^3.

D Operator = $\frac{\partial}{\partial t} + U \cdot \nabla$

D Fick diffusion coefficient, ft^2/sec.

D_v One form of the Maxwell diffusion coefficient, ft^2/sec.

f Fanning friction factor.

F_x Force in the x direction.

g Accelleration due to gravity = 32.2 ft/sec^2.

G A property of the flowing system.

K Composition correction coefficient.

$\overset{o}{m}$ Weight rate of flow, lbs/sec ft^2.

$\underline{n}_g$ Mole fraction natural gas.

$\Delta\underline{n}_g$ Correction added to composition.

$\underline{n}_g^*$ Corrected composition.

P Pressure, lbs/in^2.

r Radial coordinate.

r_o Distance from the wall to the point of the minimum concentration of gas.

R Fluctuating velocity correlation coefficient.

t time, secs.

u_i Velocity in the direction of the i coordinate.

U Time average velocity.

U_i Average velocity in the direction of the i coordinate.

U_{max} Maximum velocity in the plane of a traverse.

x Axial coordinate.

NOMENCLATURE (cont.)

x_o Distance in the direction of flow from an arbitrary datum.

X Scale of turbulence characteristic.

Y Distance traveled by a particle in direction i and time t.

Greek Letters:

γ Angular distortion.

$\underline{\varepsilon}_c$ Total conductivity, $ft^2/sec.$

ε_D Eddy diffusivity, $ft^2/sec.$

$\underline{\varepsilon}_D$ Eddy diffusivity, $ft^2/sec.$

ε_m Eddy viscosity, $ft^2/sec.$

$\underline{\varepsilon}_m$ Total viscosity, $ft^2/sec.$

θ Azimuthal coordinate.

ν Kinematic viscosity, $ft^2/sec.$

σ Specific weight of fluid, $lbs/ft^3.$

τ Shear, $lbs/ft^2.$

Dimensionless Numbers:

Re Reynolds number, $\dfrac{2r_o \bar{U}_x}{\nu}$.

Sc Turbulent Schmidt number, $\dfrac{\underline{\varepsilon}_m}{\underline{\varepsilon}_D}$.

Pr Turbulent Prandtl number, $\dfrac{\underline{\varepsilon}_m}{\underline{\varepsilon}_c}$.

Superscripts:

$'$ Fluctuating component.

$\overline{\quad}$ Time average or integrated average.

o Pure substance.

REFERENCES

1. Bakhmeteff, B.A., "The Mechanics of Turbulent Flow", Princeton University Press, 1936.

2. von Karman, T., Trans. A.S.M.E., 61, 705-10 (1939).

3. Reynolds, O., Proc. Manchester Lit. Phil. Soc., 14, 7 (1874).

4. Taylor, G.I., Proc. Roy. Soc., 151A, 421 (1935).

5. Corcoran, W.H., Ph. D. Thesis, California Institute of Technology, 1948.

6. Page, F., Jr., Ph. D. Thesis, California Institute of Technology, 1950.

7. Mason, J.L., Ph. D. Thesis, California Institute of Technology, 1950.

8. Mason, D.M., Ph. D. Thesis, California Institute of Technology, 1949.

9. Berry, V.J. Jr., Ph. D. Thesis, California Institute of Technology, 1951.

10. Jenkins, R.L., Ph. D. Thesis, California Institute of Technology, 1949.

11. Schlinger, W.G., Ph. D. Thesis, California Institute of Technology, 1949.

12. Parker, F.D., Student Report No. 146, Chem. Eng. Dept., C.I.T., (1947).

13. Cavers, S.D., Student Report No. 215, Chem. Eng. Dept., C.I.T., (1948).

14. Sherwin, R.M., Student Report No. 342, Chem. Eng. Dept., C.I.T., (1950).

15. Salvadori, M.G., Miller, K.S., "The Mathematical Solution of Engineering Problems", McGraw-Hill (1948).

16. McAdams, W.H., "Heat Transmission", McGraw-Hill (1942).

17. Sherwood, T.K., Pigford, R.L., "Absorption and Extraction", McGraw-Hill (1952).

18. Connell, W.R., Schlinger, W.G., and Sage, B.H., "A Tabulation of Eddy Properties for Uniform Flow", Ms. 5016.1, Chem. Eng. Lab., C.I.T. (1953).

19. Towle, W.L., Sherwood, T.K., Ind. Eng. Chem., 31, 457 (1939).

20. Towle, W.L., Sherwood, T.K., Seder, L.A., Ind. Eng. Chem., 31, 462 (1939).

21. Sherwood, T.K., Woertz, B.B., Ind. Eng. Chem., 31, 1034 (1939).

LIST OF TABLES

LIST OF FIGURES

LIST OF FIGURES (cont.)

TABLE I

EXPERIMENTAL DATA FOR Re 45,000 - COMPOSITION

Probe* Position (inches)	Mole Fraction Natural Gas, $\underline{n}_g$				
	$x_o = 0$	$x_o = 9$ in.	$x_o = 18$ in.	$x_o = 27$ in.	$x_o = 36$ in.
5.95	0.0801	0.0713	0.0651	0.0621	0.0620
5.80	0.0765	0.0700	0.0651	0.0621	0.0601
5.60	0.0726	0.0661	0.0632	0.0618	0.0588
5.40	0.0655	0.0613	0.0613	0.0595	0.0558
5.20	0.0596	0.0577	0.0574	0.0566	0.0555
5.00	0.0548	0.0535	0.0544	0.0531	0.0530
4.80	0.0441	0.0464	0.0486	0.0501	0.0503
4.60	0.0340	0.0386	0.0434	0.0456	0.0459
4.40	0.0288	0.0334	0.0379	0.0427	0.0439
4.20	0.0191	0.0275	0.0327	0.0395	0.0403
4.00	0.0152	0.0204	0.0292	0.0349	0.0360
3.80	0.0097	0.0149	0.0230	0.0317	0.0340
3.60	0.0065	0.0117	0.0207	0.0285	0.0308
3.40	0.0039	0.0081	0.0169	0.0269	0.0295
3.20	0.0016	0.0068	0.0149	0.0246	0.0285
3.00	0.0013	0.0062	0.0152	0.0230	0.0269
2.80	0.0026	0.0062	0.0156	0.0236	0.0275
2.60	0.0032	0.0097	0.0172	0.0259	0.0310
2.40	0.0045	0.0107	0.0211	0.0282	0.0313

*The walls of the flow channel are at probe positions 0.00 and 6.00 inches.

TABLE II

SMOOTHED DATA FOR Re 45,000 - COMPOSITION

$\left(\frac{r}{r_o}\right)^2$	Mole Fraction Natural Gas, $\underline{n}_g$				
	$x_o = 0$	$x_o = 9$ in.	$x_o = 18$ in.	$x_o = 27$ in.	$x_o = 36$ in.
0.0	0.0014	0.0062	0.0145	0.0225	0.0275
0.1	0.0141	0.0193	0.0264	0.0320	0.0355
0.2	0.0265	0.0312	0.0365	0.0403	0.0425
0.3	0.0376	0.0413	0.0449	0.0467	0.0479
0.4	0.0476	0.0495	0.0511	0.0519	0.0519
0.5	0.0563	0.0563	0.0561	0.0568	0.0550
0.6	0.0636	0.0615	0.0600	0.0586	0.0572
0.7	0.0695	0.0656	0.0628	0.0606	0.0586
0.8	0.0738	0.0684	0.0647	0.0618	0.0595
0.9	0.0765	0.0701	0.0657	0.0626	0.0599
1.0	0.0774	0.0706	0.0661	0.0629	0.0600
Std. Dev. *	0.0015	0.0008	0.0007	0.0014	0.0009

* Defined here as

$$\sqrt{\frac{\sum_{1}^{n} (\underline{n}_{g_{exp.}} - \underline{n}_{g_{smoothed}})^2}{n - 1}}$$

where $\underline{n}_{g_{exp.}}$ and $\underline{n}_{g_{smoothed}}$ are taken at the same value of $\frac{r}{r_o}$.

TABLE III

EXPERIMENTAL DATA FOR Re 45,000 - VELOCITY

Probe* Position (inches)	Velocity, U_x, ft/sec				
	$x_o = 0$	$x_o = 9$ in.	$x_o = 18$ in.	$x_o = 27$ in.	$x_o = 36$ in.
5.95	10.4	10.6	11.0	10.9	11.1
5.80	11.4	11.8	12.1	12.1	12.4
5.60	12.2	12.8	13.0	13.1	13.2
5.40	13.2	13.5	13.8	13.8	13.6
5.20	14.1	14.1	14.3	14.2	14.1
5.00	14.8	14.7	14.7	14.8	14.7
4.80	15.5	15.4	15.4	15.4	15.2
4.60	16.4	16.1	16.0	15.8	15.5
4.40	17.2	16,7	16.4	16.3	15.9
4.20	17.7	17.4	16.9	16.8	16.4
4.00	18.2	17.9	17.5	17.3	16.7
3.80	18.6	18.4	17.9	17.7	17.1
3.60	19.0	18.8	18.3	18.1	17.3
3.40	19.1	19.1	18.6	18.2	17.6
3.20	19.2	19.2	18.8	18.4	17.8
3.00	19.3	19.2	18.9	18.5	17.9
2.80	19.3	19.2	18.8	18.4	17.8
2.60	19.2	19.1	18.8	18.3	17.6
2.40	19.1	18.8	18.5	18.1	17.4

*The walls of the flow channel are at probe positions 0.00 and 6.00 inches.

TABLE IV

SMOOTHED DATA FOR Re 45,000 - VELOCITY

$\left(\frac{r}{r_o}\right)^2$	Velocity, U_x, ft/sec				
	$x_o = 0$	$x_o = 9$ in.	$x_o = 18$ in.	$x_o = 27$ in.	$x_o = 36$ in.
0.0	19.41	19.15	18.84	18.45	18.06
0.1	18.35	18.00	17.69	17.40	17.10
0.2	17.28	16.94	16.68	16.47	16.32
0.3	16.24	15.98	15.83	15.73	15.68
0.4	15.28	15.16	15.13	15.12	15.14
0.5	14.41	14.44	14.53	14.57	14.65
0.6	13.63	13.29	13.95	14.04	14.15
0.7	12.89	13.15	13.36	13.50	13.63
0.8	12.15	12.45	12.70	12.92	13.10
0.9	11.26	11.52	11.78	11.98	12.22
1.0	0	0	0	0	0
Std. Dev. *	0.12	0.08	0.11	0.08	-

* Defined here as

$$\sqrt{\frac{\sum_{1}^{n}(U_{x_{exp.}} - U_{x_{smoothed}})^2}{n-1}}$$

where $U_{x_{exp.}}$ and $U_{x_{smoothed}}$ are taken at the same value of $\frac{r}{r_o}$.

TABLE V

VARIATION OF COMPOSITION AND VELOCITY WITH AZIMUTHAL POSITION - Re 45,000

$\frac{r}{r_o} = 0.60$

		Azimuthal Position, θ					
		-120°	-60°	0°	$+60^\circ$	$+120^\circ$	$+180^\circ$
$x_o = 0$	$\underline{n}_g$ mole fract.	0.0458	0.0502	0.0452	0.0470	0.0583	0.0516
	U_x ft/sec	15.9	15.3	15.5	15.5	14.9	15.7
$x_o = 36$ in.	$\underline{n}_g$ mole fract.	0.0494	0.0502	0.0492	0.0510	0.0555	0.0515
	U_x ft/sec	15.2	14.9	15.0	15.2	14.7	15.1

TABLE VI

CORRECTIONS APPLIED TO SMOOTHED COMPOSITION DATA - Re 45,000

Radial Position $\left(\frac{r}{r_o}\right)^2$	Correction to Composition, $\Delta\underline{n}_g$[1], Mole Fraction				
	x_o = 0	x_o = 9 in.	x_o = 18 in.	x_o = 27 in.	x_o = 36 in.
	$K = 4.42 \times 10^{-3}$	$K = 2.78 \times 10^{-3}$	$K \equiv 0$	$K = -1.77 \times 10^{-3}$	$K = -2.26 \times 10^{-3}$
0	0	0		0	0
0.1	0.0008	0.0005		-0.0003	-0.0004
0.2	0.0016	0.0010		-0.0006	-0.0008
0.3	0.0023	0.0014		-0.0009	-0.0012
0.4	0.0028	0.0018		-0.0011	-0.0014
0.5	0.0033	0.0021		-0.0013	-0.0017
0.6	0.0037	0.0023		-0.0015	-0.0019
0.7	0.0040	0.0025		-0.0016	-0.0021
0.8	0.0042	0.0027		-0.0017	-0.0022
0.9	0.0044	0.0028		-0.0018	-0.0023
1.0	0.0044	0.0028		-0.0018	-0.0023

[1] $\Delta\underline{n}_g = K\left(\frac{r}{r_o}\right)^2\left(2 - \left[\frac{r}{r_o}\right]^2\right)$

TABLE VII

EXPERIMENTAL DATA FOR Re 82,300 - COMPOSITION

Probe* Position (inches)	Mole Fraction Natural Gas, n_g					
	x_o = 6 in.	x_o = 12 in.	x_o = 18 in.	x_o = 24 in.	x_o = 30 in.	x_o = 36 in.
5.95	0.0738	—	0.0680	0.0648	—	—
5.80	—	0.0698	—	0.0639	—	0.0604
5.70	—	—	—	—	0.0625	—
5.60	0.0691	—	—	0.0625	—	—
5.40	0.0634	0.0604	0.0615	0.0594	0.0586	0.0579
5.20	0.0576	—	0.0572	0.0562	0.0557	0.0552
5.10	—	0.0518	—	—	—	—
5.00	0.0502	0.0510	0.0517	0.0531	—	0.0532
4.80	0.0430	0.0438	0.0466	0.0477	—	0.0506
4.60	0.0359	0.0371	0.0420	0.0434	0.0456	0.0468
4.40	0.0281	0.0321	0.0360	0.0395	—	0.0439
4.20	0.0227	0.0270	—	0.0343	—	0.0409
4.00	0.0170	0.0220	0.0265	0.0300	0.0345	0.0377
3.80	0.0129	0.0177	0.0220	0.0266	—	0.0348
3.60	0.0088	0.0153	0.0184	0.0226	0.0284	0.0326
3.40	0.0068	0.0105	0.0151	0.0190	0.0245	—
3.20	0.0058	0.0105	—	0.0177	0.0227	0.0290
3.00	0.0053	0.0092	0.0126	0.0163	0.0213	0.0282

*The walls of the flow channel are at probe positions 0.00 and 6.00 inches.

TABLE VIII

SMOOTHED DATA FOR Re 82,300 - COMPOSITION

$\left(\frac{r}{r_o}\right)^2$	Mole Fraction Natural Gas, $\underline{n}_g$					
	x_o = 6 in.	x_o = 12 in.	x_o = 18 in.	x_o = 24 in.	x_o = 30 in.	x_o = 36 in.
0	0.0055	0.0087	0.0124	0.0168	0.0219	0.0279
.1	0.0167	0.0201	0.0234	0.0270	0.0308	0.0349
.2	0.0273	0.0305	0.0333	0.0360	0.0387	0.0411
.3	0.0375	0.0399	0.0419	0.0436	0.0451	0.0464
.4	0.0467	0.0481	0.0492	0.0499	0.0505	0.0505
.5	0.0548	0.0552	0.0552	0.0550	0.0546	0.0537
.6	0.0617	0.0610	0.0600	0.0589	0.0577	0.0560
.7	0.0673	0.0657	0.0637	0.0619	0.0600	0.0578
.8	0.0715	0.0695	0.0664	0.0640	0.0616	0.0590
.9	0.0740	0.0710	0.0680	0.0652	0.0626	0.0597
1.0	0.0749	0.0717	0.0685	0.0656	0.0629	0.0599
Std. Dev.	0.0007	0.0012	0.0006	0.0007	0.0006	0.0004

TABLE IX

EXPERIMENTAL DATA FOR Re 82,300 - VELOCITY

Probe* Position (inches)	Velocity, U_x, ft/sec					
	x_o = 6 in.	x_o = 12 in.	x_o = 18 in.	x_o = 24 in.	x_o = 30 in.	x_o = 36 in.
5.95	20.1	20.3	20.4	20.5	20.6	20.6
5.90	20.9	21.1	21.2	21.3	21.4	21.4
5.80	22.1	22.3	22.5	22.4	22.6	22.6
5.60	23.7	23.5	24.0	24.1	24.2	24.3
5.40	24.9	25.0	25.0	25.2	25.1	25.3
5.20	26.1	26.2	26.2	26.3	26.3	26.3
5.00	27.4	27.2	27.2	27.0	27.0	27.1
4.80	28.5	28.3	28.2	27.9	27.9	27.8
4.60	29.4	29.3	29.0	28.7	28.6	28.5
4.40	30.4	30.0	29.8	29.5	29.4	29.0
4.20	31.4	30.8	30.3	30.2	29.9	29.6
4.00	31.7	31.2	30.8	30.5	30.4	30.1
3.80	32.2	31.6	31.3	31.1	30.8	30.3
3.60	32.5	32.2	31.8	31.5	31.4	30.8
3.40	32.7	32.4	32.2	31.8	31.6	31.1
3.20	32.8	32.7	32.4	32.2	31.8	31.6
3.00	33.0	32.8	32.5	32.4	32.1	31.8
2.80	33.0	32.8	32.5	32.4	32.2	32.0
2.60	32.8	32.7	32.4	32.2	32.1	31.8
2.40	32.7	32.4	32.2	32.0	31.8	31.6

*The walls of the flow channel are at probe positions 0.00 and 6.00 inches.

TABLE X

SMOOTHED DATA FOR Re 82,300 - VELOCITY

$\left(\frac{r}{r_o}\right)^2$	Velocity, U_x, ft/sec					
	x_o = 6 in.	x_o = 12 in.	x_o = 18 in.	x_o = 24 in.	x_o = 30 in.	x_o = 36 in.
0	32.97	32.71	32.48	32.30	32.08	31.87
.1	31.77	31.50	31.27	31.04	30.88	30.69
.2	30.51	30.48	30.08	29.91	29.75	29.60
.3	29.24	29.06	28.92	28.82	28.71	28.62
.4	27.95	27.85	27.81	27.78	27.76	27.72
.5	26.68	26.68	26.73	26.79	26.85	26.85
.6	25.46	25.55	25.69	25.82	25.94	25.99
.7	24.29	24.45	24.64	24.81	24.97	25.05
.8	23.09	23.27	23.48	23.65	23.79	23.94
.9	21.57	21.74	21.98	22.11	22.25	22.46
1.0	0	0	0	0	0	0
Std. Dev.	0.11	0.14	0.10	0.11	0.11	0.16

TABLE XI

VARIATION OF COMPOSITION AND VELOCITY WITH AZIMUTHAL POSITION - Re 82,300

	Probe* Position	Azimuthal Position, θ					
		-60°	-30°	0°	30°	60°	90°
				n_g, mole fraction			
x_o 6 in.	5.00 in.	0.0650	0.0711	0.0519	0.0502	0.0585	0.0615
	1.00 in.	0.0512	0.0418	0.0467	0.0517	0.0572	0.0565
x_o 36 in.	5.00 in.	0.0594	0.0611	0.0688	0.0532	0.0529	0.0570
	1.00 in.	0.0536	0.0471	0.0405	0.0489	0.0508	0.0540
				U_x, ft/sec			
x_o 6 in.	5.00 in.	25.9	25.7	28.8	27.4	27.7	27.6
	1.00 in.	29.7	31.3	30.0	27.1	27.0	26.9
x_o 36 in.	5.00 in.	24.4	24.8	25.4	27.1	25.1	25.8
	1.00 in.	27.9	29.4	27.2	27.7	25.2	25.2

*The walls of the flow channel are at probe positions 0.00 and 6.00 in.

TABLE XII

CORRECTIONS APPLIED TO SMOOTHED COMPOSITION DATA - Re 82,300

Radial Position $\left(\frac{r}{r_o}\right)^2$	Correction to Composition, $\Delta\underline{n}_g^1$, Mole Fraction				
	x_o = 6 in. $K = 2.05 \times 10^{-3}$	x_o = 12 in. $K = 0.77 \times 10^{-3}$	x_o = 24 in. $K = -0.81 \times 10^{-3}$	x_o = 30 in. $K = -1.61 \times 10^{-3}$	x_o = 36 in. $K = -2.06 \times 10^{-3}$
0	0	0	0	0	0
0.1	0.0004	0.0001	-0.0001	-0.0003	-0.0004
0.2	0.0007	0.0003	-0.0003	-0.0006	-0.0007
0.3	0.0011	0.0004	-0.0004	-0.0008	-0.0011
0.4	0.0013	0.0005	-0.0005	-0.0010	-0.0013
0.5	0.0015	0.0006	-0.0006	-0.0012	-0.0015
0.6	0.0017	0.0006	-0.0006	-0.0014	-0.0017
0.7	0.0019	0.0007	-0.0007	-0.0015	-0.0019
0.8	0.0020	0.0007	-0.0007	-0.0015	-0.0020
0.9	0.0020	0.0008	-0.0008	-0.0016	-0.0020
1.0	0.0021	0.0008	-0.0008	-0.0016	-0.0021

[1] $$\Delta\underline{n}_g = K\left(\frac{r}{r_o}\right)^2\left(2 - \left[\frac{r}{r_o}\right]^2\right)$$

$K \equiv 0$ at x_o = 18 in.

TABLE XIII

CHANGE OF VELOCITY WITH DISTANCE DOWNSTREAM IN THE ABSENCE OF DIFFUSION - EXPERIMENTAL DATA

Probe* Position (inches)	Velocity, U_x, ft/sec		
	$x_o = 0$	$x_o = 18$ in.	$x_o = 36$ in.
5.95	11.2	11.7	11.7
5.80	12.6	12.9	13.1
5.60	13.6	13.9	14.0
5.40	14.4	14.7	14.8
5.20	15.4	15.4	15.4
5.00	16.3	15.9	16.0
4.80	17.0	16.5	16.5
4.60	17.7	16.8	16.7
4.40	18.3	17.5	17.0
4.20	18.6	17.7	17.4
4.00	18.9	18.0	17.6
3.80	19.1	18.2	17.8
3.60	19.2	18.4	17.9
3.40	19.2	18.5	18.0
3.20	19.2	18.6	18.1
3.00	19.2	18.8	18.2
2.80	19.2	18.8	18.3
2.60	19.1	18.7	18.3
2.40	19.0	18.6	18.2
2.20	18.7	18.5	18.1

*The walls of the flow channel are at probe positions 0.00 and 6.00 inches.

TABLE XIV

THE TOTAL DIFFUSIVITY AS A FUNCTION OF POSITION - Re 45,000

$\frac{r}{r_o}$	Total Diffusivity, ε_D - ft^2/sec				
	x_o = 0	x_o = 9 in.	x_o = 18 in.	x_o = 27 in.	x_o = 36 in.
0.0	0.0120	0.0190	0.0285	0.0250	0.0208
0.1	0.0121	0.0190	0.0284	0.0248	0.0206
0.2	0.0124	0.0192	0.0282	0.0242	0.0201
0.3	0.0130	0.0196	0.0277	0.0235	0.0196
0.4	0.0139	0.0202	0.0273	0.0231	0.0196
0.5	0.0150	0.0211	0.0272	0.0239	0.0207
0.6	0.0160	0.0221	0.0274	0.0255	0.0230
0.7	0.0163	0.0223	0.0274	0.0275	0.0260

TABLE XV

THE TOTAL VISCOSITY AS A FUNCTION OF POSITION - Re 45,000

$\frac{r}{r_o}$	Total Viscosity, ε_m - ft^2/sec				
	x_o = 0	x_o = 9 in.	x_o = 18 in.	x_o = 27 in.	x_o = 36 in.
0.0	0.0155	0.0150	0.0168	0.0193	0.0214
0.1	0.0156	0.0152	0.0169	0.0194	0.0217
0.2	0.0161	0.0157	0.0172	0.0197	0.0224
0.3	0.0168	0.0166	0.0178	0.0203	0.0236
0.4	0.0177	0.0178	0.0188	0.0212	0.0249
0.5	0.0186	0.0193	0.0202	0.0222	0.0257
0.6	0.0194	0.0209	0.0221	0.0231	0.0254
0.7	0.0194	0.0219	0.0224	0.0223	0.0228

TABLE XVI

THE TOTAL DIFFUSIVITY AS A FUNCTION OF POSITION - Re 82,300

	Total Diffusivity, ε_D - ft^2/sec					
$\frac{r}{r_o}$	x_o = 6 in.	x_o = 12 in.	x_o = 18 in.	x_o = 24 in.	x_o = 30 in.	x_o = 36 in.
0.0	0.0241	0.0305	0.0377	0.0489	0.0680	0.1030
0.1	0.0242	0.0304	0.0377	0.0488	0.0675	0.1020
0.2	0.0245	0.0305	0.0378	0.0483	0.0662	0.0986
0.3	0.0250	0.0307	0.0379	0.0480	0.0640	0.0935
0.4	0.0257	0.0312	0.0381	0.0479	0.0618	0.0881
0.5	0.0266	0.0319	0.0383	0.0479	0.0607	0.0847
0.6	0.0273	0.0323	0.0385	0.0477	0.0606	0.0835
0.7	0.0269	0.0322	0.0384	0.0473	0.0602	0.0829

TABLE XVII

THE TOTAL VISCOSITY AS A FUNCTION OF POSITION - Re 82,300

$\frac{r}{r_o}$	Total Viscosity, ε_m - ft^2/sec					
	x_o = 6 in.	x_o = 12 in.	x_o = 18 in.	x_o = 24 in.	x_o = 30 in.	x_o = 36 in.
0.0	0.0417	0.0394	0.0372	0.0356	0.0350	0.0353
0.1	0.0414	0.0393	0.0372	0.0356	0.0350	0.0352
0.2	0.0405	0.0389	0.0372	0.0357	0.0352	0.0353
0.3	0.0390	0.0382	0.0373	0.0360	0.0356	0.0357
0.4	0.0372	0.0373	0.0376	0.0367	0.0372	0.0370
0.5	0.0350	0.0361	0.0370	0.0372	0.0381	0.0388
0.6	0.0326	0.0346	0.0361	0.0370	0.0383	0.0394
0.7	0.0302	0.0320	0.0339	0.0348	0.0360	0.0361

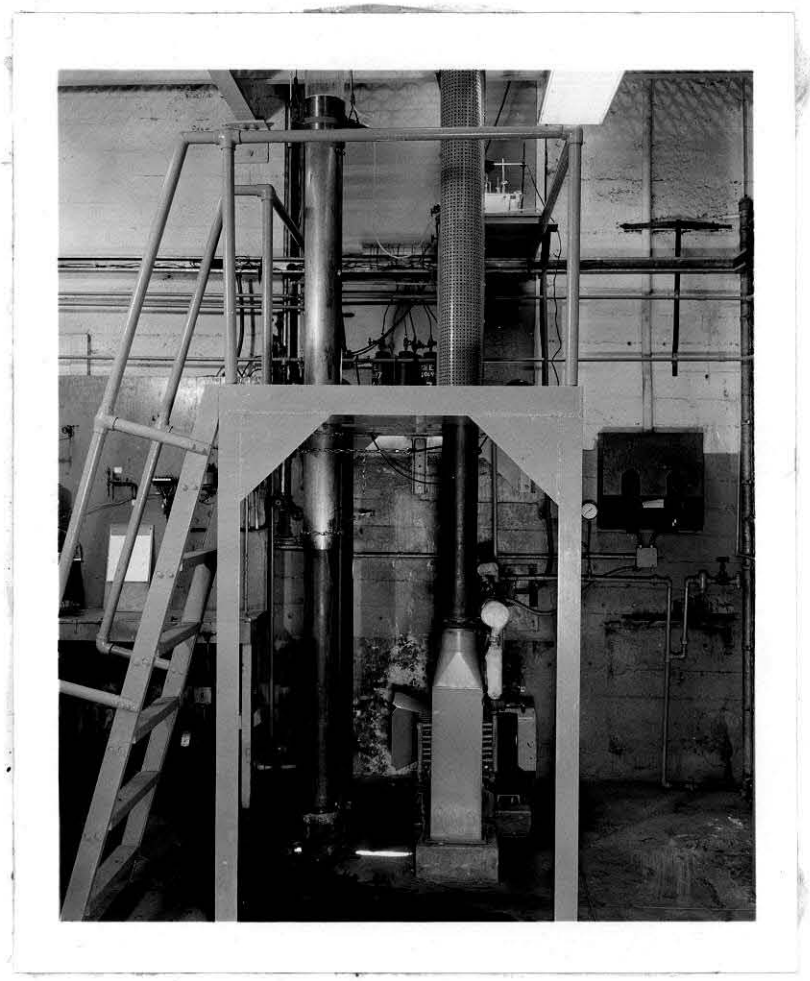

Figure 1 - The Flow Equipment

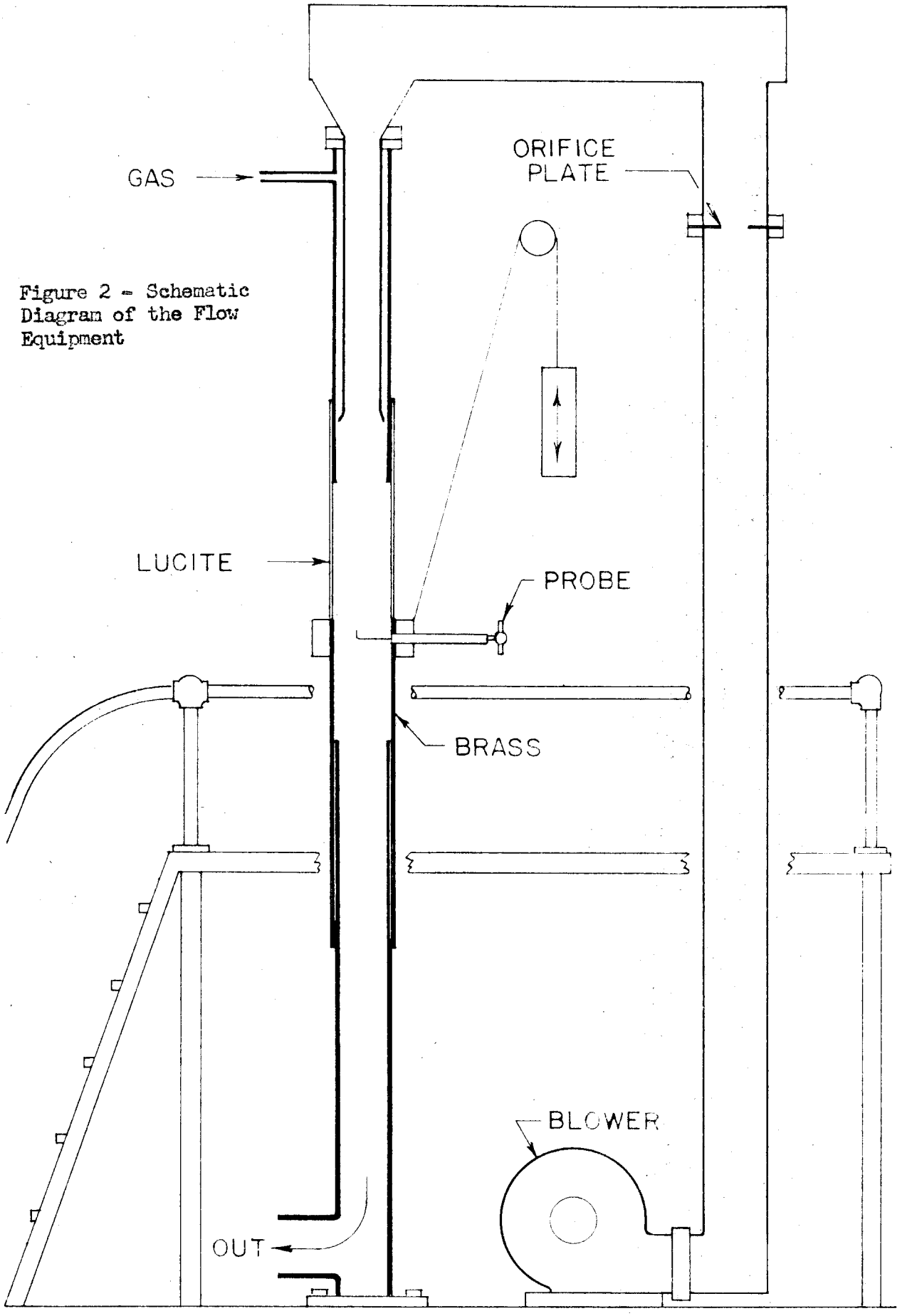

Figure 2 - Schematic Diagram of the Flow Equipment

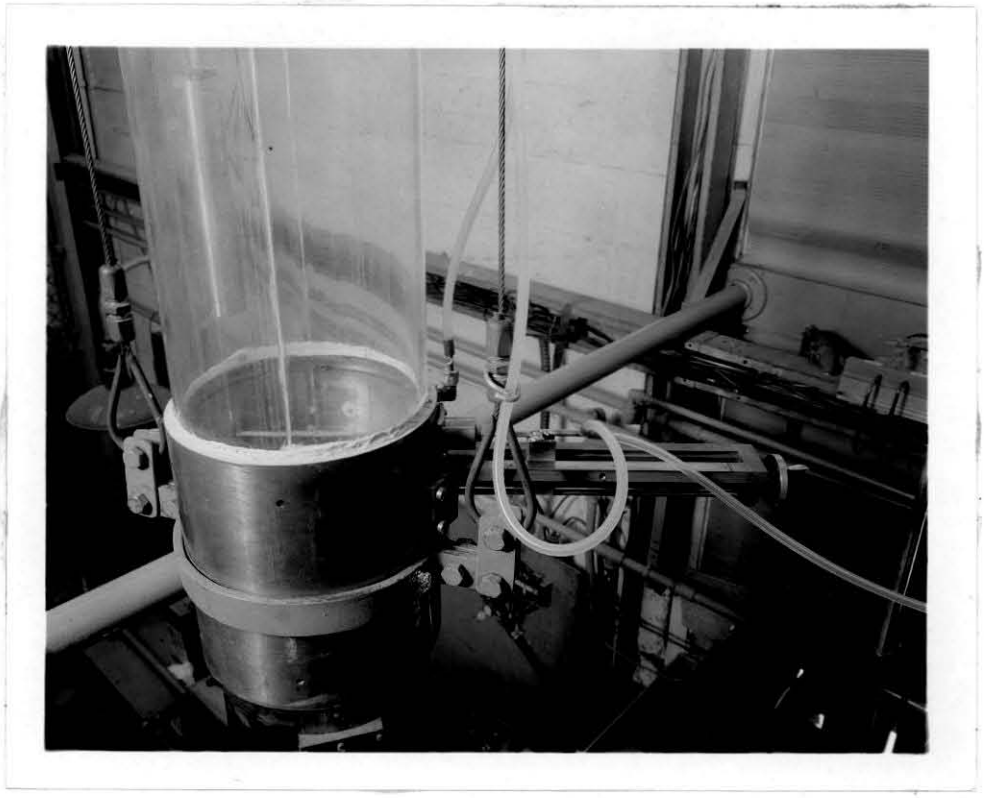

Figure 3 - The Interior of the Test Section

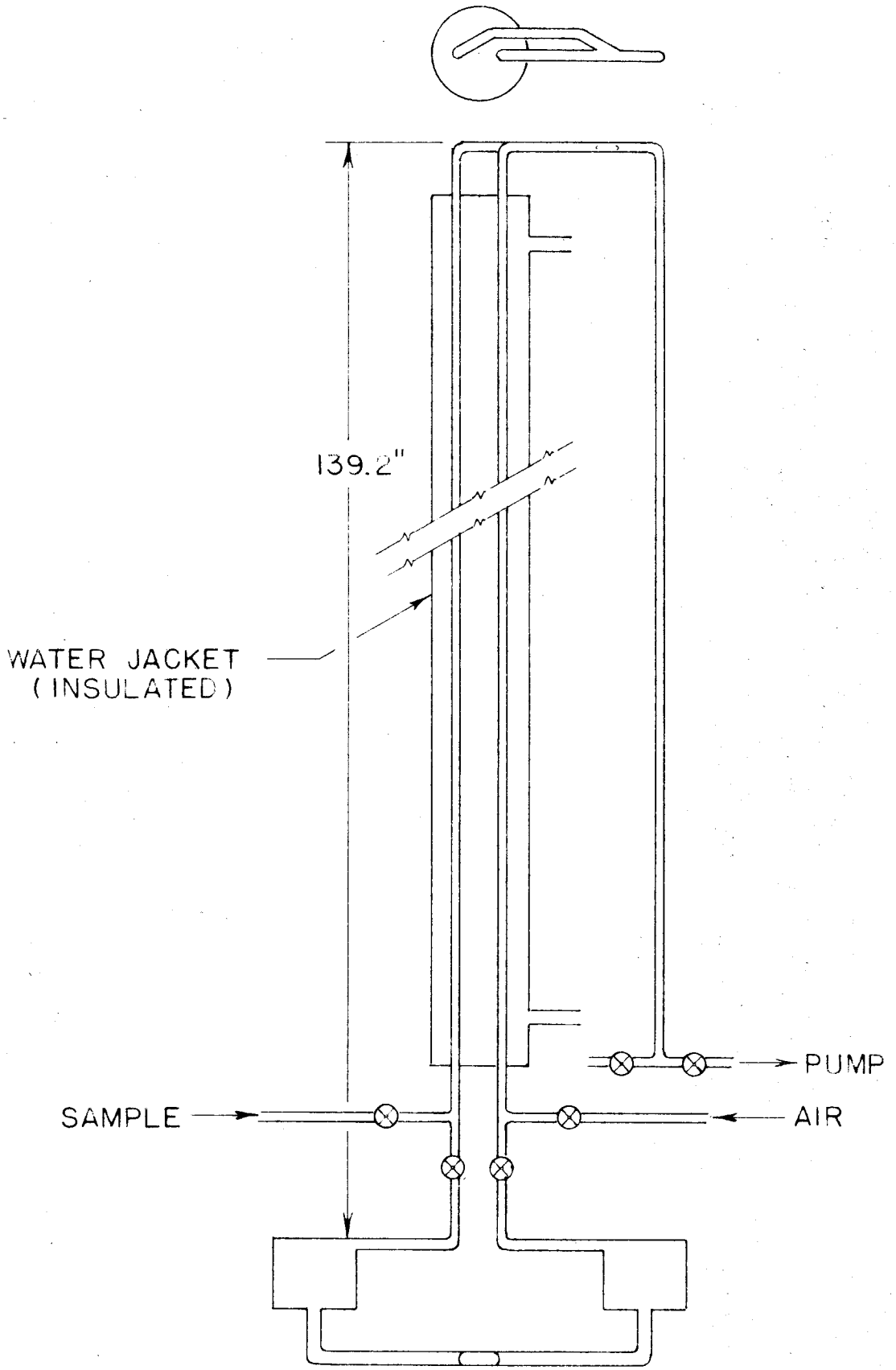

GAS ANALYSIS APPARATUS.

Figure 4

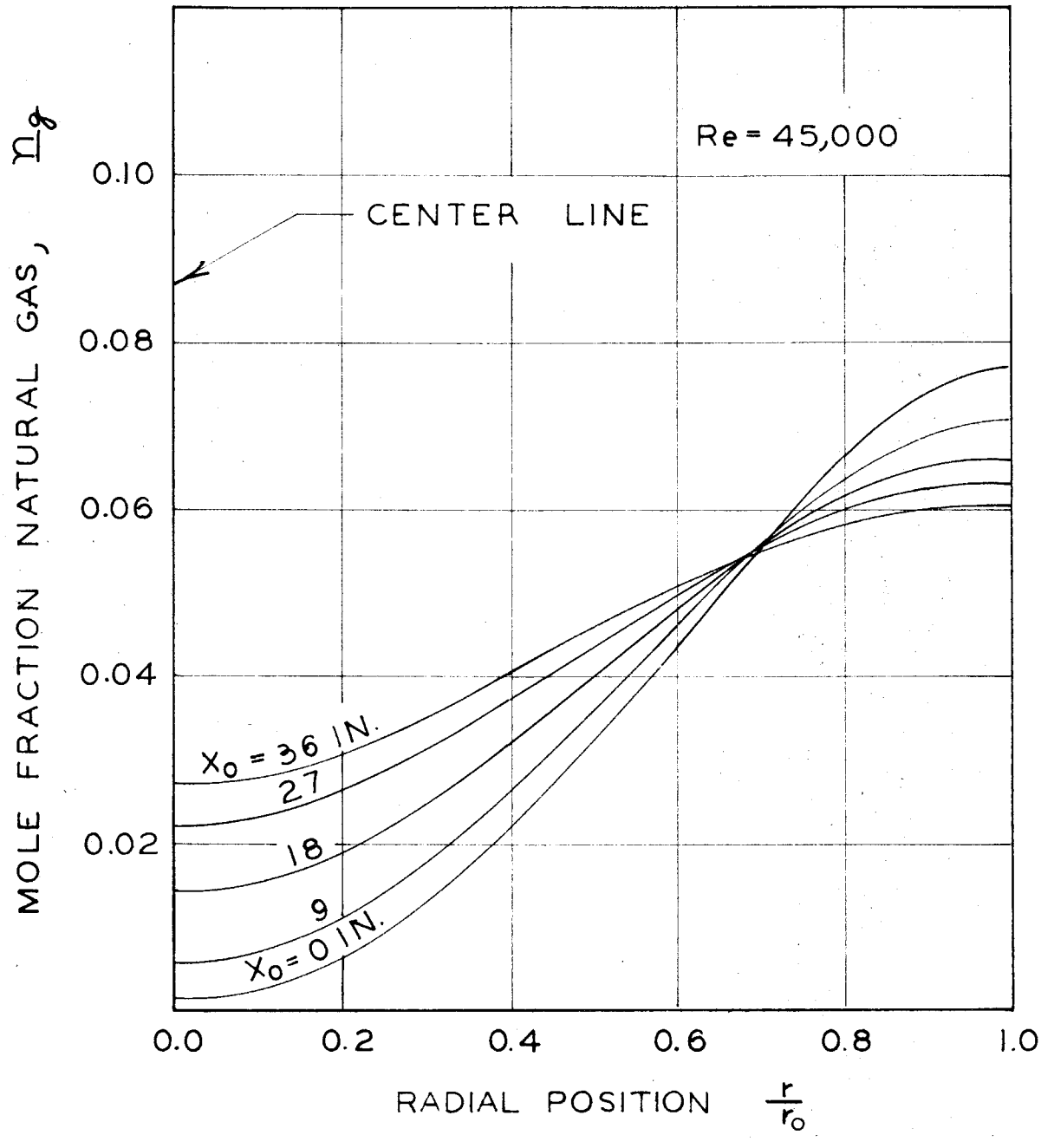

Figure 5 - Composition as a Function of Radial Position - Re 45,000

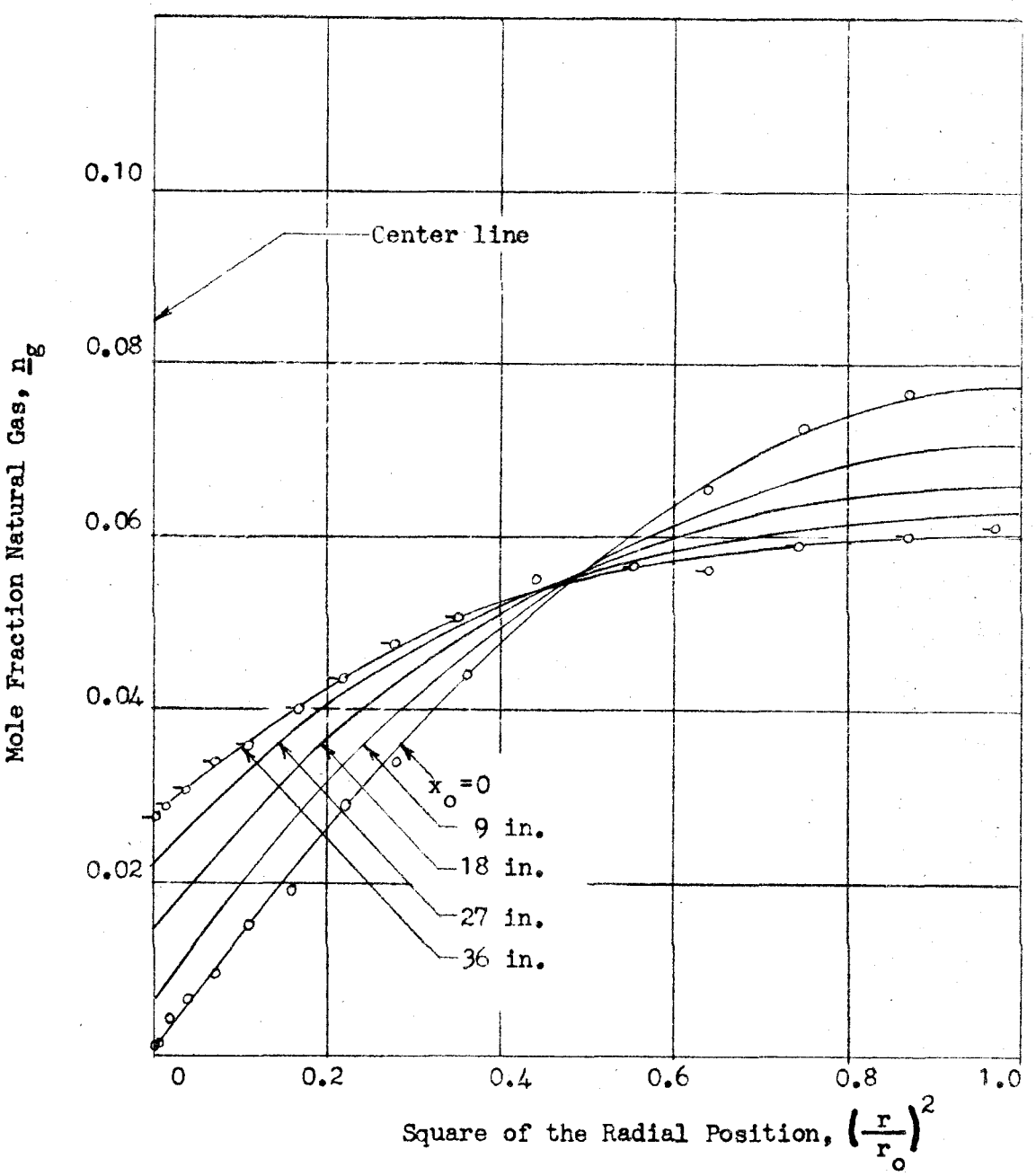

Figure 6 - Composition as a Function of the Square of the Radial Position - Re 45,000.

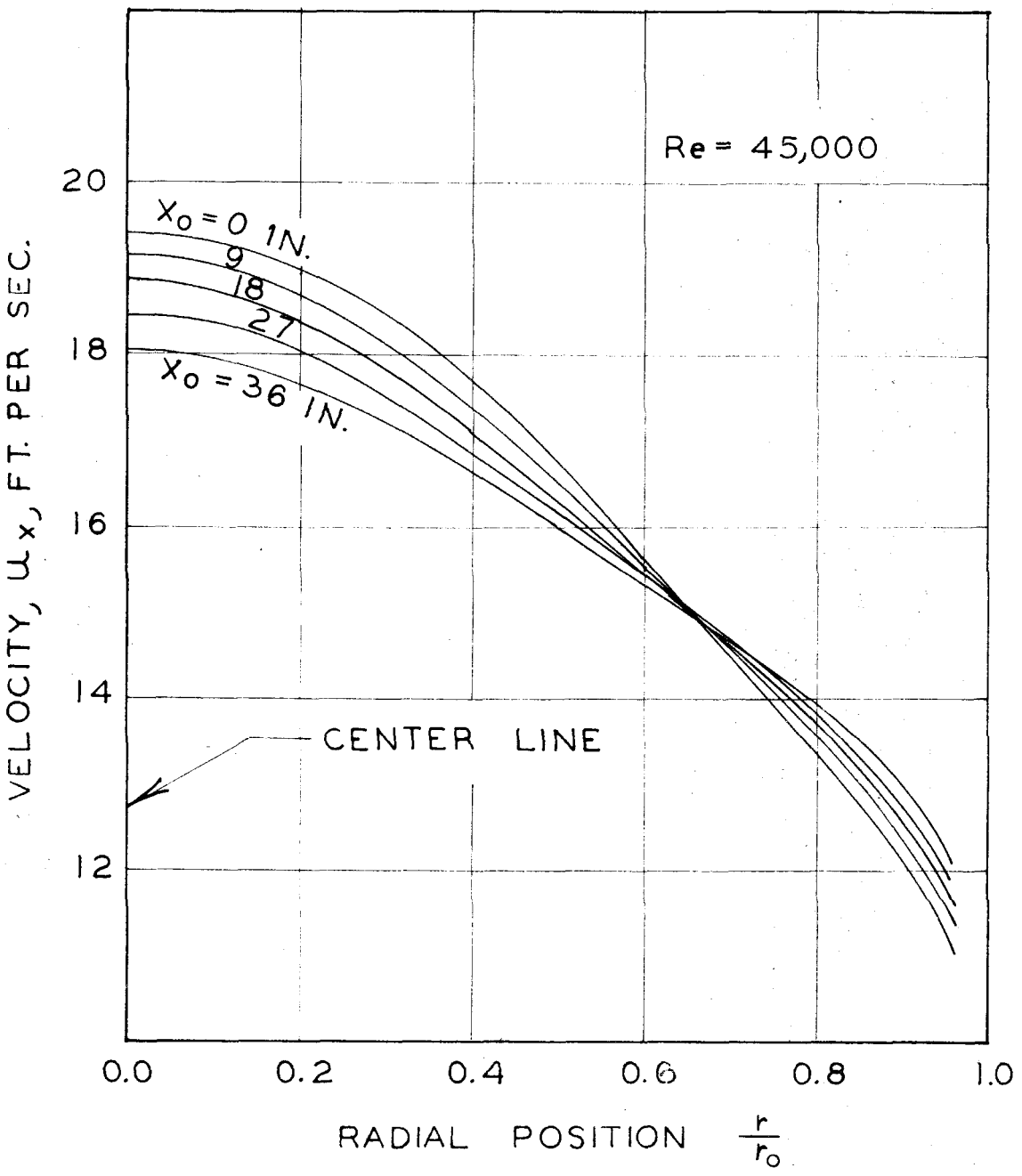

Figure 7 - Velocity as a Function of Radial Position - Re 45,000

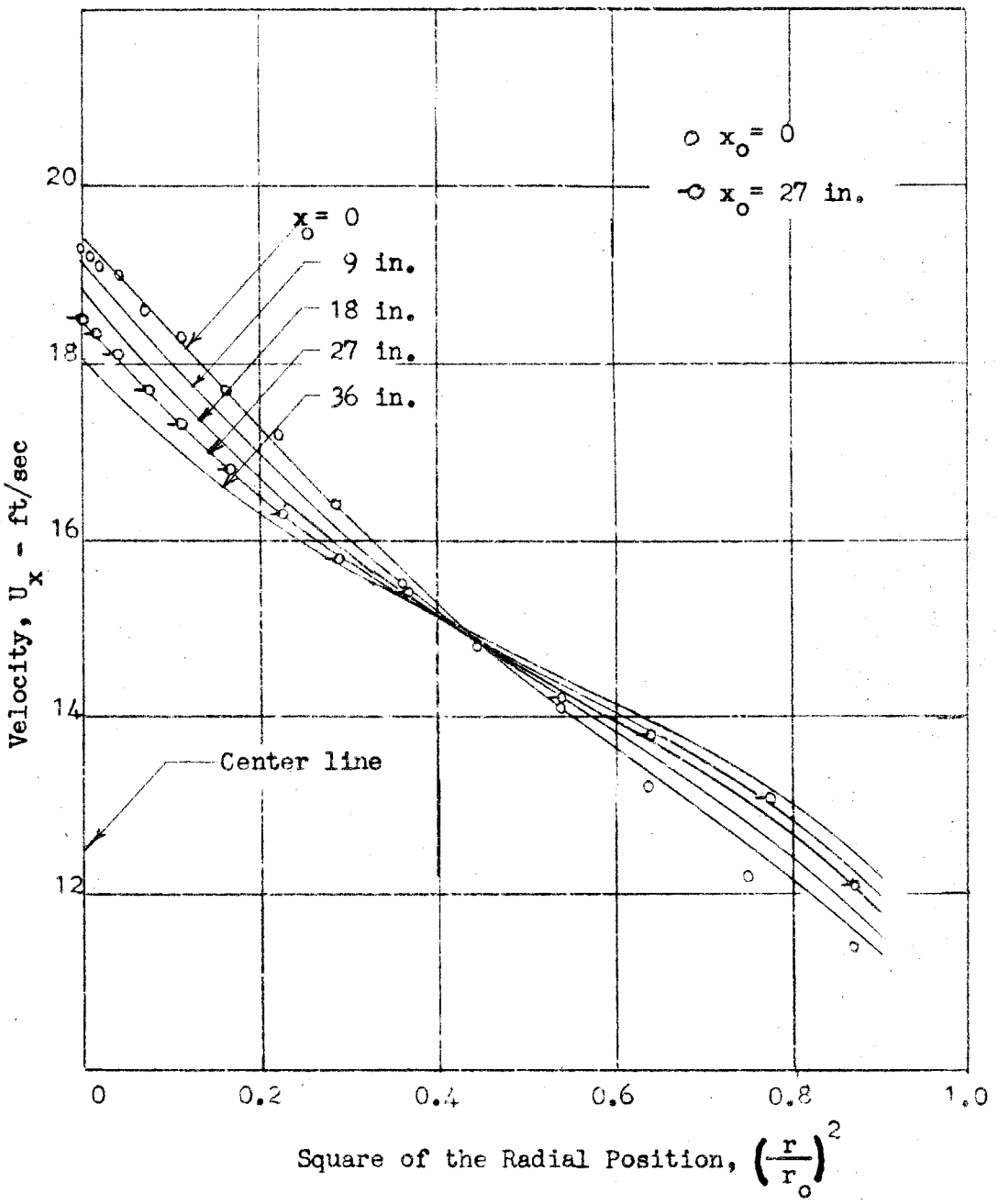

Figure 8 - Velocity as a Function of the Square of the Radial Position - Re 45,000.

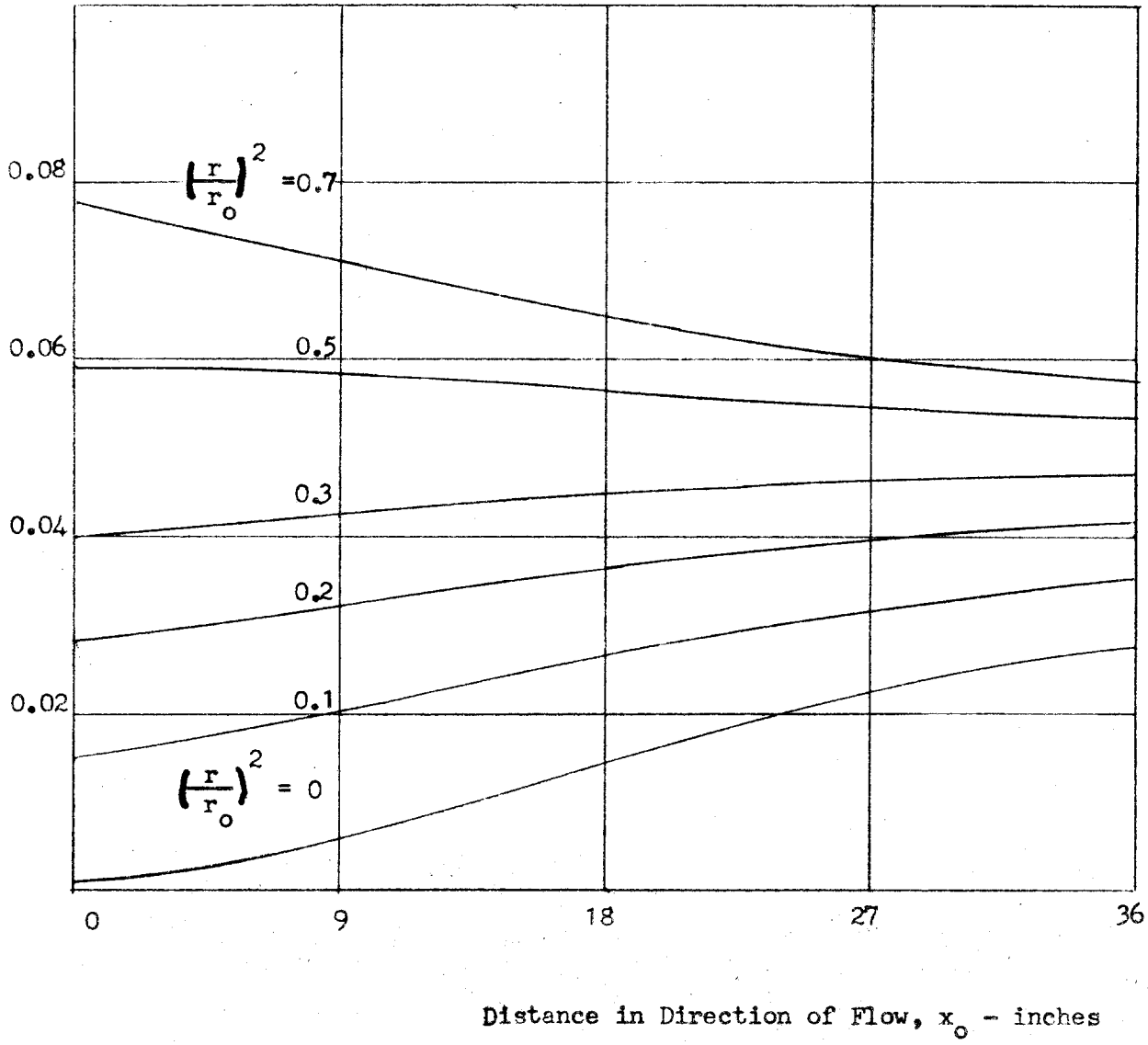

Figure 9 - Composition as a Function of Distance Downstream - Re 45,000.

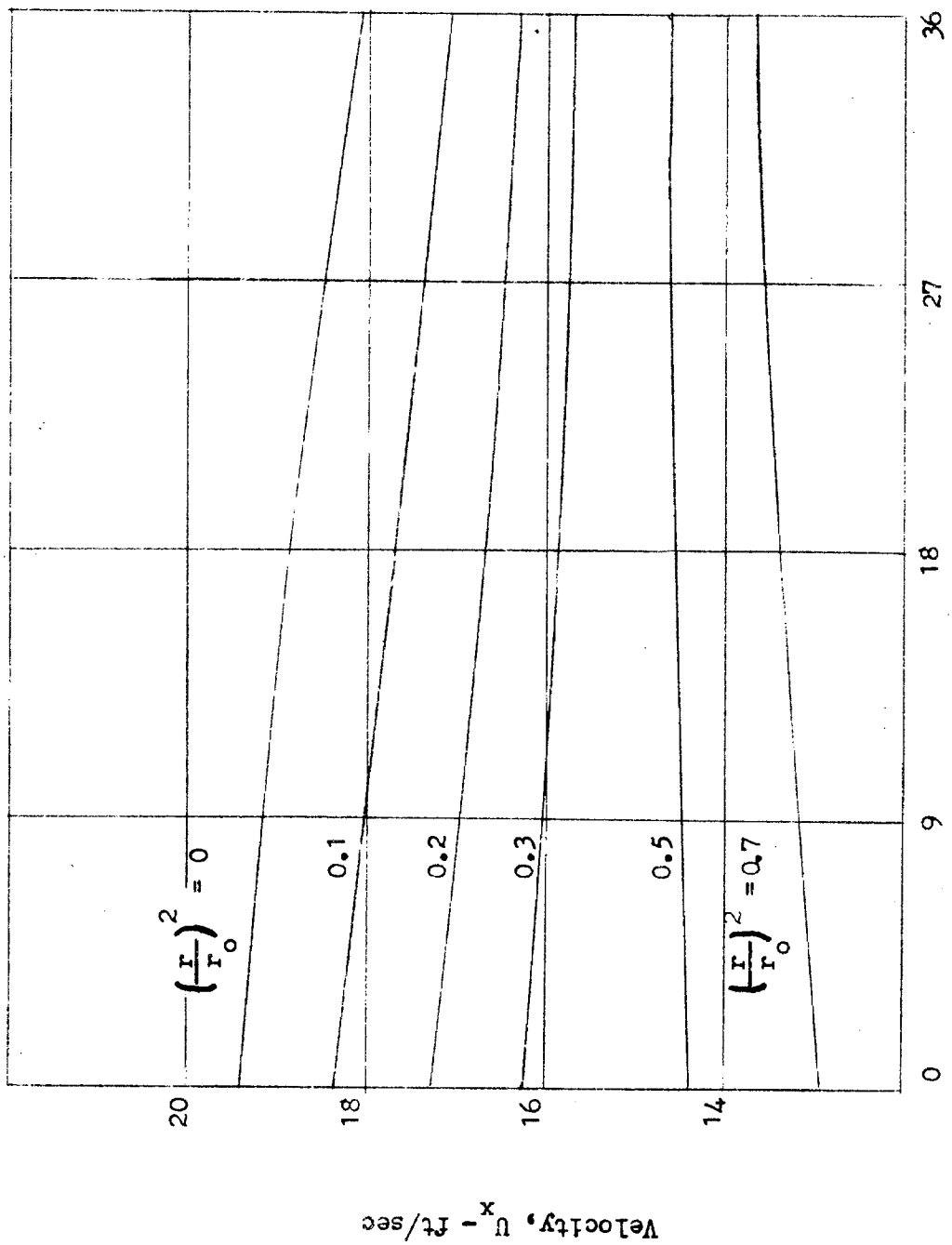

Figure 10 - Velocity as a Function of Distance Downstream - Re 45,000.

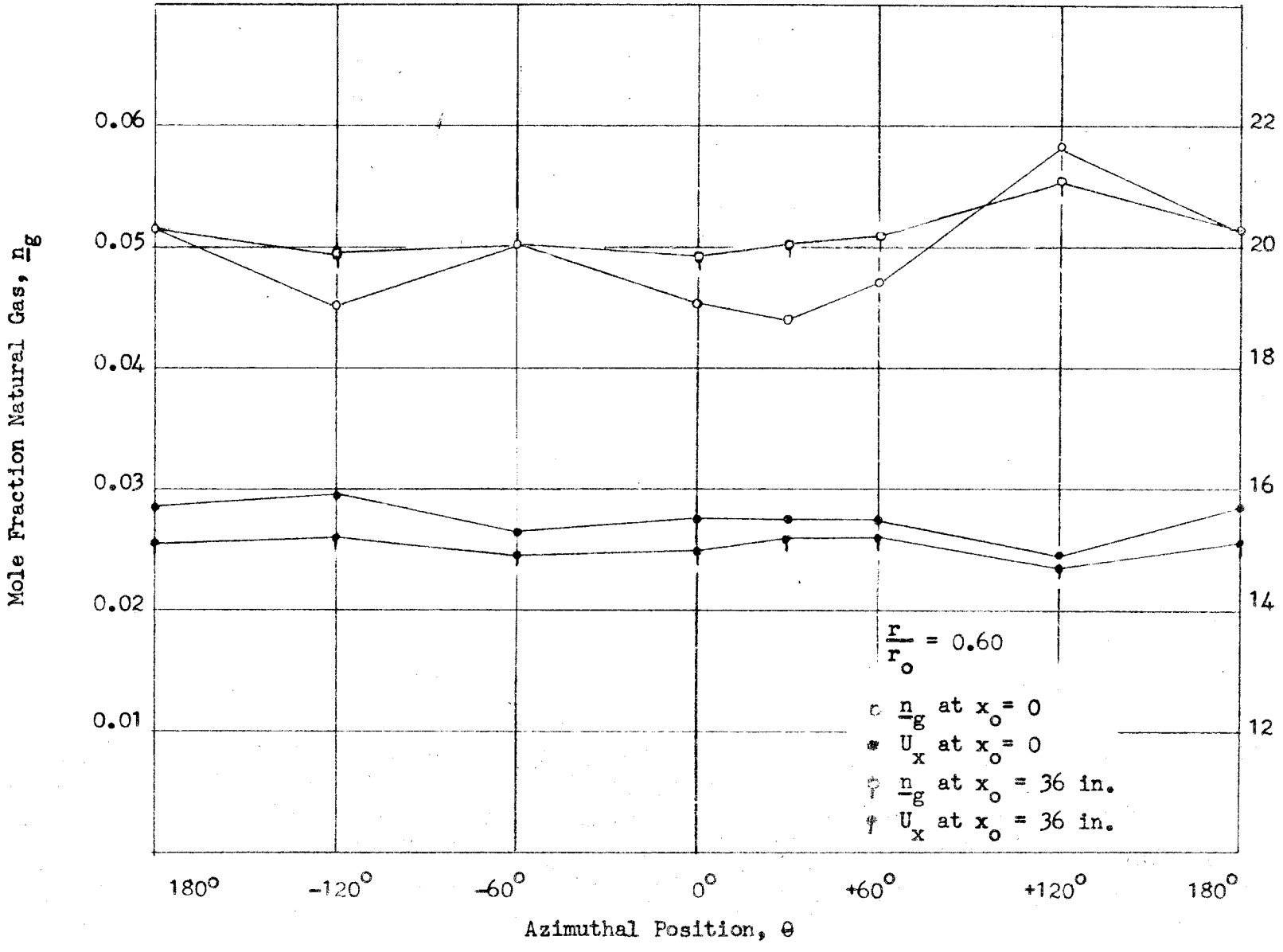

Figure 11 - Variation of Velocity and Composition with Azimuthal Position - Re 45,000.

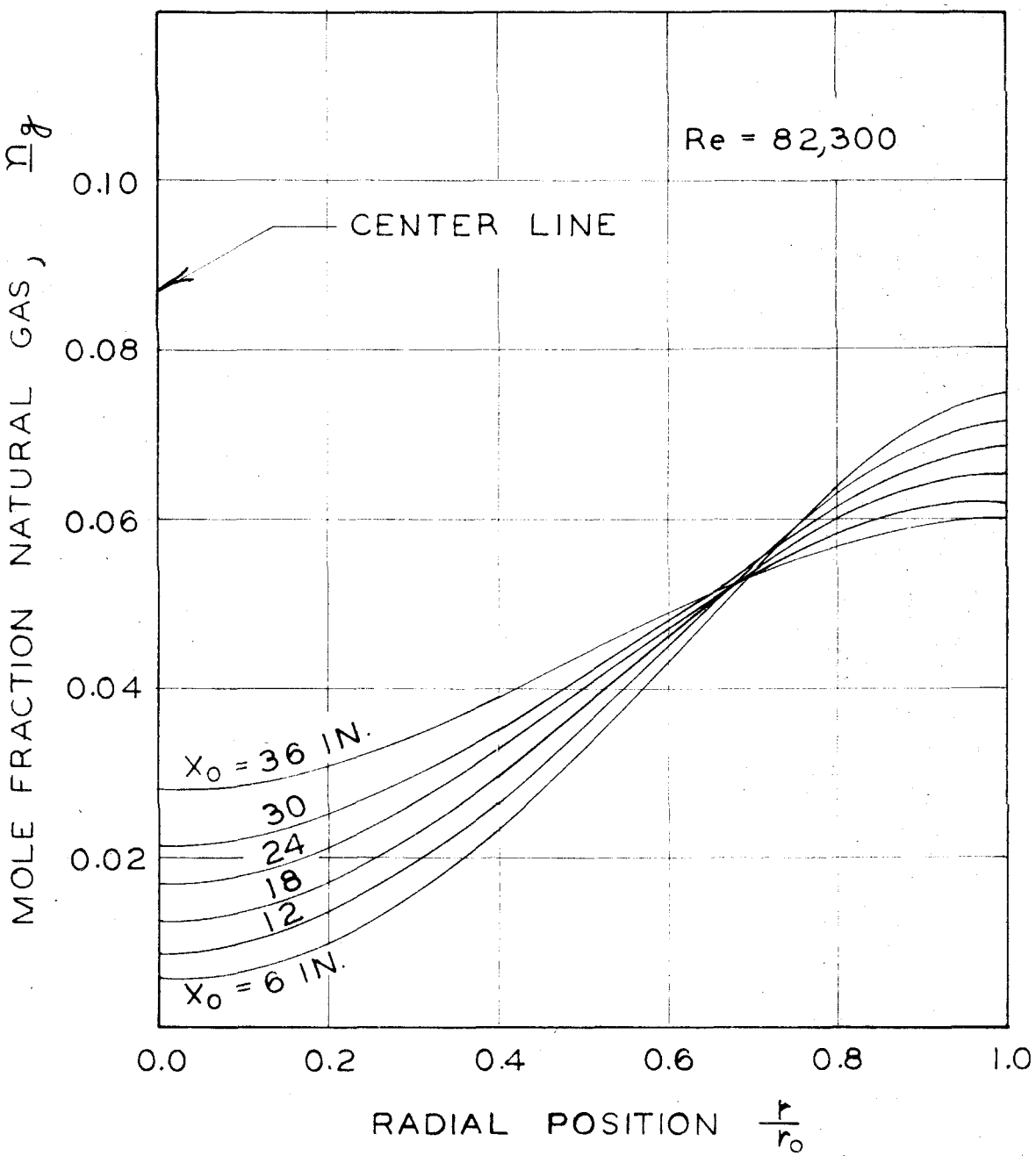

Figure 12 - Composition as a Function of Radial Position - Re 82,300

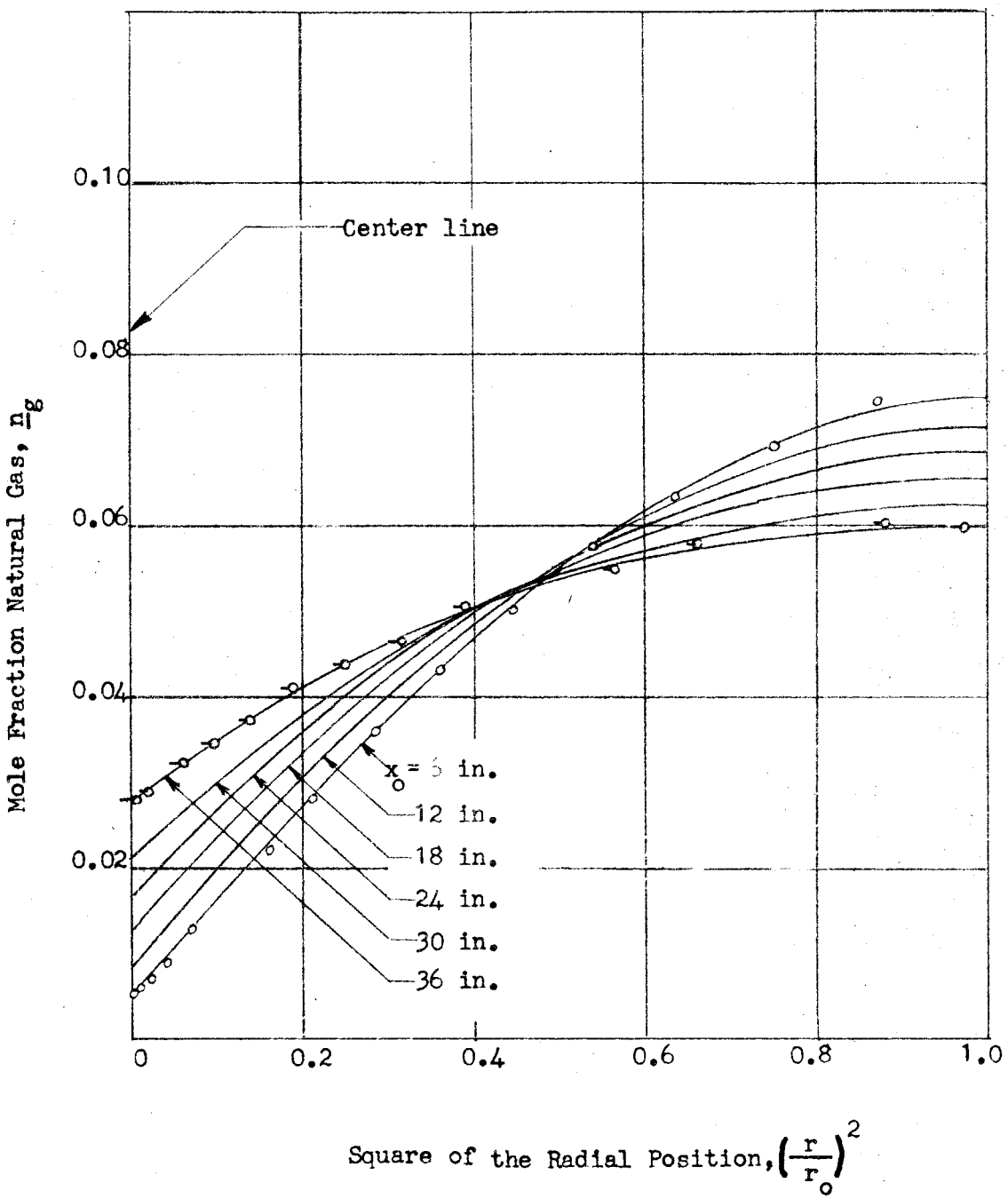

Figure 13 - Composition as a Function of the Square of the Radial Position - Re 82,300.

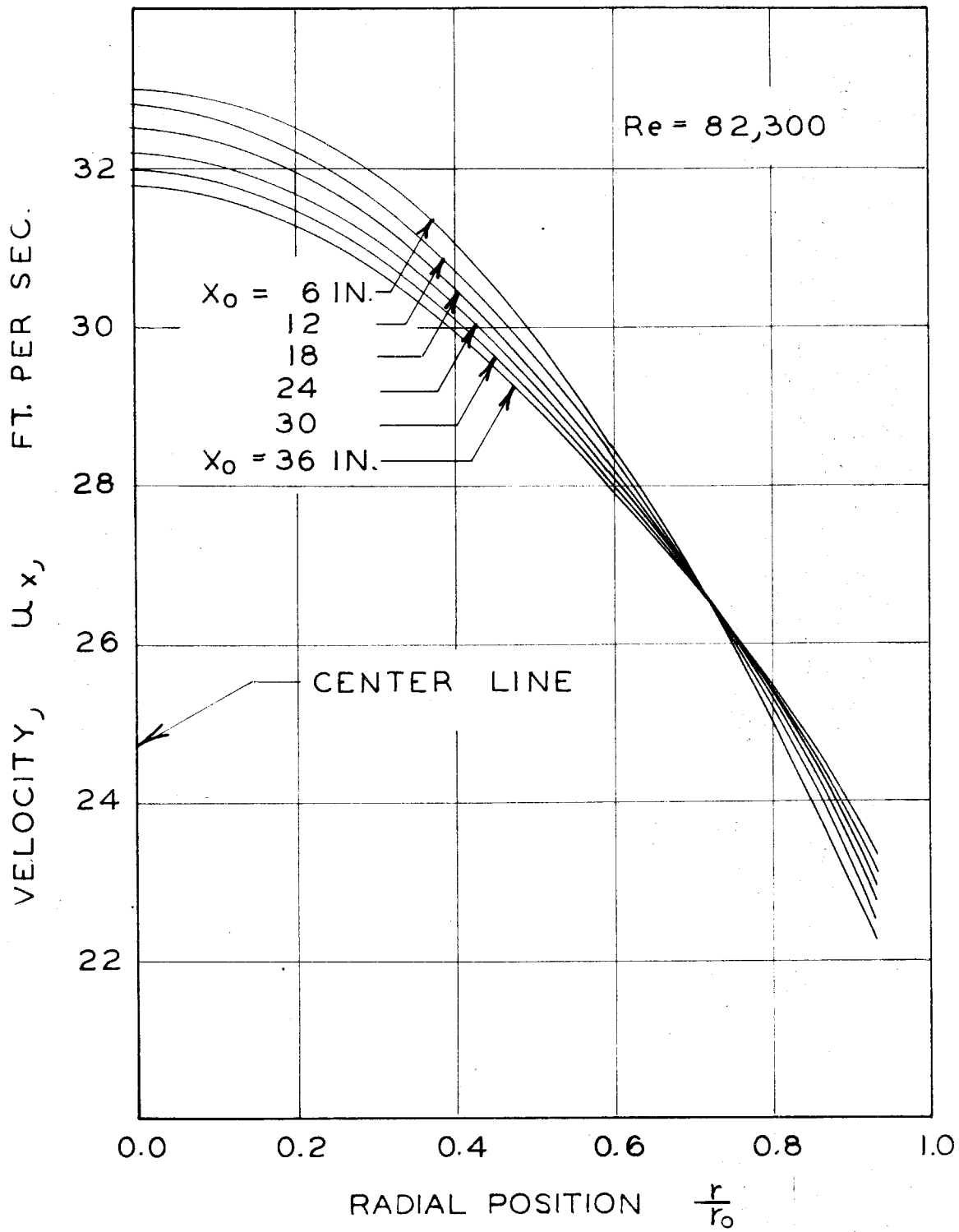

Figure 14 - Velocity as a Function of Radial Position - Re 82,300

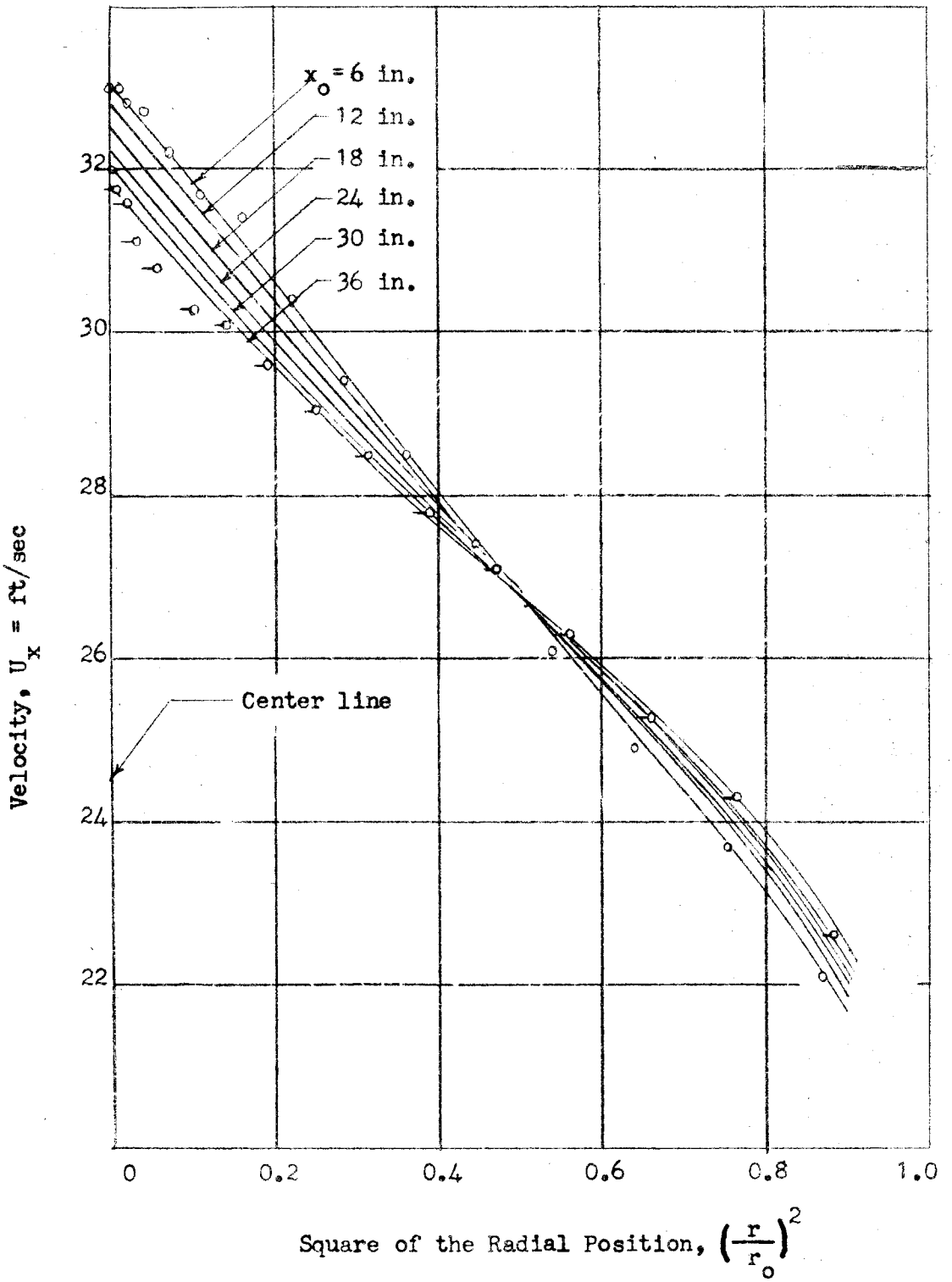

Figure 15 - Velocity as a Function of the Square of the Radial Position - Re 82,300.

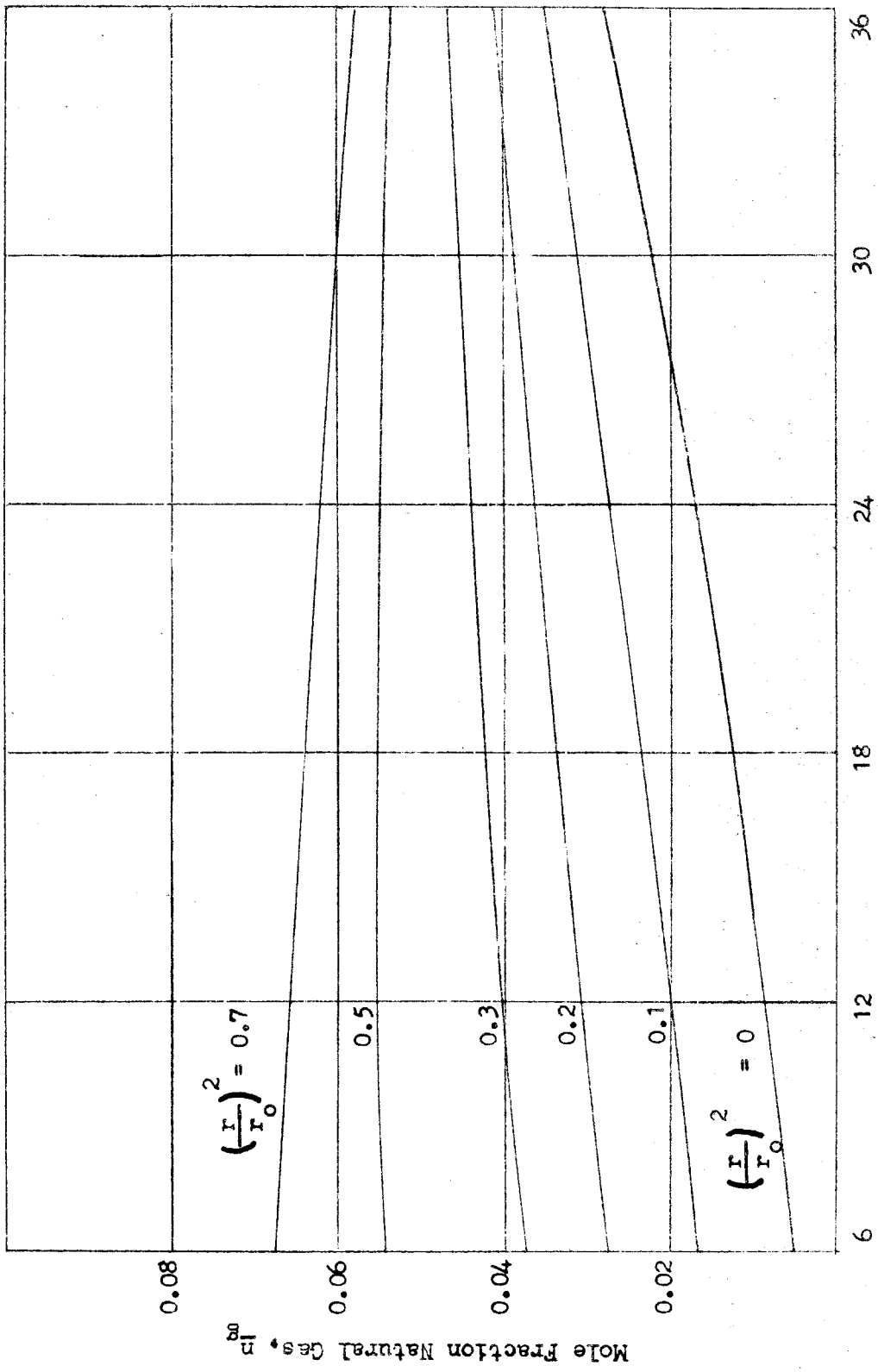

Figure 16 - Composition as a Function of Distance Downstream - Re 82,300.

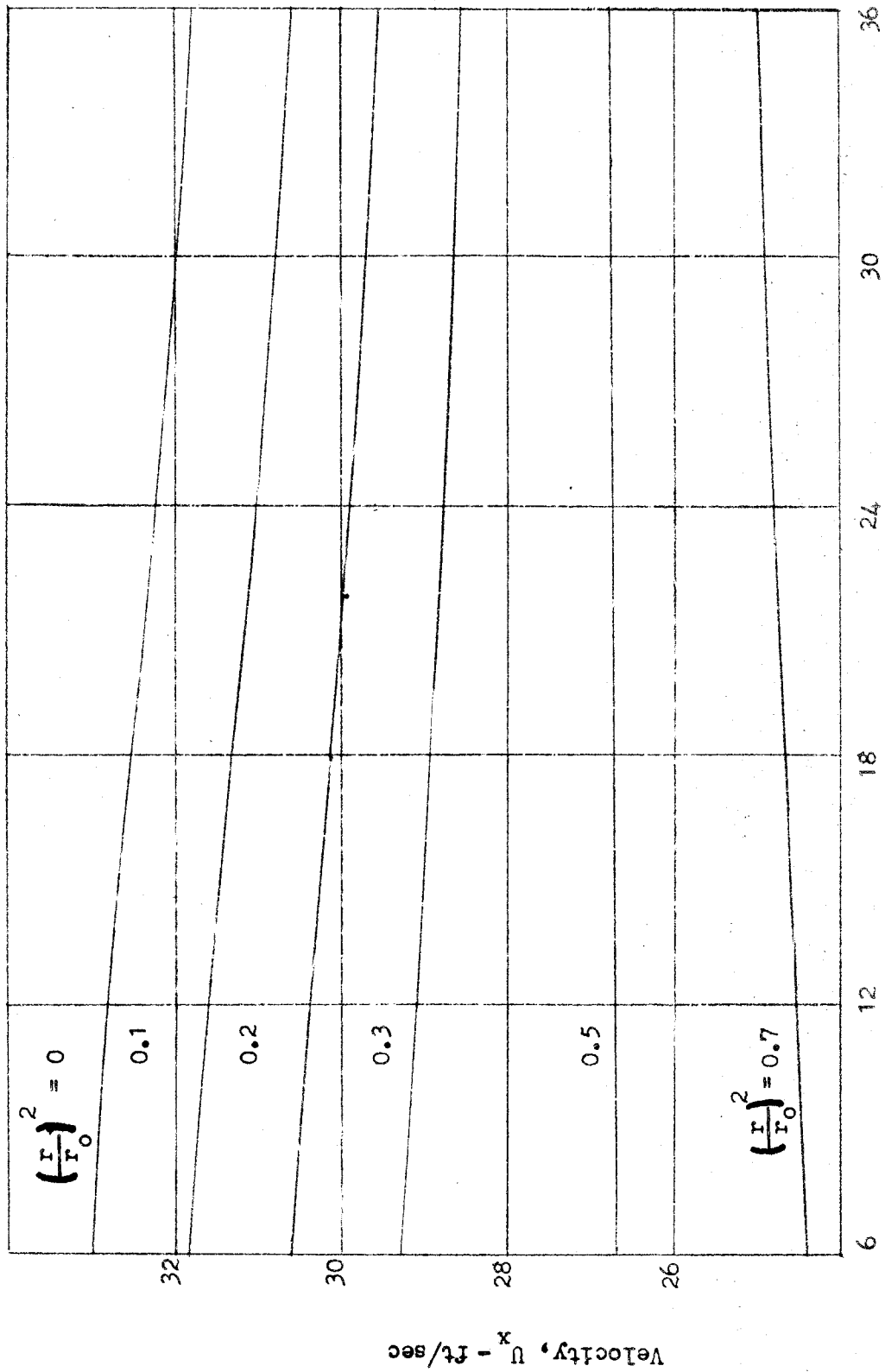

Figure 17 - Velocity as a Function of Distance Downstream - Re 82,300.

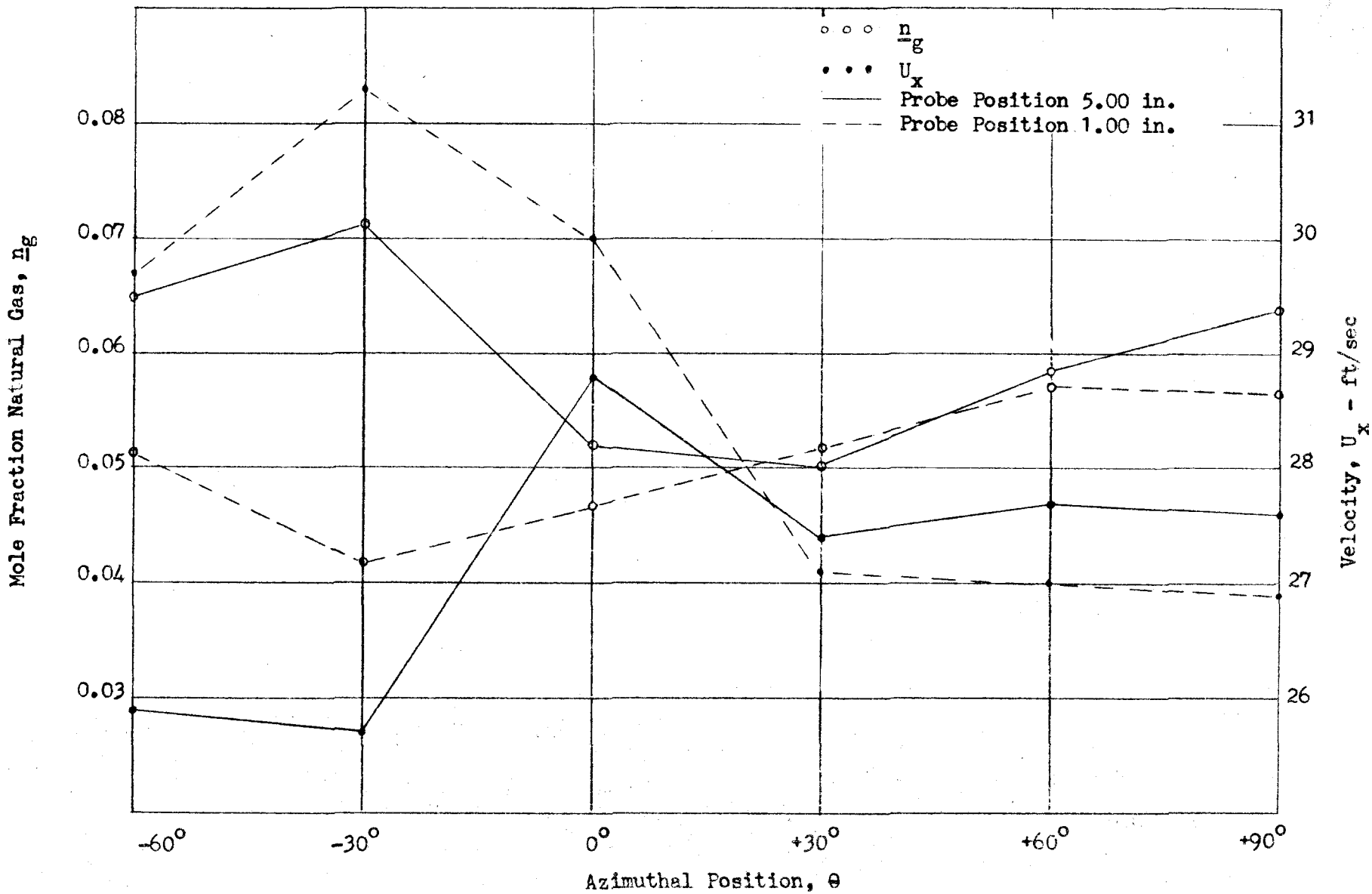

Figure 18 - Variation of Velocity and Composition with Azimuthal Position - Re 82,300 - x_o = 6 in.

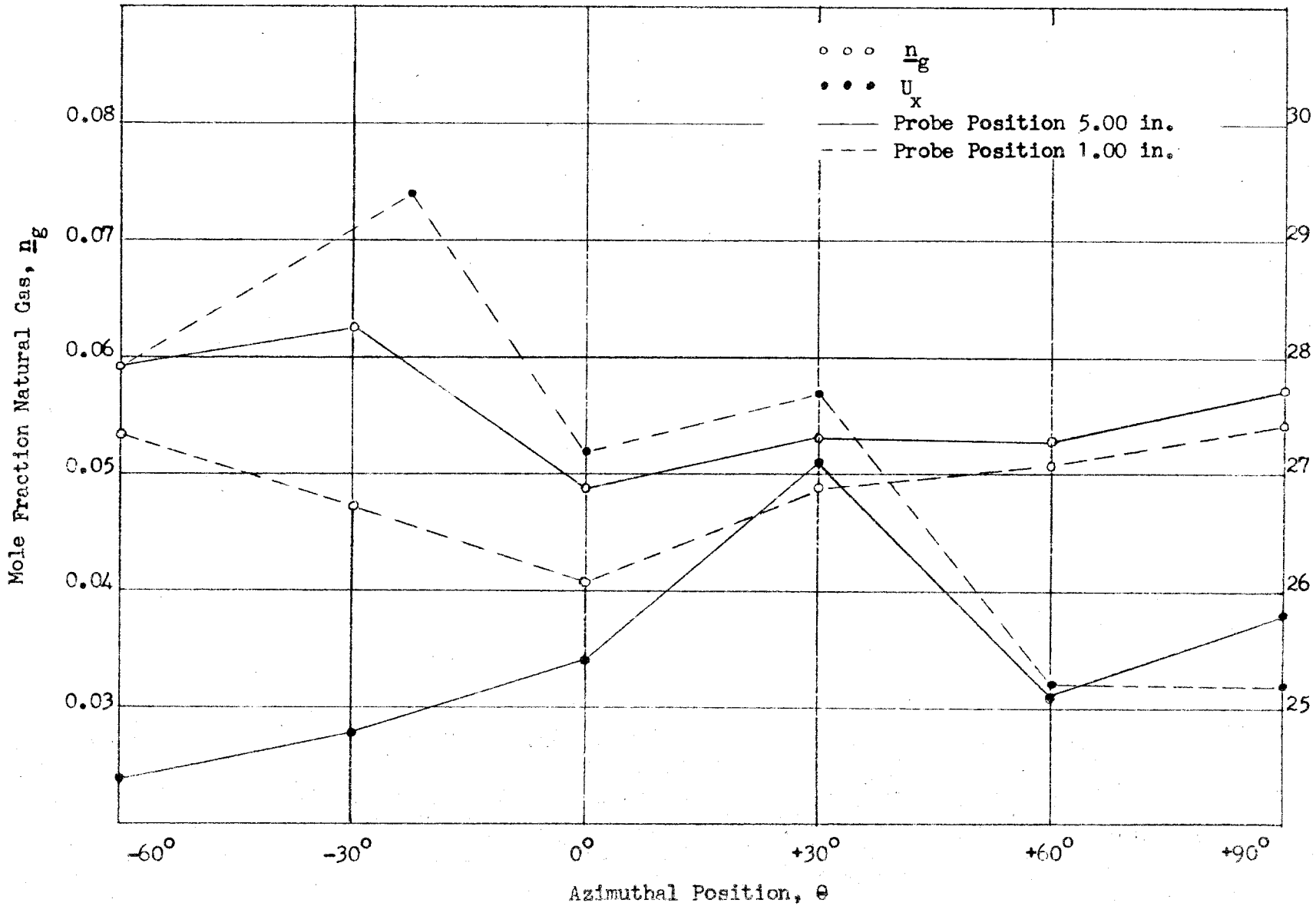

Figure 19 - Variation of Velocity and Composition with Azimuthal Position - Re 82,300 - x_o = 36 in.

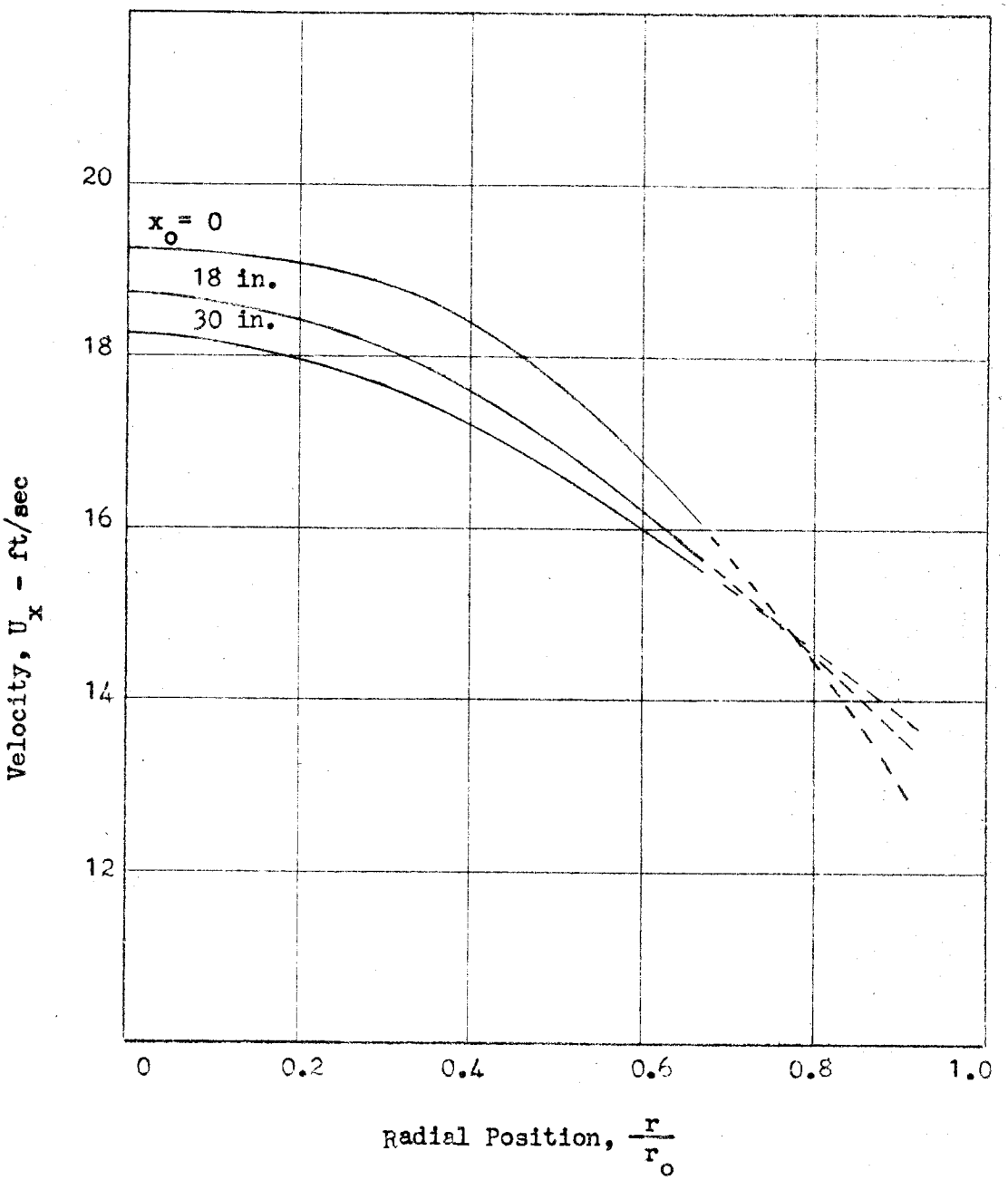

Figure 20 - Change of Velocity with Distance Downstream in the Absence of Diffusion.

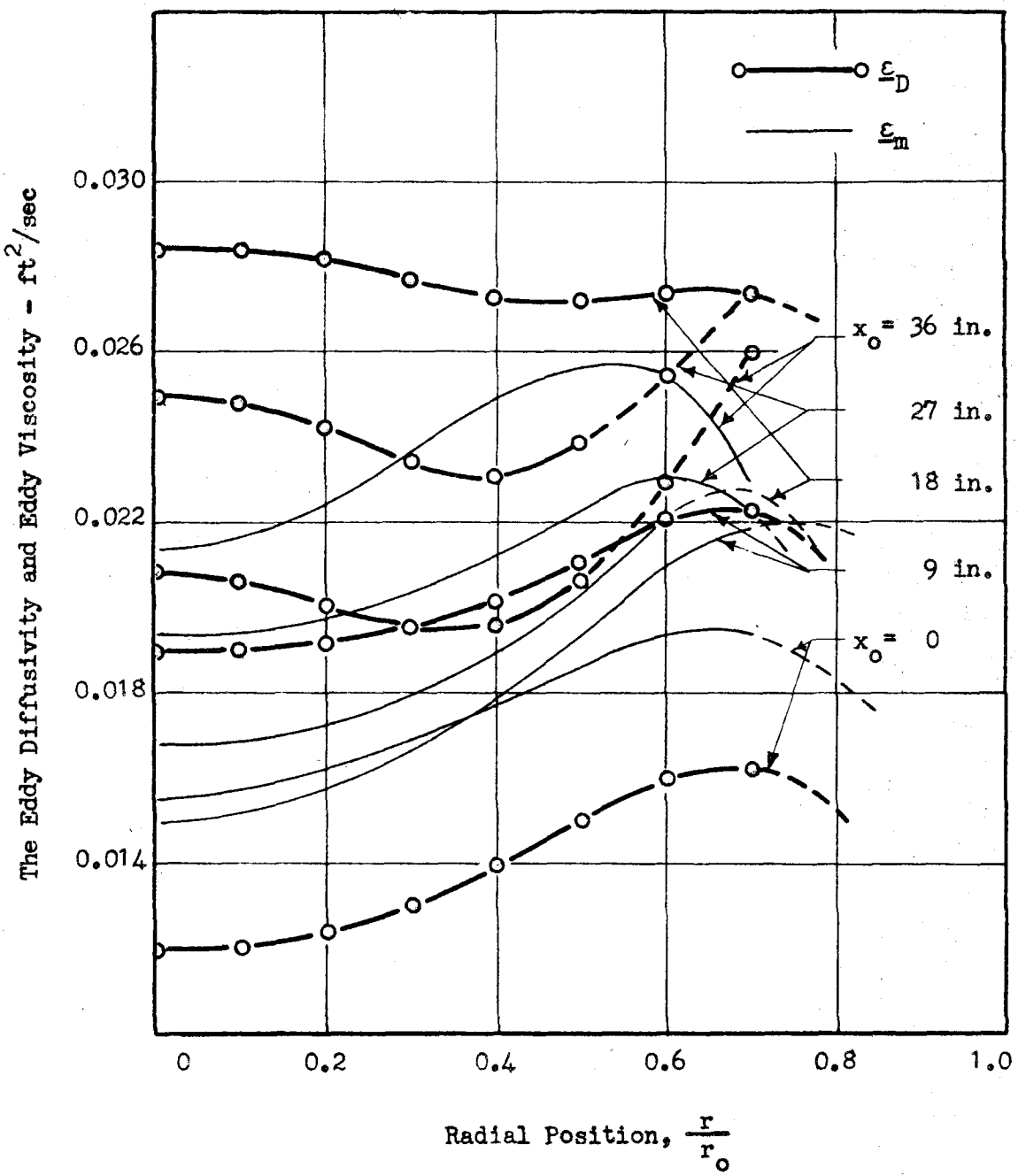

Figure 21 - The Eddy Diffusivity and Eddy Viscosity as Functions of Position - Re 45,000.

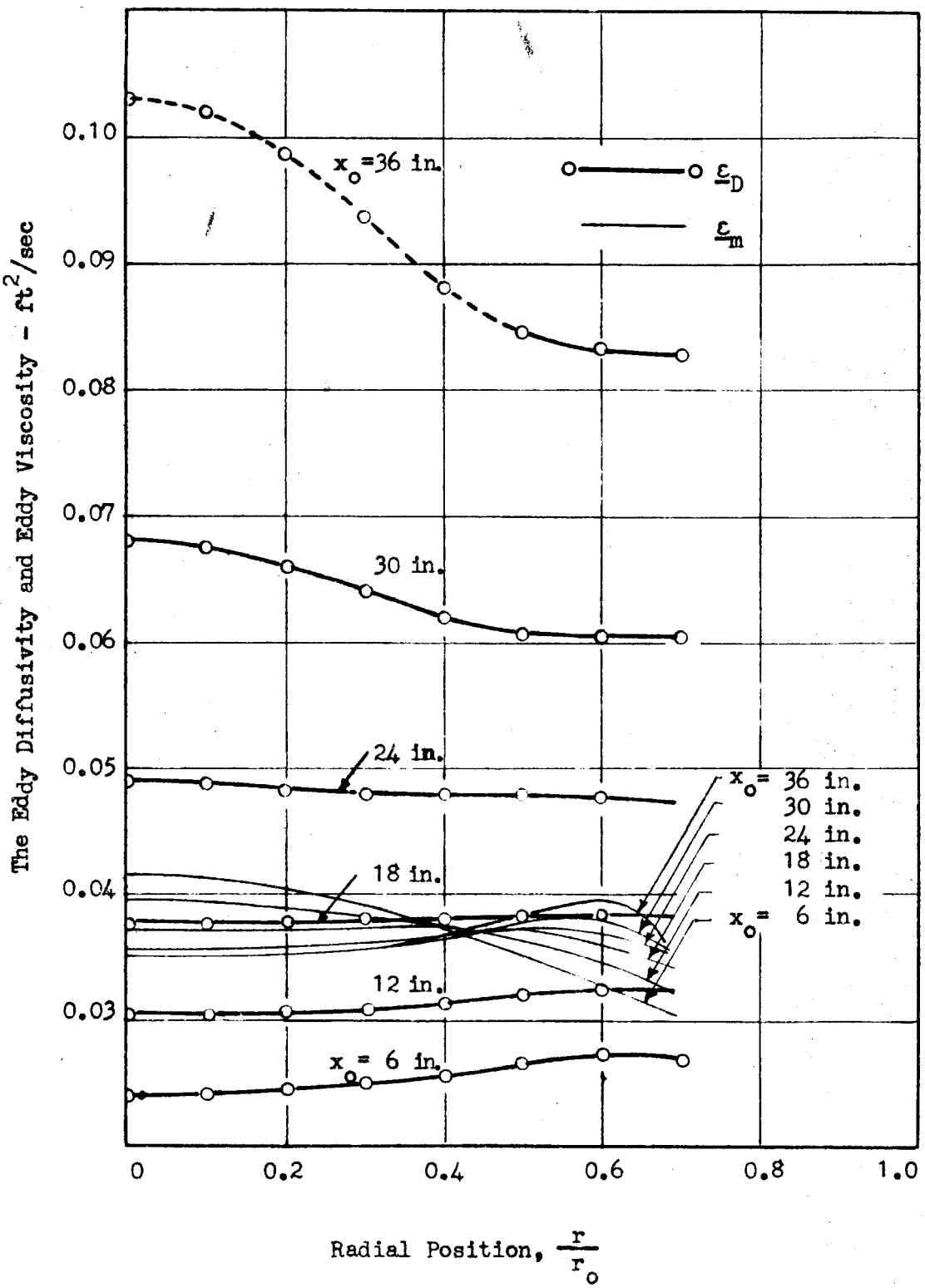

Figure 22 - The Eddy Diffusivity and Eddy Viscosity as Functions of Position _ Re 82,300

APPENDIX

A MICROMANOMETER OF HIGH SENSITIVITY

An extremely sensitive micromanometer was made on the principle first mentioned by Henry[1A] and similar to the tilting micromanometer described by Ower[2A]. In principle the instrument is very simple. The legs of the manometer were connected by a precision bore capillary tube which was horizontal and in which was placed a bubble of air. The movement of the meniscus in one of the manometer legs was thus multiplied by the ratio of areas of the leg and the capillary. As shown in the diagram of Figure 1A, this manometer was built with three sets of legs of different sizes for varying sensitivity. The legs were nominally 1, 2, and 3 in. in diameter. The inner diameter of the capillary was 0.120 in. The lowest sensitivity was 2×10^{-5} in. of manometer fluid, the highest was 2×10^{-6} in. The manometer legs were set in a brass box which was filled with water and insulated with an inch of "styrofoam" on four sides and the bottom. The water was agitated with a stirrer while measurements were being made in order to minimize temperature gradients in the manometer fluid. The position of the bubble was determined with a small microscope attached to a vernier caliper having a precision of 0.001 in. Figure 2A is a picture of the micromanometer and the lower part of the tubes of the gas analysis apparatus.

The micromanometer was calibrated using pure oxygen, nitrogen, and methane in the analysis apparatus described in the text. The movement of the bubble was found to be linear with pressure difference, and the pressure difference observed agreed with the value calculated from the dimensions of the micromanometer and the height of the tubes. The calibration procedure was repeated each day. No change was observed.

The micromanometer is not without its idiosyncrasies, and extreme care must be exercised in using it. In addition to its temperature sensitivity, it registers each slight change in position and hence should be placed on an extremely stable base such as a platform of cinder blocks set on a concrete floor.

The qualities to look for in the choice of a manometer fluid are low viscosity, low volatility, high surface tension and, above all, a liquid which does not dissolve stopcock grease. This rather improbable combination of properties is most nearly met by methyl alcohol. In a glass capillary tube coated with a silicone preparation such as Beckman "Desicote", the wall is not wet by the alcohol and flow past the bubble is negligible.

This micromanometer is preferable to the tilting type primarily because of its much lower cost[2A]. Experience has indicated that drift of the bubble past its initial equilibrium position after a reading is usually traceable to a leaky stopcock or a shift of the base when the drift amounts to more than 0.1 per cent of the reading. Hence, the sensitivity of the instrument is comparable to that of the more

elaborate instruments.

The design of the manometer could be improved in the following ways. Replacing the one millimeter stopcocks with two millimeter cocks, which are less prone to leakage; providing better access to the capillary, since the rate of solution of air in the alcohol requires replacement of the bubble every day or two; providing a pressure range just one factor of ten below that of the standard micromanometer and eliminating the present set of legs which are half way between the upper and lower range of the instrument. Only one large bulb is needed on one side of the capillary, so the three pressure ranges suggested could be obtained with four bulbs.

REFERENCES

1A Henry, A., Compt. Rend., 155, 1078 (1912).

2A Ower, E., Aer. Res. Com., Gr. Br., "Reports and Mem.", No. 1308 (1930).

LIST OF FIGURES

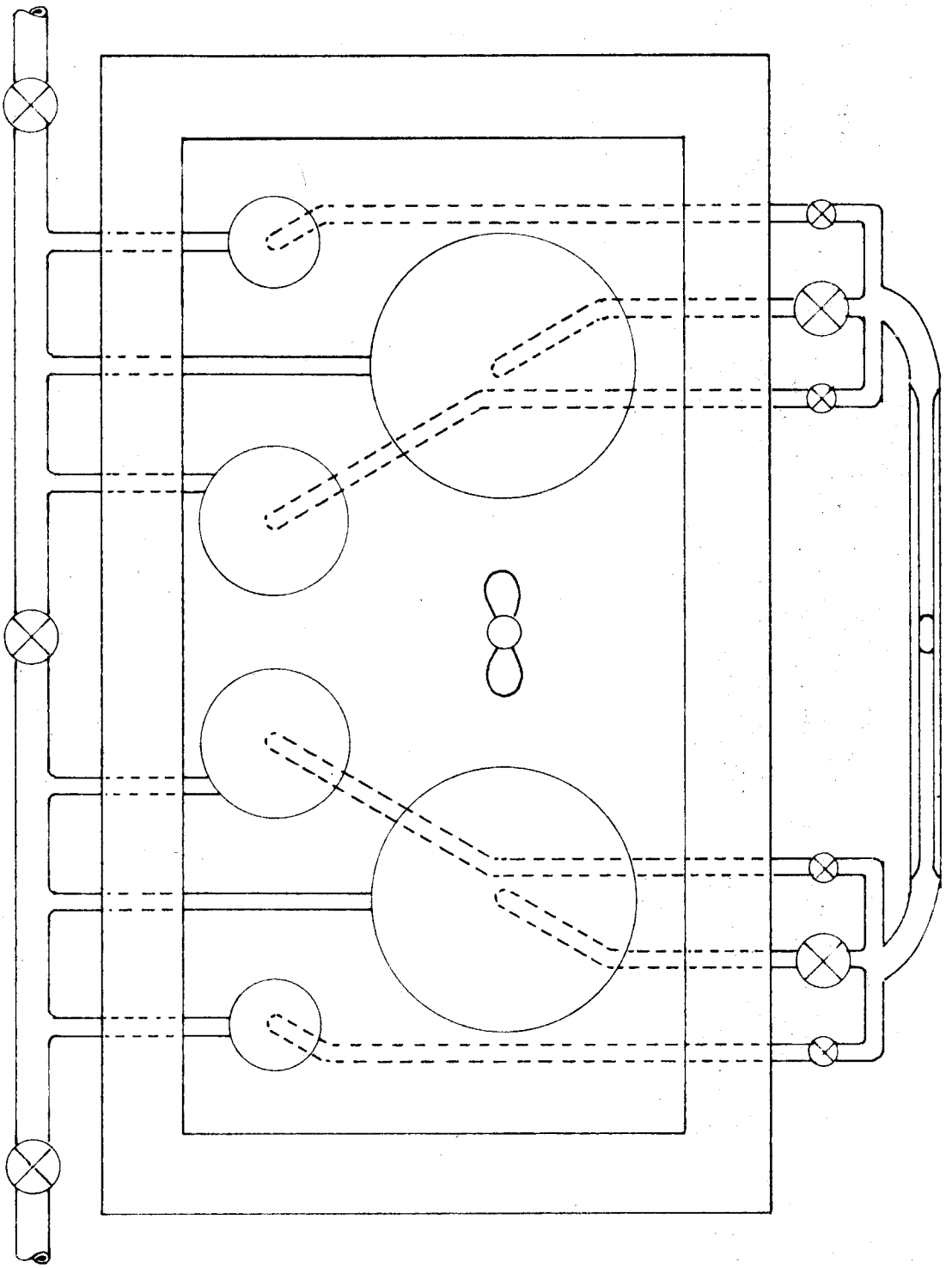

Figure 1A - Diagrammatic Sketch of the High Sensitivity Micromanometer

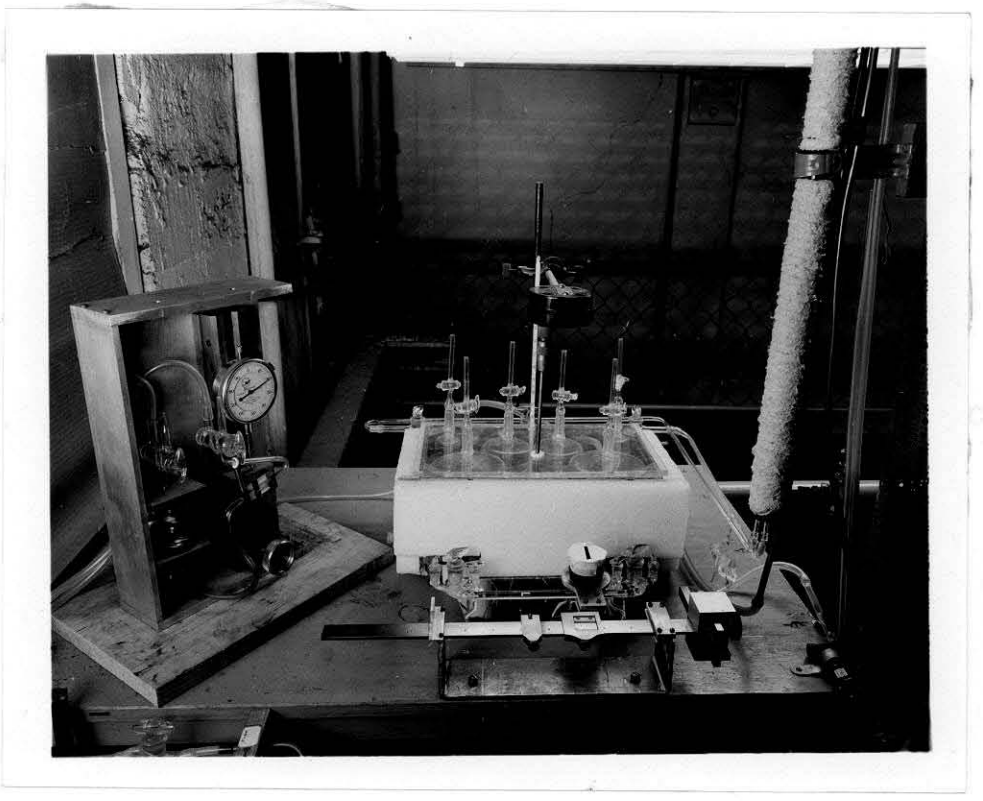

Figure 2A - High Sensitivity Micromanometer and Gas Analysis Apparatus

PART II

A. ABSORPTION OF LIGHT BY THE SYSTEM NITRIC ACID-NITROGEN DIOXIDE-WATER.

B. IONIZATION IN SOLUTIONS OF NITROGEN DIOXIDE IN NITRIC ACID FROM OPTICAL ABSORBANCE MEASUREMENTS.

II A - FOREWORD

The following report was written in conjunction with D.M. Mason and B.H. Sage, and has appeared as Progress Report No. 20-187 of the Jet Propulsion Laboratory of the California Institute of Technology. The work was done under Contract No. DA-04-495-Ord 18, Department of the Army Ordnance Corps.

TABLE OF CONTENTS

LIST OF TABLES

LIST OF FIGURES

ABSTRACT

The optical absorbance of the liquid phase of mixtures of nitric acid, nitrogen dioxide, and water was measured at 32°F at wavelengths of 500 and 425 mμ. At the longer wavelength compositions containing 0.8 or more weight fraction nitric acid were studied. At the shorter wavelength the compositions were limited to a minimum weight fraction nitric acid of 0.93. The results indicate that the absorbance varies linearly with the weight fraction nitrogen dioxide at small concentrations of this component. The optical absorbance appears to be a useful intensive property of the liquid phase to be employed as an aid in determining the composition of the ternary system.*

I. INTRODUCTION

The optical absorbance of the liquid phase of mixtures of nitric acid, nitrogen dioxide, and water is of practical interest in connection with analyses of this system. The presence of nitrogen dioxide is responsible for most of the optical absorbance experienced and thus affords a means of estimating the quantity of nitrogen dioxide in the phase without the need for more complex chemical techniques.

Only limited studies of the optical absorbance of the nitric acid--nitrogen dioxide--water system have been made. Hall and Blacet (Cf. Ref. 1) investigated the absorption spectra of nitrogen dioxide, and Dalmon and Freymann (Cf. Ref. 2), the absorbance of the nitric acid--water system at wavelengths from 950 to 1050 mμ. White (Cf. Ref. 3) employed infrared absorption in determining the composition of commercial samples of fuming nitric acid. Because of the limited background of available experimental data, measurements of the optical absorbance of the nitric acid--nitrogen dioxide--water system were made at 32°F for wavelengths of 500 and 425 mμ. The compositions investigated at 500 mμ contained a maximum of about 0.25 weight fraction of nitrogen dioxide and 0.15 of water. All measurements were carried out at atmospheric pressure.

At the shorter wavelength of 425 mμ, the compositions were limited to a maximum of 0.008 weight fraction of nitrogen dioxide and 0.01 weight fraction of water. This narrow range of compositions was investigated in sufficient detail to give insight into the ionization of nitrogen dioxide in substantially pure nitric acid and to ascertain the extent of ionization of nitric acid.

At 500 mμ for mixtures containing less than 0.03 weight fraction of water it is possible to employ the optical absorbance and the electrical conductance as means of determining the relative quantities of water and nitrogen dioxide in commercial samples of nitric acid. At higher weight fractions of water the use of a dilution technique (Cf. Ref. 4) appears desirable.

*The term nitrogen dioxide is used to designate equilibrium mixtures of nitrogen dioxide and nitrogen tetroxide.

II. DESCRIPTION OF EQUIPMENT AND METHODS

The optical absorbance was measured with a commercial spectrophotometer (Cf. Ref. 5) which was modified to permit the transmission cell to be maintained at 32°F by immersion in an ice bath. The relative optical absorbance (or, for brevity, the absorbance) is defined as -log (I/I_0), where I_0 is the intensity of light transmitted by the reference blank of air, and I is the intensity transmitted by the sample. Figure 1 is a photograph of the transmission cell and stirrer. Both the stirrer and the hypodermic syringe for adding nitrogen dioxide entered the cell through holes in the cap. Inside the stirrer was a three-junction, copper-constantan thermocouple for measuring the temperature of the contents of the transmission cell. Potentials of the thermocouple were determined by means of a potentiometer with a sensitivity of 10 μv. The temperature of the cell was 32°F with a standard deviation of 0.1°F.

Figure 2 is a photograph of the hypodermic syringe used for adding nitrogen dioxide. The position relative to the cylinder was determined by means of a micrometer screw. Jacket temperature was maintained by circulation of alcohol at a temperature within 0.1°F of 32°F. Calibration of the injector indicated that the nitrogen dioxide was added with an uncertainty less than 0.005 gram, which corresponded to 0.5 per cent of the weight of nitrogen dioxide.

In studies of the effect of nitrogen dioxide when present in small weight fractions, a mixture of nitric acid and nitrogen dioxide was employed in the glass injector. This mixture containing 0.03 weight fraction of nitrogen dioxide was used to introduce the requisite amount of nitrogen dioxide with an error of less than 1 per cent of the quantity added.

Figure 3 shows the Corex transmission cell in position on the spectrophotometer. The housing for supporting the stirrer and syringe is not included.

The absorbance of mixtures of nitric acid and nitrogen dioxide was studied semiquantitatively as a function of wavelength to ascertain appropriate frequencies for detailed investigation. These exploratory results are shown in Figure 4 and should be considered only as indicative of the trends in behavior. From these data wavelengths of 425 and 500 mμ were selected as allowing the full range of the spectrophotometer to be used for the compositions of systems to be studied. At these wavelengths the absorbance could be reproduced with the spectrophotometer with an error of 0.25 per cent. Duplicate measurements at a wavelength of 500 mμ indicated a reproducibility of results within 0.001 weight fraction of the components for the range of compositions investigated.

III. MATERIALS

The nitric acid was prepared by vacuum distillation at a temperature of approximately 100°F from a mixture of pure potassium nitrate and concentrated sulfuric acid in accordance with the procedure described by Giauque (Cf. Ref. 6). Titration of a diluted sample with sodium hydroxide indicated that the sample contained less than 0.001 weight fraction of material other than nitric acid.

Nitrogen dioxide was obtained from the Allied Chemical and Dye Corporation and was fractionated in a column provided with sixteen glass plates. The central 70 per cent portion of the overhead was dried over phosphorous pentoxide. Samples prepared in a similar fashion from the same stock yielded less than 0.2-psi change in vapor pressure with a change in quality from 0.02 to 0.5 at a temperature of 160°F. The water employed in this study was de-aerated distilled water which was not otherwise especially purified.

IV. RESULTS

The experimental measurements of absorbance at 500 mμ and 32°F for series *A* through *J* are recorded in Table I and those at 425 mμ for series *A* through *F* in Table II. The data were smoothed with respect to composition. Weight fractions of nitrogen dioxide for even values of absorbance and weight fractions of water are recorded in Table III for a wavelength of 500 mμ and in Table IV for a wavelength of 425 mμ. A portion of the ternary-composition diagram for the nitric acid--nitrogen dioxide--water system is shown in Figure 5. It is apparent that the variation in absorbance with composition at 500 mμ is relatively regular, and nearly all of the absorbance results from the presence of nitrogen dioxide in the liquid phase. This behavior is indicated by the similar effect upon the absorbance of a change in the weight fraction of nitrogen dioxide for a number of different values of the weight fraction of water in the phase, as shown in Figure 6. However, a linear change in absorbance with weight fraction of nitrogen dioxide was not realized. The behavior is more complex at compositions near the nitric acid--nitrogen dioxide system where the absorbance for small weight fractions of nitrogen dioxide reaches a minimum as the quantity of water is increased. Such behavior may be explained by the predominance of different ionic species (Cf. Refs. 7 and 8) at small and large weight fractions of water.

The corresponding behavior at a wavelength of 425 mμ is shown in Figure 7. These data, which were based upon the measurements recorded in Table II, are limited to compositions containing less than 0.01 weight fraction of nitrogen dioxide. The behavior is similar to that found with the longer wavelengths except that the variation of the absorbance with composition is more pronounced. Such behavior is also evident from a consideration of Figure 4.

A limited number of measurements at 425 mμ of the absorbance of the nitric acid--nitrogen dioxide--potassium nitrate system were made, and the experimental data for series *A* through *C* are recorded in Table V. The smoothed data are presented in Table VI. The smoothed results for this ternary system are shown in Figure 8. An increase in the weight fraction of potassium nitrate increased the absorbance at a constant weight fraction of nitrogen dioxide. In the range of concentrations shown, there is a linear relationship of absorbance to the weight fraction of nitrogen dioxide. The information upon the nitric acid--nitrogen dioxide--potassium nitrate system is limited and was obtained primarily to ascertain the comparative effects of water and potassium nitrate upon the change in absorbance with increasing amounts of nitrogen dioxide.

V. DETERMINATION OF COMPOSITION

Dilution techniques have been employed in determining the composition of the nitric acid--nitrogen dioxide--water system from conductivity measurements (Cf. Ref. 4). The combination of the absorbance and the electrical conductivity affords a means of establishing the composition without the need of dilution except for ranges of composition where the same values of absorbance and electrical conductance are obtained for two compositions. The interrelation of electrical conductance (Cf. Ref. 9) and absorbance at a wavelength of 500 mμ is shown in Figure 9. As a result of the double intersections of lines of constant absorbance and constant electrical conductance, dilution techniques must be employed for that range of composition where double intersections occur. The relatively simple relationship of absorbance to the weight fraction of nitrogen dioxide makes this intensive property particularly useful in determining the weight fraction of this variable in fuming nitric acids. The details of the methods of calculating

compositions from dilution techniques are simple (Cf. Ref. 4), and an example is presented in the Appendix.

VI. CONCLUSIONS

The absorbance of light at a wavelength of 500 mμ provides a simple method of analysis of commercial fuming nitric acids which is particularly effective in determining the weight fraction of nitrogen dioxide. The absorbance yields a somewhat simpler relationship to composition than was obtained for the electrical conductance, and for this reason it is more useful in determining by dilution techniques the weight fraction of water and nitrogen dioxide in the sample. The combination of optical absorbance and electrical conductivity affords a convenient means of direct analysis of fuming nitric acid containing less than 0.03 weight fraction water since the same values of absorbance and conductivity are not found for acids of two different compositions in this range of weight fractions of water.

TABLE I

EXPERIMENTAL MEASUREMENTS OF ABSORBANCE[a] AT 500 mμ FOR THE NITRIC ACID--NITROGEN DIOXIDE--WATER SYSTEM AT 32°F

Series A[b]		Series B[b]		Series C			Series D		
Nitrogen Dioxide (wt frac)	Absorbance	Nitrogen Dioxide (wt frac)	Absorbance	Nitrogen Dioxide (wt frac)	Water (wt frac)	Absorbance	Nitrogen Dioxide (wt frac)	Water (wt frac)	Absorbance
0	0	0	0	0	0.03165	0	0	0.03128	0
0.01997	0.064	0.01776	0.054	0.01922	0.03105	0.049	0.01736	0.03073	0.050
0.03916	0.133	0.03491	0.116	0.03772	0.03046	0.122	0.03412	0.03021	0.116
0.05761	0.215	0.05147	0.184	0.05553	0.02990	0.201	0.05033	0.02970	0.191
0.07538	0.294	0.06747	0.250	0.07271	0.02935	0.290	0.06600	0.02921	0.269
0.09259	0.375	0.08295	0.324	0.08927	0.02883	0.381	0.08117	0.02874	0.346
0.10896	0.460	0.09791	0.402	0.10525	0.02832	0.481	0.09585	0.02828	0.435
0.12485	0.551	0.11239	0.480	0.12067	0.02783	0.584	0.11006	0.02783	0.518
0.14018	0.643	0.12642	0.563	0.13557	0.02736	0.670	0.12383	0.02740	0.609
0.15500	0.731	0.14001	0.642	0.14998	0.02691	0.768	0.13719	0.02699	0.700
0.16930	0.828	0.15319	0.732	0.16391	0.02647	0.865	0.15015	0.02658	0.795
0.18313	0.930	0.16596	0.815	0.17739	0.02604	0.970	0.16272	0.02619	0.885
0.19651	1.041	0.17836	0.900	0.19555	0.02546	1.110	0.17492	0.02581	0.980
0.20945	1.122	0.19039	0.990	0.20309	0.02523	1.171	0.18678	0.02543	1.082
0.22199	1.225	0.20208	1.081	0.21535	0.02484	1.276	0.19829	0.02507	1.182
0.23413	1.327	0.21343	1.175	0.22723	0.02446	1.410	0.20949	0.02472	1.280
0.24590	1.430	0.22447	1.270	0.23877	0.02410	1.517	0.22038	0.02438	1.384
0.25732	1.535	0.23519	1.363	0.24959	0.02374	1.632	0.23097	0.02405	1.485
0.26839	1.643	0.24563	1.458	0.26083	0.02340	1.743	0.24128	0.02373	1.590
0.27914	1.755	0.25579	1.560	0.27139	0.02306	1.858	0.25132	0.02342	1.690
0.28958	1.868	0.26567	1.652	0.28165	0.02274	1.970	0.26109	0.02311	1.790
0.29971	1.980	0.27531	1.750						
		0.28467	1.850						

[a]Absorbance is defined as $-\log (I/I_0)$.

[b]These mixtures contained only nitric acid and nitrogen dioxide.

TABLE I (Cont'd)

Series *E*			Series *F*			Series *G*		
Nitrogen Dioxide (wt frac)	Water (wt frac)	Absorbance	Nitrogen Dioxide (wt frac)	Water (wt frac)	Absorbance	Nitrogen Dioxide (wt frac)	Water (wt frac)	Absorbance
0	0.04962	0	0	0.04717	0	0	0.07018	0
0.01878	0.04869	0.054	0.01708	0.04637	0.048	0.01757	0.06894	0.061
0.03676	0.04779	0.127	0.03359	0.04559	0.112	0.03453	0.06775	0.130
0.05431	0.04692	0.214	0.04955	0.04483	0.192	0.05092	0.06660	0.218
0.07113	0.04609	0.312	0.06500	0.04411	0.278	0.06677	0.06549	0.310
0.08737	0.04528	0.409	0.07996	0.04340	0.365	0.08210	0.06442	0.402
0.10304	0.04451	0.508	0.09443	0.04273	0.451	0.09693	0.06337	0.500
0.11818	0.04376	0.613	0.10846	0.04206	0.541	0.11128	0.06237	0.608
0.13282	0.04303	0.720	0.12206	0.04141	0.633	0.12519	0.06139	0.708
0.14699	0.04233	0.827	0.13526	0.04079	0.732	0.13867	0.06045	0.808
0.16069	0.04165	0.940	0.14806	0.04019	0.830	0.15174	0.05953	0.918
0.17397	0.04099	1.048	0.16049	0.03960	0.935	0.16442	0.05864	1.025
0.18683	0.04035	1.162	0.17257	0.03903	1.038	0.17673	0.05777	1.136
0.19929	0.03973	1.270	0.18430	0.03848	1.140	0.18868	0.05694	1.245
0.21138	0.03913	1.385	0.19570	0.03794	1.238	0.20028	0.05612	1.333
0.22311	0.03855	1.500	0.20678	0.03742	1.335	0.20933	0.05549	1.441
0.23450	0.03798	1.619	0.21758	0.03691	1.442	0.21818	0.05487	1.530
0.24556	0.03743	1.750	0.22807	0.03641	1.560	0.22896	0.05411	1.645
0.25630	0.03690	1.842	0.23829	0.03593	1.652	0.23945	0.05337	1.765
0.26674	0.03638	1.961	0.24824	0.03546	1.760	0.24966	0.05266	1.878
			0.25794	0.03500	1.870	0.25960	0.05196	1.970

TABLE I (Cont'd)

Series *H*			Series *I*			Series *J*		
Nitrogen Dioxide (wt frac)	Water (wt frac)	Absorbance	Nitrogen Dioxide (wt frac)	Water (wt frac)	Absorbance	Nitrogen Dioxide (wt frac)	Water (wt frac)	Absorbance
0	0.09961	0	0	0.09974	0	0	0.15118	0
0.01953	0.09809	0.131	0.01619	0.09813	0.076	0.01650	0.14860	0.114
0.03830	0.09621	0.191	0.03187	0.09657	0.160	0.03248	0.14627	0.220
0.05638	0.09440	0.295	0.04706	0.09505	0.241	0.04794	0.14393	0.332
0.07379	0.09266	0.406	0.06178	0.09358	0.336	0.06291	0.14167	0.438
0.09058	0.09099	0.522	0.07606	0.09216	0.431	0.07743	0.13947	0.542
0.10675	0.08936	0.643	0.08990	0.09708	0.529	0.09149	0.13735	0.658
0.12237	0.08780	0.763	0.10333	0.08944	0.628	0.10514	0.13529	0.768
0.13744	0.08629	0.893	0.11638	0.08814	0.725	0.11838	0.13328	0.880
0.15202	0.08483	1.025	0.12905	0.08687	0.822	0.13124	0.13134	0.989
0.16610	0.08342	1.158	0.14136	0.08564	0.935	0.14372	0.12945	1.102
0.17972	0.08206	1.297	0.15333	0.08445	1.038	0.15585	0.12762	1.213
0.19291	0.08074	1.433	0.16497	0.08329	1.144	0.16765	0.12584	1.316
0.20568	0.07946	1.562	0.17629	0.08216	1.248	0.17912	0.12410	1.450
0.21805	0.07823	1.683	0.18731	0.08106	1.351	0.19027	0.12242	1.530
0.23006	0.07703	1.805	0.19804	0.07999	1.450	0.20112	0.12077	1.610
0.24167	0.07586	1.940	0.20850	0.07895	1.550	0.21170	0.11918	1.710
0.25296	0.07473	2.07	0.21868	0.07793	1.652	0.22199	0.11762	1.808
			0.22860	0.07694	1.755	0.23202	0.11610	1.913
			0.23827	0.07598	1.850	0.24180	0.11462	2.015

~~Page 7~~

TABLE II

EXPERIMENTAL MEASUREMENTS OF ABSORBANCE[a] AT 425 mμ FOR THE NITRIC ACID--NITROGEN DIOXIDE--WATER SYSTEM AT 32°F

Series A[b]		Series B[b]		Series C[b]		Series D		
Nitrogen Dioxide (wt frac)	Absorbance	Nitrogen Dioxide (wt frac)	Absorbance	Nitrogen Dioxide (wt frac)	Absorbance	Nitrogen Dioxide (wt frac)	Water (wt frac)	Absorbance
0	0	0	0	0	0	0	0.00500	0
0.000486	0.105	0.000444	0.094	0.000432	0.083	0.00043	0.00491	0.084
0.000952	0.202	0.000871	0.183	0.000848	0.172	0.00085	0.00481	0.163
0.001402	0.298	0.001282	0.270	0.001249	0.255	0.00125	0.00473	0.239
0.001835	0.392	0.001679	0.359	0.001635	0.340	0.00164	0.00464	0.311
0.002252	0.487	0.002061	0.440	0.002009	0.420	0.00201	0.00456	0.380
0.002655	0.580	0.002430	0.520	0.002370	0.500	0.00237	0.00448	0.448
0.002983	0.650	0.002786	0.600	0.002718	0.580	0.00272	0.00440	0.513
0.003419	0.770	0.003131	0.674	0.003055	0.652	0.00306	0.00433	0.579
0.003783	0.840	0.003463	0.743	0.003382	0.725	0.00338	0.00426	0.640
0.004133	0.900	0.003785	0.815	0.003697	0.797	0.00370	0.00419	0.705
0.004473	0.970	0.004097	0.885	0.004003	0.860	0.00400	0.00412	0.763
0.004802	1.045	0.004399	0.950	0.004300	0.922	0.00430	0.00406	0.820
0.005120	1.115	0.004691	1.017	0.004587	0.985	0.00486	0.00394	0.940
0.005429	1.185	0.004975	1.077	0.004866	1.045	0.00539	0.00383	1.045
0.005728	1.260	0.005516	1.190	0.005400	1.165	0.00589	0.00372	1.150
0.006019	1.330	0.006027	1.295	0.005903	1.275	0.00636	0.00361	1.250
0.006300	1.395	0.006509	1.410	0.006378	1.380	0.00681	0.00351	1.340
0.006574	1.440	0.006964	1.515	0.006828	1.490	0.00723	0.00342	1.425
0.007097	1.570					0.00762	0.00333	1.500
0.007593	1.680							

[a] Absorbance is defined as $-\log (I/I_0)$.

[b] These mixtures contained only nitric acid and nitrogen dioxide.

TABLE II (Cont'd)

Series *E*			Series *F*		
Nitrogen Dioxide (wt frac)	Water (wt frac)	Absorbance	Nitrogen Dioxide (wt frac)	Water (wt frac)	Absorbance
0	0.009736	0	0	0.009741	0
0.000458	0.009558	0.073	0.000426	0.009563	0.065
0.000900	0.009386	0.149	0.000836	0.009390	0.126
0.001327	0.009228	0.220	0.001231	0.009224	0.193
0.001739	0.009061	0.295	0.001614	0.009064	0.255
0.002136	0.008907	0.362	0.001983	0.008909	0.334
0.002520	0.008758	0.430	0.002340	0.008759	0.395
0.002892	0.008614	0.497	0.002685	0.008614	0.453
0.003252	0.008474	0.565	0.003018	0.008474	0.519
0.003600	0.008339	0.628	0.003341	0.008338	0.575
0.003945	0.008208	0.691	0.003654	0.008207	0.632
0.004264	0.008081	0.755	0.003957	0.008080	0.690
0.004581	0.007959	0.815	0.004251	0.007956	0.743
0.004888	0.007839	0.880	0.004536	0.007837	0.797
0.005187	0.007724	0.940	0.004812	0.007720	0.855
0.005476	0.007611	0.995	0.005341	0.007498	0.950
0.005758	0.007502	1.050	0.005841	0.007288	1.045
0.006031	0.007396	1.105	0.006313	0.007090	1.145
0.006296	0.007293	1.155	0.006771	0.006902	1.240
0.006503	0.007136	1.212	0.007185	0.006724	1.325
0.006806	0.007095	1.265	0.007588	0.006555	1.410
0.007052	0.007000	1.315			
0.007289	0.006908	1.365			

TABLE III

ABSORBANCE[a] AT 500 mμ FOR THE NITRIC ACID--NITROGEN DIOXIDE--WATER SYSTEM AT 32°F

Absorbance	Nitrogen Dioxide (wt frac)						
	for 0.00 wt frac water	for 0.0100 wt frac water	for 0.0200 wt frac water	for 0.0300 wt frac water	for 0.0400 wt frac water	for 0.0500 wt frac water	for 0.0600 wt frac water
0	0	0	0	0	0	0	0
0.050	0.0155	0.0171	0.0182	0.0186	0.0181	0.0171	0.0158
0.100	0.0300	0.0315	0.0325	0.0328	0.0322	0.0308	0.0291
0.150	0.0531	0.0445	0.0453	0.0449	0.0436	0.0413	0.0392
0.200	0.0556	0.0558	0.0559	0.0550	0.0537	0.0516	0.0491
0.300	0.0777	0.0768	0.0753	0.0739	0.0718	0.0691	0.0662
0.400	0.0976	0.0952	0.0928	0.0902	0.0880	0.0851	0.0822
0.500	0.1161	0.1129	0.1094	0.1063	0.1032	0.1000	0.0968
0.600	0.1332	0.1293	0.1251	0.1213	0.1178	0.1140	0.1106
0.700	0.1490	0.1446	0.1398	0.1356	0.1314	0.1276	0.1239
0.800	0.1641	0.1592	0.1540	0.1492	0.1448	0.1403	0.1363
0.900	0.1782	0.1728	0.1672	0.1620	0.1571	0.1524	0.1480
1.000	0.1919	0.1860	0.1799	0.1743	0.1690	0.1641	0.1595
1.100	0.2045	0.1982	0.1919	0.1859	0.1804	0.1752	0.1704
1.200	0.2165	0.2099	0.2032	0.1969	0.1910	0.1858	0.1809
1.300	0.2283	0.2211	0.2130	0.2080	0.2007	0.1961	0.1919
1.400	0.2393	0.2317	0.2244	0.2178	0.2118	0.2062	0.2012
1.500	0.2501	0.2425	0.2349	0.2281	0.2217	0.2159	0.2107
1.600	0.2607	0.2527	0.2447	0.2376	0.2310	0.2254	0.2205
1.700	0.2708	0.2621	0.2537	0.2462	0.2399	0.2347	0.2300
1.800	0.2809	0.2718	0.2630	0.2556	0.2490	0.2438	0.2394

[a]Absorbance is defined as $-\log (I/I_0)$.

TABLE III (Cont'd)

Absorbance	Nitrogen Dioxide (wt frac)						
	for 0.0700 wt frac water	for 0.0800 wt frac water	for 0.0900 wt frac water	for 0.1000 wt frac water	for 0.1100 wt frac water	for 0.1200 wt frac water	for 0.1300 wt frac water
0	0	0	0	0	0	0	0
0.050	0.0146	0.0131	0.0120	0.0109	0.0099	0.0092	0.0084
0.100	0.0274	0.0252	0.0231	0.0211	0.0191	0.0174	0.0157
0.150	0.0371	0.0347	0.0325	0.0303	0.0282	0.0263	0.0244
0.200	0.0470	0.0443	0.0410	0.0392	0.0369	0.0348	0.0326
0.300	0.0638	0.0607	0.0570	0.0551	0.0521	0.0493	0.0465
0.400	0.0791	0.0729	0.0729	0.0698	0.0666	0.0637	0.0606
0.500	0.0938	0.0905	0.0874	0.0841	0.0811	0.0779	0.0747
0.600	0.1071	0.1037	0.1005	0.0971	0.0938	0.0903	0.0869
0.700	0.1203	0.1167	0.1131	0.1096	0.1059	0.1024	0.1088
0.800	0.1326	0.1288	0.1250	0.1224	0.1170	0.1141	0.1107
0.900	0.1439	0.1398	0.1370	0.1324	0.1280	0.1253	0.1219
1.000	0.1551	0.1510	0.1470	0.1433	0.1396	0.1361	0.1333
1.100	0.1660	0.1618	0.1577	0.1539	0.1504	0.1468	
1.200	0.1764	0.1722	0.1682	0.1646	0.1699	0.1572	
1.300	0.1867	0.1827	0.1780	0.1750	0.1713	0.1677	
1.400	0.1968	0.1925	0.1885	0.1850	0.1812	0.1777	
1.500	0.2061	0.2018	0.1981	0.1946	0.1919	0.1896	
1.600	0.2162	0.2121	0.2081	0.2048	0.2009	0.1973	
1.700	0.2260	0.2221	0.2185	0.2149	0.2114	0.2079	
1.800	0.2352	0.2316	0.2279	0.2243	0.2210	0.2174	

TABLE IV

ABSORBANCE[a] AT 425 mμ FOR THE NITRIC ACID--NITROGEN DIOXIDE--WATER SYSTEM AT 32°F

Absorbance	Nitrogen Dioxide (wt frac)		
	for 0.00 wt frac water	for 0.00300 wt frac water	for 0.00600 wt frac water
0	0	0	0
0.200	0.00093	0.00102	0.00111
0.400	0.00185	0.00204	0.00220
0.600	0.00277	0.00305	0.00331
0.800	0.00369	0.00406	0.00436
1.000	0.00462	0.00507	0.00540
1.200	0.00554	0.00604	0.00642
1.400	0.00647	0.00705	0.00741
1.600	0.00743	0.00804	0.00842

[a]Absorbance is defined as $-\log (I/I_0)$.

TABLE V

EXPERIMENTAL MEASUREMENTS OF ABSORBANCE[a] AT 425 mμ FOR THE NITRIC ACID--NITROGEN DIOXIDE--POTASSIUM NITRATE SYSTEM AT 32°F

Series *A*			Series *B*			Series *C*		
Nitrogen Dioxide (wt frac)	Potassium Nitrate (wt frac)	Absorbance	Nitrogen Dioxide (wt frac)	Potassium Nitrate (wt frac)	Absorbance	Nitrogen Dioxide (wt frac)	Potassium Nitrate (wt frac)	Absorbance
0	0.02764	0	0	0.05541	0	0	0.05548	0
0.00044	0.02710	0.132	0.00044	0.05443	0.151	0.00041	0.05450	0.141
0.00087	0.02658	0.255	0.00087	0.05348	0.308	0.00080	0.05356	0.280
0.00128	0.02607	0.373	0.00128	0.05257	0.448	0.00118	0.05265	0.410
0.00168	0.02561	0.490	0.00168	0.05169	0.590	0.00155	0.05177	0.538
0.00206	0.02512	0.602	0.00207	0.05084	0.720	0.00191	0.05092	0.650
0.00243	0.02468	0.702	0.00244	0.05002	0.840	0.00225	0.05009	0.768
0.00278	0.02424	0.797	0.00280	0.04922	0.965	0.00258	0.04930	0.875
0.00312	0.02382	0.893	0.00315	0.04845	1.092	0.00291	0.04853	0.980
0.00346	0.02325	0.975	0.00349	0.04770	1.205	0.00322	0.04778	1.080
0.00378	0.02303	1.060	0.00383	0.04697	1.310	0.00352	0.04705	1.180
0.00409	0.02263	1.143	0.00414	0.04627	1.410	0.00382	0.04635	1.270
0.00444	0.02221	1.238	0.00445	0.04558	1.510	0.00410	0.04567	1.355
0.00475	0.02193	1.300	0.00475	0.04492	1.610	0.00438	0.04500	1.460
0.00496	0.02159	1.370	0.00504	0.04428	1.700	0.00465	0.04436	1.525
0.00523	0.02125	1.445	0.00532	0.04365	1.790	0.00491	0.04373	1.600
0.00550	0.02093	1.520	0.00560	0.04304	1.870	0.00516	0.04310	1.680
0.00600	0.02032	1.650				0.00541	0.04253	1.755
0.00648	0.01980	1.775						
0.00693	0.01919	1.890						

[a]Absorbance is defined as $-\log (I/I_0)$.

TABLE VI

ABSORBANCE[a] AT 425 mμ FOR THE NITRIC ACID--NITROGEN DIOXIDE--POTASSIUM NITRATE SYSTEM AT 32°F

Absorbance	Nitrogen Dioxide (wt frac)	
	for 0.02000 wt frac Potassium Nitrate	for 0.04000 wt frac Potassium Nitrate
0	0	0
0.200	0.00072	0.00058
0.400	0.00144	0.00120
0.600	0.00216	0.00185
0.800	0.00292	0.00244
1.000	0.00365	0.00310
1.200	0.00440	0.00373
1.400	0.00511	0.00433
1.600	0.00583	0.00495

[a] Absorbance is defined as $-\log (I/I_0)$.

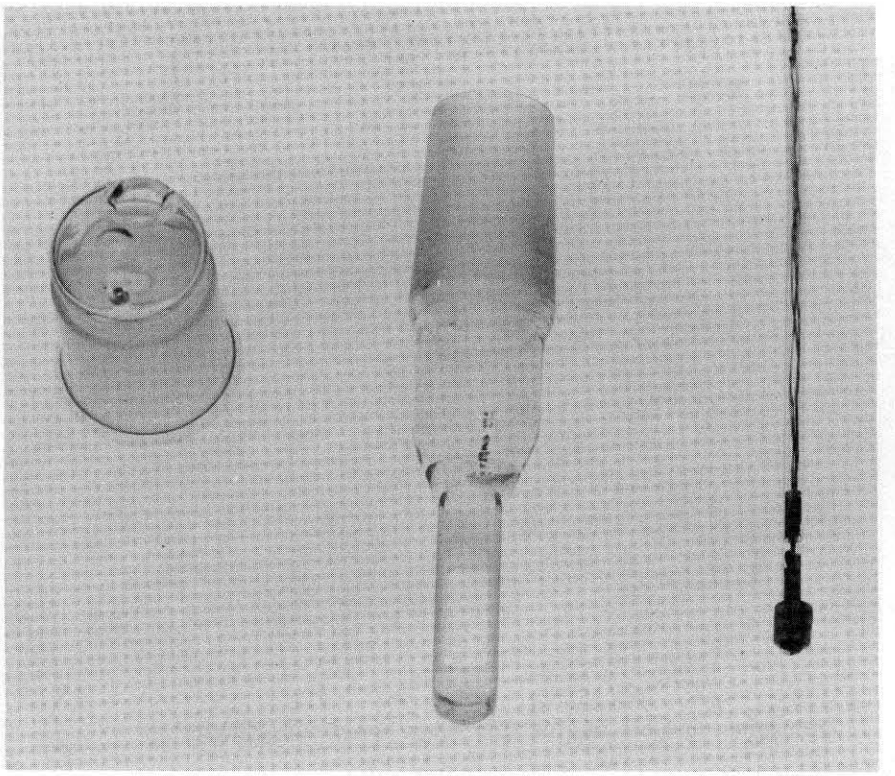

Figure 1. Transmission Cell and Stirrer with Thermocouple

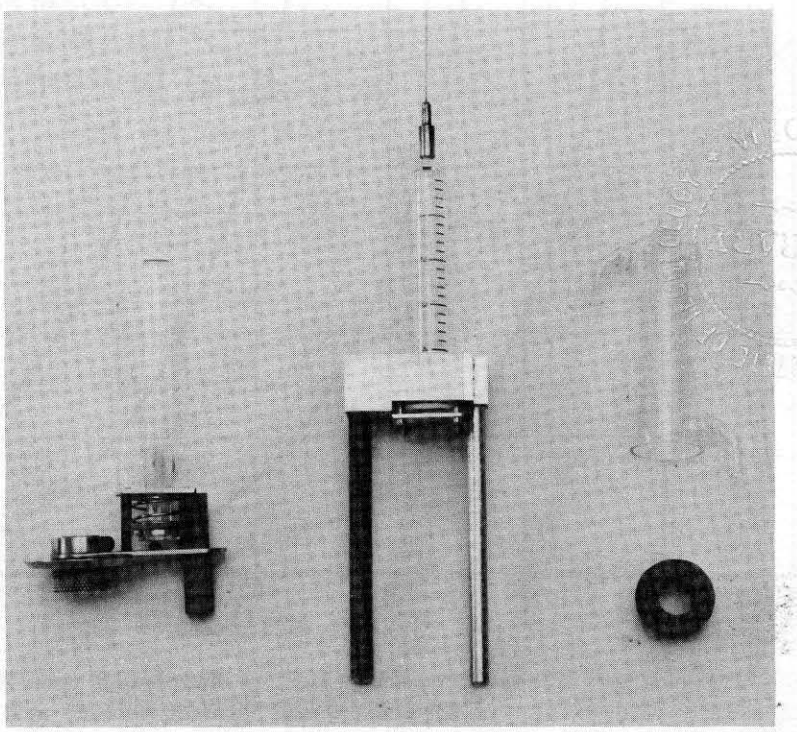

Figure 2
Details of Syringe

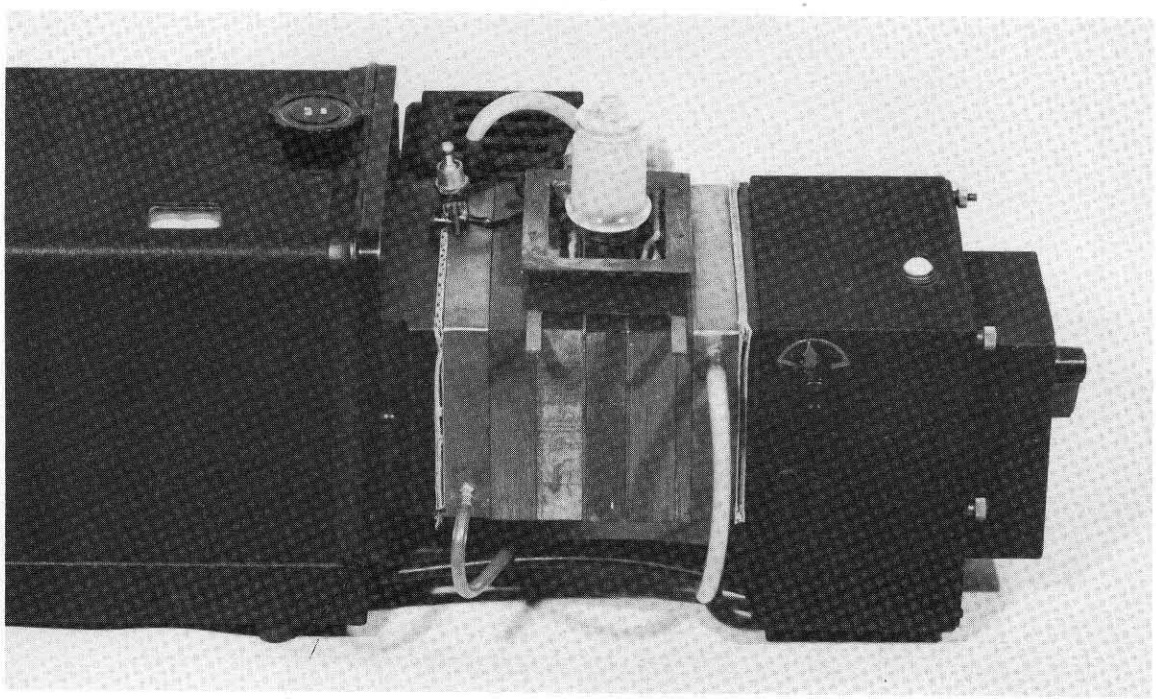

Figure 3. Transmission Cell in Position upon Spectrophotometer

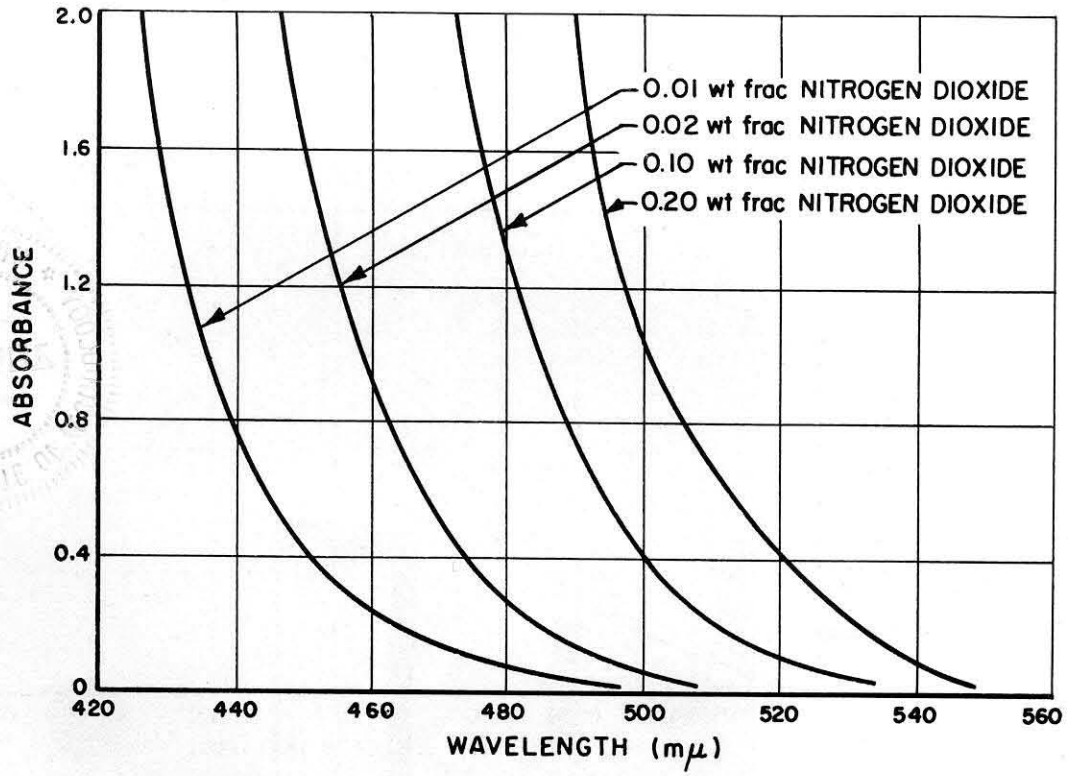

Figure 4. Semiquantitative Effect of Wavelength upon Absorbance of Mixtures of Nitric Acid and Nitrogen Dioxide at 32°F

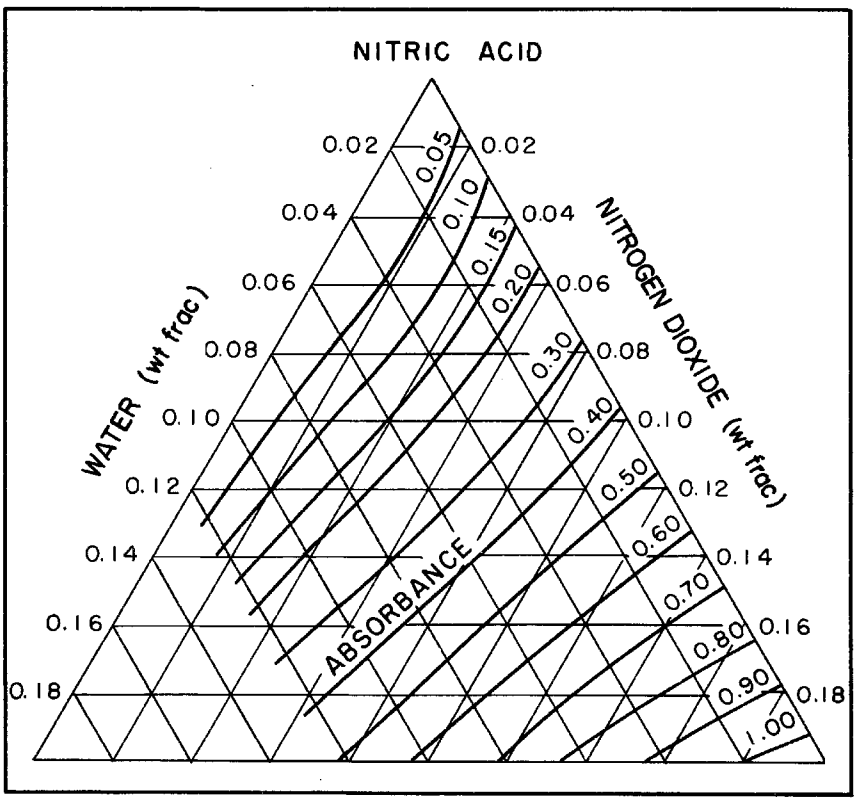

Figure 5. Effect of Composition upon Absorbance at 500 mμ

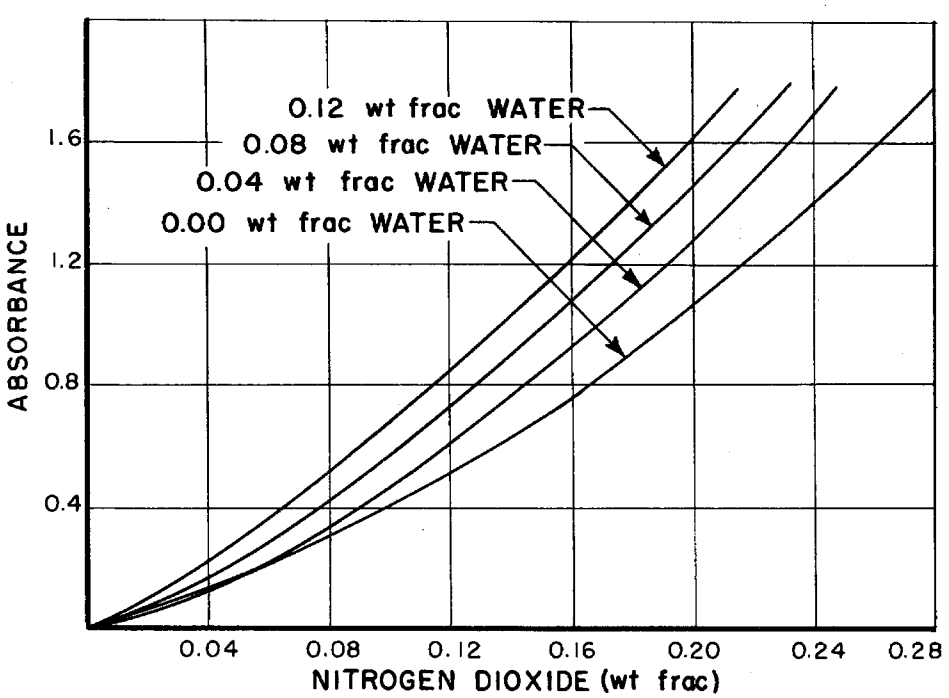

Figure 6. Absorbance of the Nitric Acid–Nitrogen Dioxide–Water System at 500 mμ

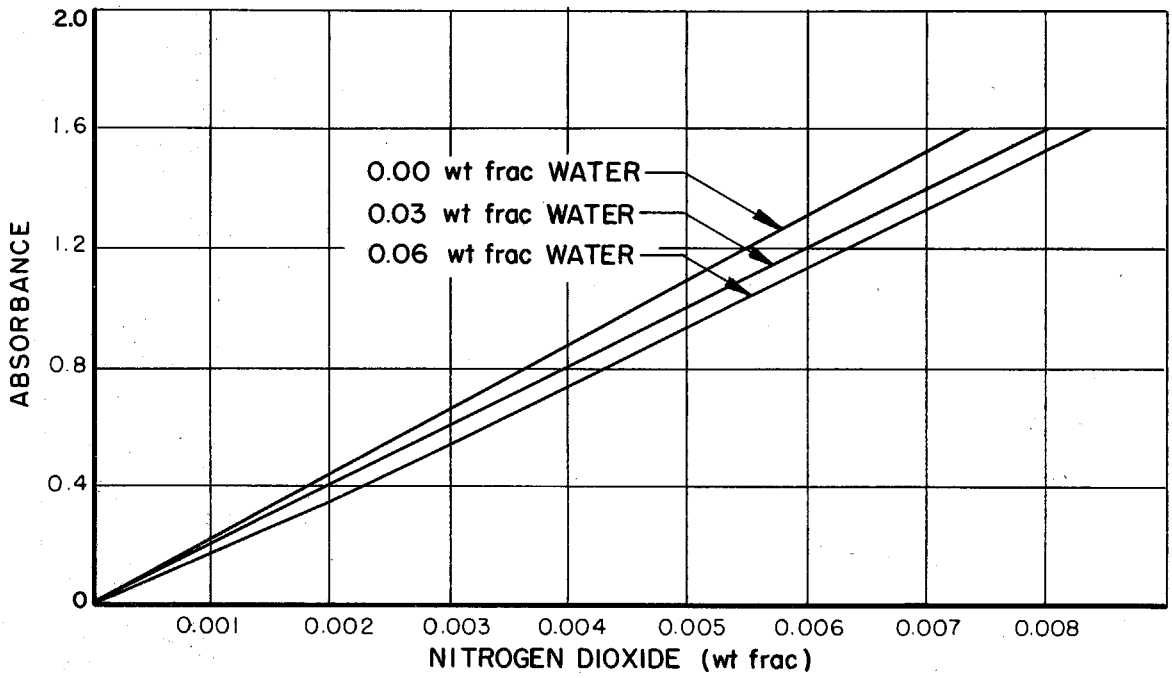

Figure 7. Absorbance of the Nitric Acid--Nitrogen Dioxide--Water System at 425 mμ

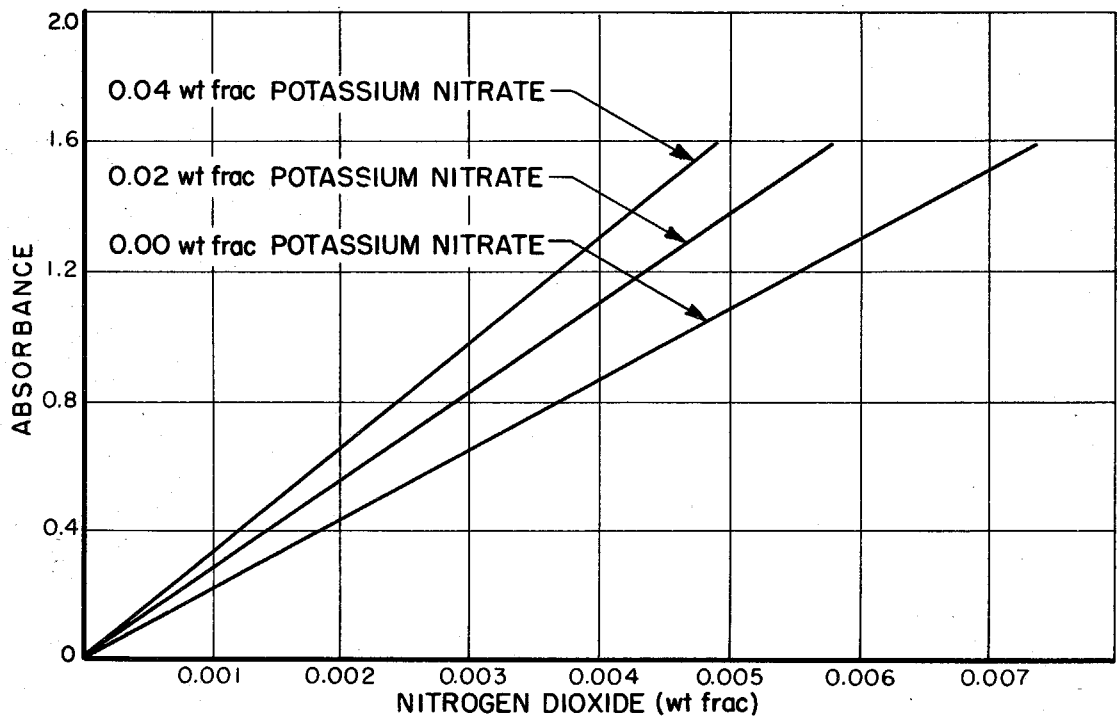

Figure 8. Absorbance of the Nitric Acid--Nitrogen Dioxide--Potassium Nitrate System at 425 mμ

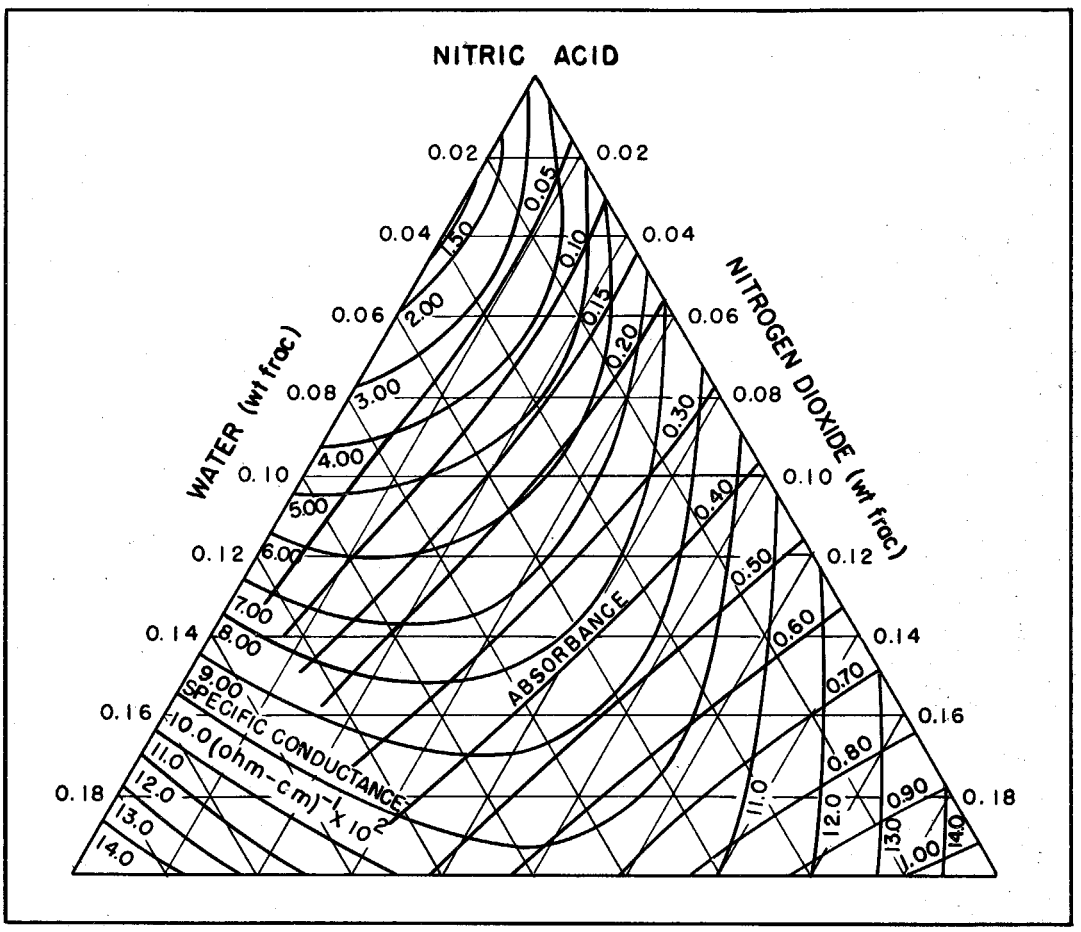

Figure 9. Effect of Composition upon Absorbance and Specific Conductance of the Nitric Acid--Nitrogen Dioxide--Water System

APPENDIX

A POSSIBLE METHOD OF ANALYSIS

It can be shown (Cf. Ref. 10) that on a triangular, ternary diagram the composition of a solution obtained by mixing two liquids of compositions A and B must lie on a straight line connecting these points. If a measured quantity of acid of known composition is added to an established weight of acid of unknown composition, the points representing the composition of the original unknown, that of the resulting mixture, and that of the acid of known composition must lie on a straight line on a triangular, ternary composition diagram. A unique solution of a material-balance equation for any one component can be found by taking compositions on a line that is drawn from the point of known composition and intersects the lines representing the absorbances of the original sample and the final mixture. The composition of the unknown is thus established where the line giving the unique solution to the material balance intersects the contour representing the absorbance of the unknown.

For example, if M grams of the unknown are weighed into an optical cell and found to have an absorbance A at 500 mμ and 32°F and if N grams of a mixture containing 0.90 weight fraction of nitric acid and 0.10 weight fraction of water are weighed into the cell and the resulting solution has an absorbance B, the composition of the unknown may be calculated in the following way:

Let α be the weight fraction of nitrogen dioxide in the unknown and β be the weight fraction of nitrogen dioxide in the mixture after dilution of the unknown with the standard acid. Since the total quantity of nitrogen dioxide is not changed by the dilution, it follows that

$$\alpha(M) = \beta(M + N) \tag{A-1}$$

$$\frac{\alpha}{\beta} = \frac{M + N}{M} \tag{A-2}$$

In the following procedure line 1 is drawn from the point corresponding to 0.1 weight fraction of water and 0.9 weight fraction of nitric acid as shown in Figure A-1, and the weight fraction of nitrogen dioxide may be read at the intersections of the line with the contours of constant absorbance A and B. The ratio of the weight fractions of nitrogen dioxide may be taken and compared with the ratio, $(M + N)/M$. This trial procedure is repeated until a line is found where the ratio of weight fractions of nitrogen dioxide at the intersections of the line with contour A and B is equal to $(M + N)/M$. The composition of the unknown acid is that at the intersection of the line and the absorbance contour A.

The method described permits the composition of an unknown to be determined with an uncertainty of 0.001 in the weight fraction of the components. A standard acid of any known composition may be used if Equations (A-1) and (A-2) are suitably modified. The described diluent acid is suggested because of its stability when stored out of contract with light.

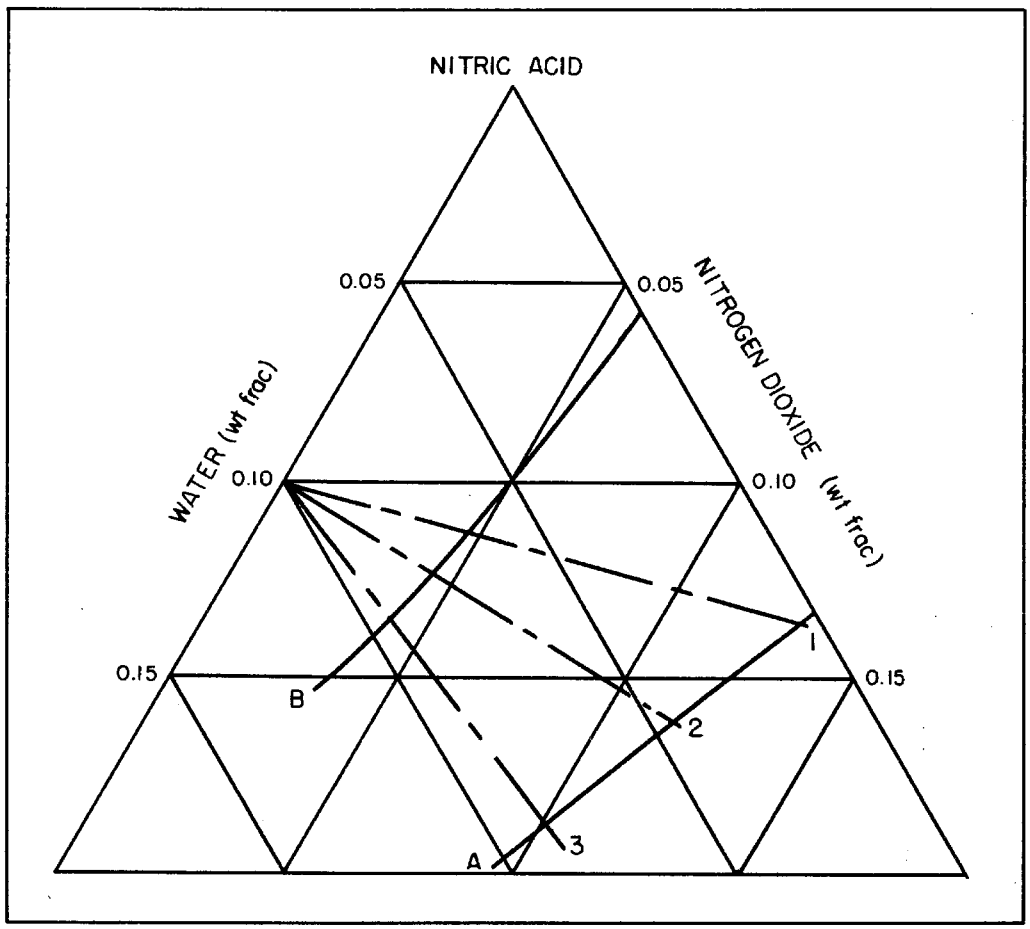

Figure A-1. Graphical Analysis of Composition of Nitric Acid--Nitrogen Dioxide--Water Samples Using Absorbance Data

REFERENCES

1. Hall, T. C., and Blacet, F. E., "Separation of the Absorption Spectra of NO_2 and N_2O_4 in the Range of 2400-2500A," *Journal of Chemical Physics*, 20:1745-1749, 1952.

2. Dalmon, R., and Freymann, R., "Infrared Absorption Spectrum of 100% Nitric Acid and of Its Aqueous Solutions," *Comptes rendus*, 211:472-474, 1940.

3. White, Locke, Jr., "Determination of Water in Fuming Nitric Acid by Infrared Absorption" (speech given at symposium sponsored by Committee on Fuels and Lubricants, September 8, 1951), in *Symposium on Analysis of Nitric Acids* (pp. 43-53). Washington: Department of Defense, Research and Development Board, December 31, 1951.

4. Clark, John, "A Field Assay for White Fuming Nitric Acid" (speech given at symposium sponsored by Committee on Fuels and Lubricants, September 8, 1951), in *Symposium on Analysis of Nitric Acids* (pp. 65-81). Washington: Department of Defense, Research and Development Board, December 31, 1951.

5. Gibson, K. S., and Balcolm, M. M., "Transmission Measurements with the Beckman Quartz Spectrophotometer," Research Paper 1798, *Journal of Research, National Bureau of Standards*, 38:601-616, 1947.

6. Forsythe, W. R., and Giauque, W. F., "The Entropies of Nitric Acid and Its Mono and Tri-hydrates. Their Heat Capacities from 15 to 300°K. The Heats of Dilution at 298.1°K. The Internal Rotation and Free Energy of Nitric Acid Gas. The Partial Pressures over Its Aqueous Solutions," *Journal of the American Chemical Society*, 64:48-61, 1942.

7. Ingold, C. K., Hughes, E. D., and Reid, R. I., "Mechanism of Aromatic Nitration," *Journal of the Chemical Society*. 1950 (September):2400-2440.

8. Goulden, J. D. S., and Millen, D. J., "Vibrational Spectra of Ionic Forms of Oxides and Oxyacids of Nitrogen," *Journal of the Chemical Society*, 1950 (October):2620-2627.

9. Robertson, Glenn D., Mason, David M., and Sage, B. H., *Electrolytic Conductance of the Ternary System of Nitric Acid--Nitrogen Dioxide--Water at 32°F and Atmospheric Pressure*, Progress Report No. 20-155. Pasadena: Jet Propulsion Laboratory, November 12, 1951.

10. Roozeboom, H. W. B., *Die Heterogenen Gleichgewichte vom Standpunkte der Phasenlehre*, vol. 3. Braunschweig: Friedrich Vieweg und Sohn, 1913.

II B - FOREWORD

The following report was written in conjunction with D.M. Mason and W.H. Corcoran as Ms. 2644 of the Chemical Engineering Laboratory. The data are taken from Part II A and the report has been forwarded to the Jet Propulsion Laboratory for publication in form of a progress report.

INTRODUCTION

Although Raman-spectral (1,2), conductance (3,4), and cryoscopic (5) measurements have given evidence of the existence of nitrosonium (NO^+) and nitronium (NO_2^+) ions, it was believed desirable to obtain further information about the existence of these ionic species. Use of another physical property such as optical absorption was thought to be a possible approach to the determination of the extent of their presence in solutions of nitrogen dioxide and nitric acid. The optical absorbance* at 425 mμ was selected as a means of analyzing the solutions since it was believed that at this wave length the nitrogen dioxide molecule could be assumed to be the only absorbing species. Two ternary systems, nitric acid-nitrogen dioxide-water and nitric acid-nitrogen dioxide-potassium nitrate, along with the binary system, nitric acid-nitrogen dioxide, were used in the absorbance measurements.

---

* Defined here as $-\log I/I_o$ where I_o is the intensity of light transmitted by a reference blank of air and I is the intensity of light transmitted by the sample.

EQUIPMENT AND METHODS

The equipment used and the procedures followed have been described in detail in a previous report (6). The absorbance of light was measured with a Beckman model DU spectrophotometer modified to allow the cell to be placed in an ice bath. The concentration range studied was from zero to 0.8 per cent nitrogen dioxide by weight. Samples were prepared by adding volumetrically a three per cent solution of nitrogen dioxide in acid to pure acid in small increments by means of a hypodermic syringe. The weight of nitrogen dioxide added was known with a maximum uncertainty of 0.5 per cent. The absorbance readings were reproducible within $\pm$ 0.3 per cent.

RESULTS

Figure 1 and Table II show the effect of small amounts of water and potassium nitrate on the absorbance of solutions of nitrogen dioxide in nitric acid. The experimental data were also previously recorded (6). In the analysis presented here the formal concentrations were obtained by assuming zero partial specific volumes of potassium nitrate and nitrogen dioxide in nitric acid. The partial specific volume of water was taken as its specific volume in the liquid state at 32° F. A value of 96.329 pounds per cubic foot was used for the specific weight of pure nitric acid at 32° F. Volumetric data for the nitric acid-nitrogen dioxide-water system were available (7), but for the small concentrations of nitrogen dioxide and water in the nitric acid, the approximation used here appeared acceptable.

Qualitatively, the absorption behavior is what would be expected by assuming that the absorption is due solely to the nitrogen dioxide molecule. Further, the following equilibria, which were first proposed on the basis of Raman spectra (1,2), appear to be in accord with the data:

$$2\,NO_2 \rightleftharpoons NO^+ + NO_3^- \qquad (1)$$

$$2\,HNO_3 \rightleftharpoons NO_2^+ + NO_3^- + H_2O \qquad (2)$$

$$H_2O + HNO_3 \rightleftharpoons H_3O^+ + NO_3^- \qquad (3)$$

Reaction (2) is presumed to predominate over reaction (3) in acid containing less than three per cent water whereas the reverse is presumed true when the concentration of water is greater than this. Qualitatively, this seems to be the case, as shown by conductivity measurements (3,4), freezing point measurements (5), and absorbance measurements (6). Considering only reactions (1) and (2) it is seen that the addition of

potassium nitrate will shift the equilibrium shown in reaction (1) to the left, increasing the concentration of nitrogen dioxide and thus the absorbance for a given formal concentration of nitrogen dioxide. On the other hand, the addition of small amounts of water will drive reaction (2) to the left, reducing the concentration of nitrate ion and giving more nitric acid. By a reduction in the concentration of the nitrate ion, more nitrogen dioxide will dissociate according to reaction (1) and thus reduce the absorbance for a given formal concentration of nitrogen dioxide.

In the above considerations it was assumed that the nitrogen dioxide molecule was the only species absorbing light at the wave lengths of the measurements. It is known (8) that nitrogen tetroxide does not absorb at these wave lengths when in the gas phase and hence is not likely to absorb in the liquid phase. Nitrosonium, the only other ion not present in pure nitric acid, has an even number of electrons and forms a colorless crystalline perchlorate and bisulfate the solutions of which in sulfuric acid are also colorless. Hence it would not be expected to absorb light in the visible range in solutions of nitric acid. Since the nitronium ion, nitrate ion, and the water molecule are present in pure nitric acid, which is colorless, these species may also be considered colorless.

Calculations using the absorbance data as a basis were made to establish the values of the dissociation of nitrogen dioxide and nitric acid according to equations (1) and (2) respectively. They were to be compared with quantitative data obtained from cryoscopic measurements (5,9)

and Raman spectra (2,10). In the calculations the following equilibrium expressions were used:

$$K_1 = \frac{[NO^+][NO_3^-]}{[NO_2]^2} \tag{4}$$

$$K_2 = \frac{[NO_2^+][NO_3^-][H_2O]}{[HNO_3]^2} \tag{5}$$

In the use of these equations it was assumed that the activity coefficient for each species was independent of concentration.

To develop the necessary equations for application of the equilibrium constants in order to establish the dissociation of the nitrogen dioxide and nitric acid, use was made of data shown in Figure 1. For one set of calculations at a given absorbance, data were taken from three curves. The curve for pure nitric acid was used in each instance along with any two other curves. For any arbitrary value of the absorbance in the range of Figure 1, assuming that the nitrogen dioxide molecule is the only color absorbing species, the following typical relationship may be written:

$$[NO_2]_a = [NO_2]_b - [NO_2]_c \tag{6}$$

In this equation the subscripts designate the selected curves intersected by the line of constant absorbance. Combining equation (6) with equations (4) and (5) gives six simultaneous equations with six unknowns which are the values of the dissociation of nitric acid and nitrogen dioxide according to equations (1) and (2). In this treatment the quantity γ, the dissociation of nitric acid according to equation (3), was neglected as it was considered small in the calculations compared to α and β when less than three per cent water was present (3,4,5).

The six simultaneous equations were solved by trial and error for α_b and β_b, the dissociations of nitrogen dioxide and of nitric acid respectively in mixtures of the two. Values were obtained at absorbances of 0.600, 0.900, and 1.200. All combinations of the curves shown in Figure 1 fitting the described procedure were used in the calculations so that six values of α_b and β_b were obtained at each absorbance. It was found that the results were very sensitive to the relationships between absorbances and concentrations. A summary of the calculations is given as follows:

Absorbance	$\bar{\alpha}_b$[a]	σ	$\bar{\beta}_b$[a]	σ
0.600	0.68	0.32	0.043	0.024
0.900	0.69	0.25	0.045	0.018
1.200	0.71	0.27	0.48	0.021

[a] Average of six values. In each group of six one value for α_b was greater than 1.0. Since 1.0 represents complete ionization, it was taken as the maximum allowable value; and where necessary β_b was accordingly corrected.

To determine the validity of assuming γ small with respect to α and β, additional equations were developed by using four curves in Figure 1 for a given analysis. Values of α and β obtained as a first approximation in the simplified case were used in solving for γ. It was found that γ was practically zero, giving a corresponding value of zero for K_3. The original assumption in regard to γ thus appeared valid.

Values for the dissociation of anhydrous nitric acid according to equation (2) have been reported in the literature. Using cryoscopic techniques, Gillespie et al. (9) obtained a value of 0.034 at -40° C. and Dunning and Nutt (5) a value of 0.08. Ingold and Millen (10) made Raman spectra measurements and found the dissociation to be 0.03 at -15° C. These data for anhydrous nitric acid can be compared with values of β_b, the dissociation of nitric acid containing less than 0.008 weight fraction of nitrogen dioxide.

Goulden and Millen (2) showed that α_b, the dissociation of nitrogen dioxide in the nitric acid solution, had a value of about 1.0. Their data were obtained at 20° C. and apply to dilute solutions of nitrogen dioxide in nitric acid.

DISCUSSION

It is apparent from the calculations that have been made, based only on absorption data, that not all salient features have been taken into account. One major example is in the treatment of α_b. The variation of optical absorbance with the weight fraction of nitrogen dioxide in pure nitric acid is a straight line as shown in Figure 1,

and Beer's law suggests that a_b is therefore constant. The equilibrium expressions, however, show that, if K_1 and K_2 are constant, a_b bears a quartic relationship to the formal concentration of nitrogen dioxide.

The uncertainty of the identity of the absorbing species contributes to the possibilities of error in calculating a quantity such as a_b. In addition, there would be a contribution to the error from the fact that the activity coefficient for each species in the solutions was assumed not to change with composition. Presence of ions other than those stated is another possible source of uncertainty separate from the problem as to which of these ions is involved in the optical absorption.

Optical absorbance data are difficult to interpret in describing thermodynamic equilibria since there are uncertainties as to the nature and effect of the absorbing species. It is believed, however, that by making reasonable assumptions as was done here, the information on optical absorbance can at least be used to show the order of magnitude of the dissociations. It appears that the work at least qualitatively supports the existence of equilibria as shown in equations (1) and (2). For further investigation it would be desirable to supplement the absorption data with more direct information such as would be available in magnetic susceptibility measurements on solutions of nitrogen dioxide in nitric acid. The fact that in this system nitrogen dioxide is the only molecule having paramagnetic properties would allow direct measurements of its presence (11,12).

LIST OF TABLES

LIST OF FIGURES

REFERENCES

1. Hughes, E. D., Ingold, C. K., and Reed, R. I., "Kinetics and Mechanism of Aromatic Nitration. Part II. Nitration by the Nitronium Ion, NO_2^+, Derived from Nitric Acid," Journal of the Chemical Society, 1950: 2400-2440.

2. Goulden, J. D. S., and Millen, D. J., "Vibrational Spectra of Ionic Forms of Oxides and Oxyacids of Nitrogen. Part VI. Raman-spectral Evidence of the Ionization of Dinitrogen Tetroxide in Nitric Acid. The Nitrosonium Ion, NO^+ and the Nitrosonium-Nitrogen Dioxide Ion, $N_2O_3^+$," Journal of the Chemical Society, 1950: 2620-2627.

3. Robertson, G. D., Jr., Mason, D. M., and Sage, B. H., "Electrolytic Conductance of the Ternary System Nitric Acid-Nitrogen Dioxide-Water at 32° F. and One Atmosphere," JPL Progress Report 20-155, 1952; "Electrolytic Conductance of the Nitric Acid-Nitrogen Dioxide-Water System at 32° F.," Industrial and Engineering Chemistry, 44: 2928-2930 (1952).

4. Taylor, E. G., Lyne, L. M., and Follows, A. G., "Conductance Measurements in Water-Nitric Acid-Nitrogen Pentoxide Mixtures at Various Temperatures," Canadian Journal of Research, 29, 439-451 (1951).

5. Dunning, W. J., and Nutt, C. W., "Freezing Point of Nitric Acid-Water Solutions," Transactions of the Faraday Society, 47, 15-25 (1951).

6. Lynn, S., Mason, D. M., and Sage, B. H., "Optical Absorbance of the System Nitric Acid-Nitrogen Dioxide-Water at 32° F. and One Atmosphere," JPL Progress Report 20-187 (1953).

7. Klemenc, A., and Rupp, J., "Zur Kenntnis der Salpetersaure. VI.," Zeitschrift fur anorganische und allgemeine Chemie, 194, 51-72 (1930).

8. Hall, T. C., Jr., and Blacet, F. E., "Separation of the Absorption Spectra of NO_2 and N_2O_4 in the Range of 2400-2500 A," Journal of Chemical Physics, 20, 1745-1749 (1952).

9. Gillespie, R. T., Hughes, E. D., and Ingold, C. K., "Cryoscopic Measurements in Nitric Acid. Part I. The Solutes Dinitrogen Pentoxide and Water. The Self-Dissociation of Nitric Acid.," Journal of the Chemical Society, 1950: 2552-2558.

10. Ingold, C. K., and Millen, D. J., "Vibrational Spectra of Ionic Forms of Oxides and Oxy-acids of Nitrogen. Part V. Raman-spectral Evidence of the Ionization of Dinitrogen Pentoxide in Nitric Acid and of the Constitution of Anhydrous Nitric Acid," Journal of the Chemical Society, 1950: 2612-2619.

11. Yost, D. M., and Russell, H., "Systematic Inorganic Chemistry," New York, Prentice-Hall, p. 27, 1946.

12. Sone, T., "Magnetic Susceptibility of Six Nitrogen Oxides," Tohuku Imperial University Science Reports, 5, 11, 139-157 (1922).

TABLE I.

NOMENCLATURE

K	equilibrium constant
log	logarithm to the base 10
α	fractional dissociation of NO_2 into NO^+ and NO_3^-
β	fractional dissociation of HNO_3 into NO_2^+ , NO_3^-, and H_2O
γ	fractional dissociation of HNO_3 into H_3O^+ and NO_3^-
σ	standard deviation

Subscripts

a	point on an absorbance curve of system containing nitric acid-nitrogen dioxide-potassium nitrate
b	point on an absorbance curve of system containing nitric acid-nitrogen dioxide
c	point on an absorbance curve of system containing nitric acid-nitrogen dioxide-water
1	reference to equation 1
2	reference to equation 2
3	reference to equation 3

Superscript

—	denotes mean values

TABLE II.

WEIGHT FRACTION OF NITROGEN DIOXIDE IN NITRIC ACID SOLUTIONS FOR EVEN VALUES OF ABSORBANCE AT 425 mμ AND 32° F.

Absorbance[a]	Weight Fraction Potassium Nitrate		Acid	Weight Fraction Water	
	0.02	0.04		0.003	0.006
0	0	0	0	0	0
0.200	0.00072[b]	0.00058	0.00093	0.00102	0.00111
0.400	0.00144	0.00120	0.00185	0.00204	0.00220
0.600	0.00216	0.00185	0.00277	0.00305	0.00331
0.800	0.00292	0.00244	0.00369	0.00406	0.00436
1.000	0.00365	0.00310	0.00462	0.00507	0.00540
1.200	0.00440	0.00373	0.00554	0.00604	0.00642
1.400	0.00511	0.00433	0.00647	0.00705	0.00741
1.600	0.00583	0.00495	0.00743	0.00804	0.00842

[a] Absorbance is defined as $-\log \frac{I}{I_o}$.

[b] Values in table are weight fractions of nitrogen dioxide.

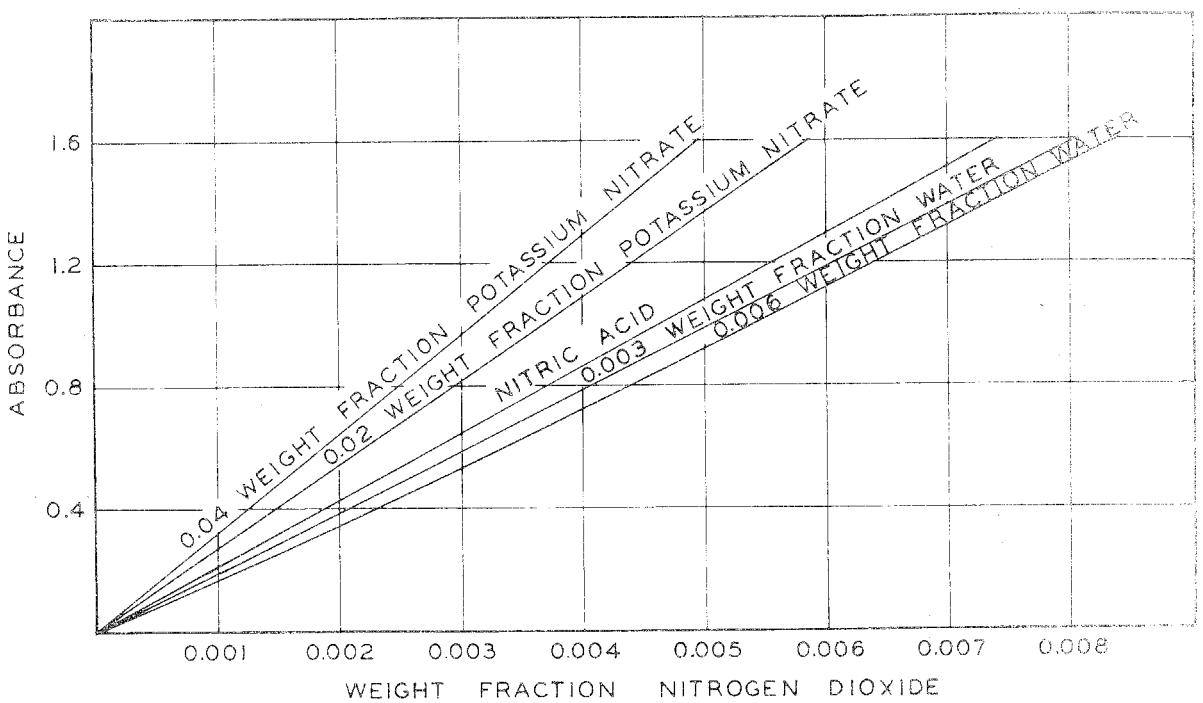

Fig. 1. Absorbance at 425 mμ and 32° F of Nitrogen Dioxide in Nitric Acid Solutions

PART III

KINETICS OF THE DECOMPOSITION OF SODIUM DITHIONITE

INTRODUCTION

Solutions of $Na_2S_2O_4$ are used as powerful and rapid reducing agents for vat dyeing, bleaching, and for the manufacture of various chemicals. The inherent instability of this compound with respect to both decomposition and atmospheric oxidation in aqueous solutions, however, lowers the efficacy of the solutions after prolonged storage. The present study was undertaken to determine some of the factors affecting the rate of thermal decomposition and atmospheric oxidation of sodium dithionite in aqueous solutions. Jellinek (1,2), Nicloux (3), and Baatard (4) measured the rates of these reactions in aqueous solution. In the temperature range of 0 - 60° C Jellinek (1) found for the thermal decomposition reaction that the rate of change of the concentration of $S_2O_4^{=}$ with time was second order with respect to $S_2O_4^{=}$ and in the presence of excess HSO_3^{-} the reaction was catalyzed, the rate of change of the concentration of $S_2O_4^{=}$ being second order with respect to both the concentration of $S_2O_4^{=}$ and HSO_3^{-}. It was quantitatively established by Jellinek (1) that the reaction proceeded towards completion according to the stoichiometric equation:

$$2\ Na_2S_2O_4 + H_2O \longrightarrow 2\ NaHSO_3 + Na_2S_2O_3 \qquad (1)$$

Nicloux (3) established that aqueous solutions of $Na_2S_2O_3$ react with oxygen according to the stoichiometry:

$$Na_2S_2O_4 + O_2 + H_2O \longrightarrow NaHSO_4 + NaHSO_3 \qquad (2)$$

A comprehensive review of the miscellaneous physicochemical properties of $Na_2S_2O_4$ is given by Yost (5), Jellinek (6), and Bassett and Durant (7).

The purpose of the present investigation was to obtain more experimental data on the rate of thermal decomposition of aqueous solutions of $Na_2S_2O_4$ with the exclusion of O_2 and also on the rate of atmospheric oxidation of these solutions with the objective of finding conditions under which the rate of these reactions is reduced. The measurements were made at 50°, 60°, and 70° C. The effect of various additives in the solutions on the rates of reaction was also measured. These additives included $NaHSO_3$, Na_2SO_3, $Na_2S_2O_3$, Na_2S, NaOH, NaCl, and $NaHCO_3$ for measurements of decomposition and NaOH for the atmospheric oxidation reaction. The reactions appear to be sufficiently complicated that no exact kinetic mechanism was ascertained from the present experimental data.

EXPERIMENTAL

Chemicals:- Analytical-grade reagents produced by Baker Co. and Mallinckrodt Co. were used without purification as additives for the kinetics studies. $Na_2S_2O_4$ as "Virginia Sodium Hydrosulfite" was contributed by the Virginia Smelting Co., and this supplier gave as an analysis of the lot of their product received: $Na_2S_2O_4$, 92 - 94 per cent; NaCl-Na_2CO_3, 8 per cent max; metallic impurities, 0.035 per cent max; insoluble in H_2O, 0.01 per cent max. This solid material as received was treated by completely dissolving it in warm water under an

atmosphere of nitrogen and then cooling the solution to the ice point so as to obtain reasonably pure $Na_2S_2O_4$ by differential solution and fractional crystallization. The nitrogen used throughout was a 99.98 per cent grade supplied by the Mathieson Co. containing but minute quantities of oxygen. A saturated solution of a third crystallized fraction of $Na_2S_2O_4$ was made and kept in an atmosphere of nitrogen at the ice point. Measured volumes of the saturated solution of $Na_2S_2O_4$ were used to make up solutions of known concentrations of $Na_2S_2O_4$ in the decomposition vessels. These saturated solutions had a turbid appearance due probably to the presence of discrete particles of sulfur and the amount of this sulfur present may depend on the washing procedure used. As will be discussed later this sulfur has a measurable effect on the rate of decomposition of $Na_2S_2O_4$.

Analytical Procedure:- Since the measurement of the rate of decomposition of $Na_2S_2O_4$ was to be made in the presence of various reducing agents such as $NaHSO_3$, Na_2SO_3, $Na_2S_2O_3$, and Na_2S present sometimes in concentrations one hundred times the concentration of $Na_2S_2O_4$, it was necessary to adopt an analytical procedure which could determine $Na_2S_2O_4$ specifically in the presence of these other reducing agents. The analytical procedure used for most of the measurements called for methylene blue as the standard reagent. One mole of methylene blue is reduced from an intense blue color to an almost colorless leucoform by one mole of $Na_2S_2O_4$. This reagent has been used previously in

the determination of $Na_2S_2O_4$ (8). However, in methods recommended by other investigators the solutions must be warmed to increase the speed of the reduction. At elevated temperatures the large excesses of the other reducing agents listed above reduced the methylene blue. It was found experimentally that in aqueous solutions the rate of the reaction between $Na_2S_2O_4$ and methylene blue is too low to give a clear, precise end-point near room temperature due to two factors. One factor, of course, is the lower temperature. In addition the leuco-form of methylene blue is relatively insoluble in water at room temperature and the solid leuco-compound has a tendency to adsorb unreacted methylene blue during the titration causing a lowered overall rate of reaction due to the necessity of the diffusion of the $Na_2S_2O_4$ to the surface of the solid before reaction can ensue. In about 10 per cent by volume of an organic solvent such as acetone or methanol the solid leuco-compound dissolves and the reactions are accelerated by eliminating the necessity of diffusion. Under these conditions $S_2O_3^=$, $SO_3^=$, and $S^=$ in quantities greater than one hundred times the concentration of $S_2O_4^=$ do not interfere in the reaction between methylene blue and $S_2O_4^=$ in the temperature range 0° - 30° C when the solution is about 0.01 - 0.05 N in KOH and as low as 0.0001 F in $S_2O_4^=$ and contains an organic solvent. The standard solution of methylene blue is rapidly titrated into a solution containing an unknown amount of $S_2O_4^=$, and the end-point is marked by the persistence of the intense methylene blue color. The end-point is sharp and is rapidly attained at room temperature.

Oxygen is excluded during the titration by the continuous bubbling of nitrogen through the solution or by use of a carbon dioxide generator described in the literature (9). The solution of methylene blue is standardized by quantitative precipitation with an excess of standard solution of I_2 by a procedure described in detail elsewhere (10). The precipitate is filtered and the filtrate is analyzed for excess I_2 by conventional iodometric procedures (11). The precision of the analytical procedure in determining concentrations of $S_2O_4^{=}$ is about ± 1 per cent.

The selective reduction of chromium to the trivalent state by $S_2O_4^{=}$ is another possible analytical procedure. The trivalent chromium is precipitated as the hydroxide, which is filtered and thoroughly washed with ammonia water. In a solution of K_2CrO_4 0.1 F in KOH large excesses of $S_2O_3^{=}$ and $SO_3^{=}$ do not interfere in the reaction between $CrO_4^{=}$ and $S_2O_4^{=}$, although a large excess of $S^{=}$ does. The $Cr(OH)_3$ precipitate is dissolved from the filter with 1 N HNO_3 and the trivalent chromium in the filtrate is oxidized to the hexavalent state using $HClO_4$ and $AgNO_3$ in a procedure described in the literature (12). The $Cr_2O_7^{=}$, and thus the equivalents of $S_2O_4^{=}$, are determined iodometrically. Due to the accuracy and rapidity of the analytical method using methylene blue it was adopted in preference to the very accurate yet more tedious chromate method in most cases. A test employing the chromate method is included in the results for comparison with the methylene blue procedure.

Apparatus and Procedures:- For most of the tests 125-ml Kjeldahl flasks equipped with neoprene stoppers were used to contain the solutions undergoing decomposition. Intermittent agitation within the flasks was provided by means of a glass-covered-steel agitator moved manually from without by means of a powerful horseshoe magnet. In a few cases a 500-ml round-bottom extraction flask equipped with a continuous mercury-sealed stirrer was used. Through a glass tube in the stopper of the flasks a positive gauge pressure of nitrogen of about 0.1 atm was maintained inside the flasks to preclude entry of air to the flask. The nitrogen used for the pressurization was 99.98 per cent Mathieson grade which was thoroughly scrubbed through a concentrated basic solution of $Na_2S_2O_4$ and then stored in a five-gallon bottle over a basic solution of $Na_2S_2O_4$. The hydrostatic pressure of this solution was used to give the positive pressure in the system. This procedure was designed to eliminate as completely as possible the entry of oxygen in the flask during the measurement of decomposition.

A measured volume of distilled water, about 100 ml for the Kjeldahl flasks and 400 ml for the extraction flasks, which had been vigorously boiled to facilitate the removal of air was added to the flask in which a stream of nitrogen continuously flowed. Additives to be included were then dissolved in the water. A layer of kerosene which had also been boiled to remove air was placed on the surface of the water in the decomposition flask to reduce further any chance for atmospheric contamination during addition or withdrawal of material from the flasks in the

course of the decomposition measurements. The flask and added water were immersed in a water bath controlled by a mercury thermo-regulator to within 0.1° C of the desired temperature.

Suitable amounts of samples of a saturated solution of $Na_2S_2O_4$ at 0° C prepared as previously described were added to the solution in the flask by inserting through the neoprene stopper a long hypodermic needle attached to a conventional glass syringe which had been flushed out by moving the plunger back and forth several times while the needle tip was in an atmosphere of N_2. Measured volumes of solutions were withdrawn with the same apparatus. The precision of the volumetric measurements was $\pm$ 0.2 per cent. After addition of an amount of saturated solution of $Na_2S_2O_4$ to the mixture in the decomposition flask to give the desired initial concentration of $S_2O_4^{=}$, the contents were very thoroughly agitated by the magnetic stirrer or the mercury-sealed stirrer so that a uniform mixture resulted. The temperature of the contents of the flask was not lowered appreciably by the addition of the saturated solution. The resulting solution was withdrawn at various times and immediately added to a 125 ml conical flask containing about 25 ml of the deaerated solution of KOH and methanol or acetone previously described. The solution was subsequently titrated with methylene blue. Nitrogen was continuously bubbled through this solution until the titration with methylene blue was completed.

The concentrations of methylene blue solutions were selected to give burette readings which were sufficiently precise. The color of

methylene blue is so intense that a drop of 0.0001 F solution of this reagent gives a clearly discernible blue color under the above conditions. However, for the bulk of the tests methylene blue solutions of about 0.001 F were used.

The time of withdrawal from the decomposition flask was assumed to be that at which the KOH solution and the $Na_2S_2O_4$ solution were mixed. The rate of decomposition of $Na_2S_2O_4$ in the KOH solution was assumed to be negligible for the few minutes required for the titration. In Test 11 the solution from the decomposition flask was added to basic chromate solution and the analyses were performed in bulk at the conclusion of the withdrawal of all the samples.

In a few cases the concentration of H^+ in the solution of $Na_2S_2O_4$ was measured with a Beckmann Model G pH meter equipped with a sleeve-type glass electrode. Temperature corrections for measurements above 25° C were made on the pH readings as prescribed by the manufacturer. In several tests the turbidity of the solution as a function of time was followed by a measurement of the optical absorbance of the solution at 400 mμ. A Beckman model DU spectrophotometer was used with a constant-temperature bath attachment to make the measurements.

In the measurements of the rate of atmospheric oxidation of $Na_2S_2O_4$ in aqueous solutions, air at near atmospheric pressure was allowed to bubble at a measured volumetric rate of flow through the solution in the Kjeldahl flasks. Similar sampling and analytical techniques to those described above were used in these measurements.

RESULTS

Decomposition of Aqueous Solutions of $Na_2S_2O_4$ at 60° C:- An aqueous solution of pure $Na_2S_2O_4$ appears to decompose very slowly at first. The decomposition accelerates rapidly after a certain elapsed time as is evident from Figure 1 and Table I, Tests 1 and 2. Such behavior is in keeping with a degenerate branching chain mechanism (13). Other examples of this type of reaction in aqueous solution are known, as for example the decomposition of nitrosyl disulfonate ion (14,15). For Test 2, the concentration of H^+, which is a measure of the amount of HSO_3^- formed in the decomposition according to equation (1), is also plotted versus time and it is seen that this curve is nearly a mirror image of the concentration of $S_2O_4^{=}$ versus time curve.

In Figure 1, Tests 1 and 2 represent measurements on two separate samples of $Na_2S_2O_4$ prepared as previously described. It is noteworthy that the concentration-time relationship is not identical in the case of these two samples. Also the lines in Figure 2 have different slopes. The slightly higher initial $S_2O_4^{=}$ concentration may partially account for the earlier drop-off of Test 2 as will be seen subsequently. However, the major cause of this lack of reproducibility may be due to the presence of differing amounts of suspended sulfur particles in the original saturated solution of $Na_2S_2O_4$ in these two cases.

A degenerate branching chain reaction approximately follows the law:

$$-\frac{dC}{d\theta} = A^{B\theta} \qquad (3)$$

Where C is concentration of reacting species, θ is the time, and A and B are constants. Thus it is seen by integration of equation (3) that one of the criteria for this type of a mechanism is that there be a linear relationship between log $(C_o - C)$ and θ. C_o is the initial concentration and C is the concentration at time θ. In Figure 2 is a plot of the log $(C_o - C)$ versus θ for part of the concentration range. The data are also shown in Table II. The linearity of these data indicate that $Na_2S_2O_4$ in pure aqueous solutions decomposes in a fashion similar to a degenerate branching chain reaction. It is apparent from Figure 1 that the reaction starts off slowly via some reaction of undetermined order before the onset of the rapid decomposition.

In certain tests, such as 3 and 4 shown in Figure 3 and Table III, where the concentrations of $S_2O_4^{=}$ and H^+ are plotted against time, it is seen that there are peculiar oscillations. The oscillations are most apparent in the curves of the concentration of $S_2O_4^{=}$ versus time but are measurable in the curves of the concentration of H^+ versus time. The fact that in some portions of the $S_2O_4^{=}$-time curves the concentration of $S_2O_4^{=}$ increases with time is rather unusual. Initial mixing was thorough so that incomplete mixing is not a source of error. There is a possibility that some intermediate product of the decomposition of $S_2O_4^{=}$ reduces methylene blue and thus the increase in the concentration of $S_2O_4^{=}$ is only apparent. The ultimate products of the decomposition, $NaHSO_3$ and $Na_2S_2O_3$, do not reduce methylene blue under the conditions of

the analytical procedures as previously described. Also Na_2S and an acidified solution of $Na_2S_2O_4$ where much sulfur and polythionous acid are produced do not reduce the methylene blue under the conditions of the analytical procedure. Thus no known species accounts for the apparent increase in the concentration of $S_2O_4^{=}$ with time. Chemical reactions where the velocity varies periodically with time are known and such behavior may be found in systems where coupled autocatalytic reactions occur and where physical phenomena such as supersaturation are present (16). In the reaction between H_2O_2 and HIO_3 such periodicity occurs and the concentration of I_2 is found to increase with time during the oscillations (17). It is suspected that the presence of colloidal or discrete sulfur particles in the present system may account partially for this behavior, as will be discussed subsequently, although no definite mechanism has been established. From a comparison of Tests 3 and 4 in Figure 3 it is again evident that there is a lack of reproducibility between two separate tests. Also the fluctuations appearing in Tests 3 and 4 do not appear in Tests 1 and 2.

It is interesting to note that there is reproducibility in the concentration versus time relationships in similar tests on pairs of samples prepared from the same saturated solution of $Na_2S_2O_4$, as evidenced in Figures 9, Tests 13ab, and Figure 10b, Tests 15abcd. These data for decomposition with and without added products of decomposition will be discussed more fully subsequently, but these figures show that the concentration-time relationships of Tests 13ab without fluctuations

are similar and so are the Tests 15abcd with fluctuations. Because of this seeming dependence of the concentration-time curves on the original saturated solution of $Na_2S_2O_4$ each test number in the paper designates a single saturated solution from which several samples a,b,c etc. were taken.

Figure 4 and Table IV, Tests 5abcd, show the effect of initial concentration in the range 0.009 - 0.09 F of $Na_2S_2O_4$ on the decomposition reaction. Included in these solutions was enough NaCl in each case to give a uniform ionic strength of 1.00. It is seen from these data that the higher the initial concentration the sooner the accelerated portion of the curve of the concentration of $S_2O_4^{=}$ versus time is reached and the sooner the second, lower rate leg is reached, except for Test 5d. Also note that at 120 minutes about a quarter of the original $Na_2S_2O_4$ remains in Test 5d whereas a much smaller fraction of the original $Na_2S_2O_4$ remains in Tests 5abc. It is particularly apparent from Tests 5c and 5d that the second, lower rate leg appears in the concentration-time curves when the products of the decomposition, $NaHSO_3$ and $Na_2S_2O_3$, reach sufficiently high concentrations relative to the undecomposed $Na_2S_2O_4$. As will be discussed subsequently this portion of the decomposition rate is first order with respect to the concentration of $Na_2S_2O_4$.

An increase in ionic strength by increasing the concentration of NaCl in solution results in a reduction of the half life of $S_2O_4^{=}$, as is evident from Figure 5 and Table V, Tests 5abcd. This positive salt

effect might, on the basis of Brönsted's theory, be interpreted as an indication that reacting ions of like sign are principally responsible for the rate determining step of the autocatalytic decomposition (18). However, the possibility that NaCl may have a specific catalytic effect on the reaction is not precluded. No quantitative analysis of these data on the basis of the Brönsted theory was made. Practically, the addition of NaCl to the commercial samples of "Sodium Hydrosulfite" mentioned previously seems inadvisable from the point of view of stability.

Catalytic Effect of $NaHSO_3$ and Several Other Compounds on the Decomposition:- In the presence of initial concentrations of $NaHSO_3$ equimolar to or less than the initial concentration of $Na_2S_2O_4$, the branching chain type of thermal decomposition of the latter is initially catalyzed as seen in Figure 6, Test's 7abcd, and Table VI, Tests 7a and 8abcd. The tests in Figure 6 are for a constant ionic strength of 0.02, which was attained by adding appropriate amounts of NaCl to the solutions. Figures 5 and 6 show that $NaHSO_3$ has a pronounced catalytic effect on the decomposition reaction. With the presence of concentrations of $NaHSO_3$ greater than that of the $Na_2S_2O_4$ the autocatalytic nature of the reaction disappears, as a comparison of Tests 10abc, Figure 7a, with Test 7c in Figure 6 shows. Actually, as will be seen presently, the reaction becomes first order with respect both to HSO_3^- and $S_2O_4^=$ in this composition range. Thus there appear to be two regions of different

rate behavior. They are the chain branching and the first order regions, depending on whether the $NaHSO_3$ concentration is greater or less than the equivalent (according to equation (1)) amount of $Na_2S_2O_4$. In both regions HSO_3^- catalyzes the decomposition.

With H^+ concentration greater than 10^{-3} obtained by adding $NaHSO_4$ to the solution, $Na_2S_2O_4$ decomposed immeasurably rapidly.

In the region of initial concentration of HSO_3^- greater than the initial concentration of $S_2O_4^=$, the rate of decomposition appears to be first order with respect to both the HSO_3^- and the $S_2O_4^=$ concentrations and the rate may be expressed:

$$-\frac{d(S_2O_4^=)}{d\theta} = k(S_2O_4^=) = k'(HSO_3^-)(S_2O_4^=) \qquad (4)$$

k is the specific first order rate constant for the reaction. Typical data showing the rate dependence of the decomposition of $S_2O_4^=$ on the concentration of HSO_3^- are shown in Figures 7a, Tests 10abcd, 11, and Table VII, Tests 9abcd, 10abcd, 11, and 12ab for nominal concentrations of HSO_3^- varying between 0 - 0.5 F. The ionic strength for these tests was maintained constant at 2.0 by the addition of appropriate amounts of NaCl to the solutions. From Figure 7a it is evident that with increasing concentration of HSO_3^- the rate of decomposition is increased. In Figure 7a are evident again fluctuations in the rate of the decomposition and, although the overall reaction proceeds in a first order

fashion, there is inherent periodicity in the rate (16).

It is interesting to note in Figure 7b and Table VII, Test 12 that the addition of 1 F $NaHCO_3$ to the solution inhibits the decomposition and effectively causes the chain branching mechanism to disappear. The concentration of H^+ in this solution is 7.75×10^{-6} molar, which is in the range that might be encountered in buffered solutions of $NaHSO_3$ - Na_2SO_3 . However, the rate of decomposition of $Na_2S_2O_4$ in this solution appears to be very much lower than with the same concentration of H^+ in a solution of $NaHSO_3$ - Na_2SO_3. From Tests 25ab in Figure 7b it is evident that 0.1 F NaOH or 0.5 F Na_2SO_3 greatly inhibit the reaction. This inhibition may be due in part to the reduced amount of the catalytic species HSO_3^- in the solutions of these compositions. $S^=$ does not appear to have a specific catalytic effect, at least not in solutions of 0.1 F Na_2S, which are basic, where the rate of decomposition of $Na_2S_2O_4$ is reduced nearly to that in 0.1 F NaOH, as is seen in Table VII, Test 25b.

Tests 10abd are shown in Figure 8ab and the first order nature of the overall thermal decomposition with respect to the concentration of $S_2O_4^=$ is noted from the linear relationship between the logarithm of the concentration of $S_2O_4^=$ and time. A plot of the reciprocal of the concentration of $S_2O_4^=$ versus time does not give a linear relationship for the data of Table VII and thus it may be concluded that under the present set of conditions the reaction is not second order with respect to the concentration of $S_2O_4^=$ as Jellinek found. In his experiments

Jellinek worked with solutions initially about 0.28 F in $Na_2S_2O_4$, studying the rate of decomposition of the pure substance at 60° C, and the rate of decomposition in the presence of 10 - 30 per cent by weight $NaHSO_3$ at 18° and 32° C. The periodicity of the rate superimposed on the overall reaction rate is demonstrated by the dotted lines for Test 10d. It is noteworthy that although the average slopes of the linear first order relationship of Figure 8a can be precisely reproduced for the same initial bulk concentrations of species, the frequency of the fluctuations is reproduced with certainty only with samples prepared from a common saturated solution of $Na_2S_2O_4$.

From the specific rate constants obtained by taking slopes of lines such as shown in Figure 8a, it is found that the rate expression given by equation (4) is essentially correct, the rate being first order with respect to the concentrations of $S_2O_4^{=}$ and HSO_3^{-} and independent of the concentrations of $SO_3^{=}$ and H^{+} in buffered solutions of $NaHSO_3$ - Na_2SO_3. There is a slight dependence of the rate on the initial concentration of $S_2O_4^{=}$. In Figure 8b and Table VIII are given the values of these rate constants for a variety of initial conditions. In Figure 8b where k in min^{-1} is plotted versus initial concentration of HSO_3^{-} it is seen that a linear relationship results and the rate increases with increasing concentration of HSO_3^{-} for initial concentrations of $S_2O_4^{=}$ of approximately 0.01 F. As seen from Table VIII, these data represent about an eighty-five fold variation in H^{+} and a variation in initial formal concentration of $SO_3^{=}$ from 0 - 0.5 F, yet over this range of composition

the rate constant appears to be directly proportional to the concentration of HSO_3^-. That the rate is somewhat dependent on the initial concentration of $S_2O_4^=$ is indicated by the deviation of the points for Tests 12a and b, for about 0.05 and 0.10 F $S_2O_4^=$, respectively, from the line in Figure 8b as was stated.

Catalytic Effect of $Na_2S_2O_3$ and $NaHSO_3$ on the Decomposition:- $Na_2S_2O_3$, when present alone, catalyzes the chain-branching-type decomposition of $Na_2S_2O_4$. In Figure 9 and Table IX, Tests 13abcd, are shown the effects of both $Na_2S_2O_3$ and precipitated sulfur on the thermal decomposition reaction. Tests 13a and b represent runs with and without a large glass wool surface exposed to the reacting solution to measure possible heterogeneous catalysis by glass surface. The similarity of the concentration of $S_2O_4^=$ versus time curves for this pair of tests indicates glass surface to be ineffective in catalyzing the decomposition. Also this pair of curves shows that the chain branching reaction is reproducible with a common initial solution. With Test 13c the catalytic effect of about 0.01 F $S_2O_3^=$ is evident, thus showing further the autocatalytic nature of the reaction. Also, sulfur precipitated by acidifying $Na_2S_2O_3$ and filtered and thoroughly washed has a marked catalytic effect on the decomposition.

In Figures 10ab, Tests 14ab and 15abcd, and Table X, Tests 12cd, 14ab, 15abcd, 16abcd, 17ab, and 18abc, are shown data on the effect of $Na_2S_2O_3$ and $NaHSO_3$ when present in greater concentrations than $Na_2S_2O_4$

on the rate of decomposition of the latter. For comparison in Figure 10b are Tests 15ab for decomposition of pure $Na_2S_2O_4$ by chain branching.

From a comparison of Tests 14a and b it is evident that 0.1 F $Na_2S_2O_3$ catalyzes the branching chain leg of the reaction. However, the combination of 0.1 F $Na_2S_2O_3$ with 0.1 F $NaHSO_3$ causes a first order reaction to appear. When both $Na_2S_2O_3$ and $NaHSO_3$ are present, as will be subsequently discussed, the specific rate constant is approximately proportional to both. Also in Tests 15cd the addition of $S_2O_3^{=}$, HSO_3^{-} and $SO_3^{=}$ again causes the curve of the concentration of $S_2O_4^{=}$ versus time to become first order with respect to the concentration of $S_2O_4^{=}$. Evident in Tests 15abcd is the periodicity in the rates. The remarkable duplication of these fluctuations in each pair of curves is shown in Figure 10b.

The first order nature of the thermal decomposition in the presence of excess $S_2O_3^{=}$, HSO_3^{-}, and $SO_3^{=}$ is shown by representative data in Figure 11a where the logarithm of the concentration of $S_2O_4^{=}$ is linear with time. In Table XI values of specific first order rate constants k for the various tests of Table X are calculated from the slopes of lines such as shown in Figure 11a. From Figures 11ab and Table XI it is evident that the rate of thermal decomposition increases with both $S_2O_3^{=}$ and HSO_3^{-}. The presence of marked periodicity in Tests 17ab and its absence in Tests 16d are evident in this plot. The plot of the reciprocal of the concentration of $S_2O_4^{=}$ versus time is non-linear over the whole range of time, showing that the reaction is not second order with respect to the concentration of $S_2O_4^{=}$.

The nature of the catalysis of the decomposition of $S_2O_4^{=}$ by HSO_3^- and $S_2O_4^{=}$ as well as by H^+ is shown in Figure 11b where the specific first order rate constant k, is plotted versus the concentration of $S_2O_3^{=}$ times the concentration of HSO_3^-. For constant values of the concentration of H^+ and the initial concentration of $S_2O_4^{=}$, the rate constant varies in a regular manner with increasing value of the product of the concentrations. The rate constant is dependent on initial concentration of $S_2O_4^{=}$, as seen in this figure, and unlike the case of catalysis of HSO_3^- alone, in the presence of $S_2O_3^{=}$ H^+ catalyzes the decomposition of $S_2O_4^{=}$. It is interesting to note that in studies of acid decomposition of $Na_2S_2O_3$ the time of formation of particles of sulfur depends on $(H^+)^{\frac{1}{2}}$ and $(S_2O_3^{=})^{>1}$ (19). The rate of this reaction is of the same order of magnitude as for the $S_2O_4^{=}$ decomposition but the concentration of H^+ in the solutions was much higher in the former. That sulfur apparently plays some role in the decomposition was seen in Figure 9.

Role of Sulfur in the Decomposition of $Na_2S_2O_4$:- The turbidity of aqueous solutions of $Na_2S_2O_4$ decreases as thermal decomposition progresses. This turbidity is probably due to the presence of colloidal particles of sulfur. A Beckman model DU spectrophotometer with corex cells of 1 cm depth placed in a constant temperature bath was used to measure the rate of change of optical absorbance at 400 mμ. Air was used as a reference for the absorbance measurements. The measurement of direct absorbance in this manner instead of measuring scattering of light has been used

by other investigators in the study of the formation of discrete sulfur particles (19). In Figure 12 is shown a plot of the logarithm of both optical absorbance and the concentration of $S_2O_4^{=}$ as a function of time for solutions containing HSO_3^-, $S_2O_3^{=}$ and $SO_3^{=}$. For solutions obeying the Beer-Lambert law the absorbance is proportional to the concentration of the light absorbing species. Assuming that this law applies approximately in dithionite solutions, it follows that the light absorbing species reacts according to a first order law. In Figure 12, Tests 19abcd, and Table XII, Test 19abcd, and 20ab, it is seen that the disappearance of the sulfur particles with time occurs at about the same rate as $S_2O_4^{=}$ decomposes. Comparing Test 19a with 19b it is seen that the rate of disappearance of sulfur is less than the rate of decomposition of the $S_2O_4^{=}$. However, in Tests 19cd these rates are more nearly identical. No periodic fluctuations occur in the absorbance-time relationships, although in Tests 19ac there is evidence of these fluctuations in the $S_2O_4^{=}$-time relationship. The precise role of sulfur in the decomposition has not been established other than the observation that it disappears at nearly the same rate as does $S_2O_4^{=}$. Also the presence of this solid phase potentially gives conditions which lead to supersaturation phenomena and periodic reactions (16,17).

Effect of Temperature on the First Order Decomposition of $Na_2S_2O_4$ in the Presence of $NaHSO_3$ and $Na_2S_2O_3$:- In Figure 13 and Table XIII, Tests 21ab and 22ab, are shown data for the first order thermal decomposition of $Na_2S_2O_4$. These data are for solutions 0.01 F in $Na_2S_2O_4$. The

solutions of Tests 21a and 22a are 0.5 F in HSO_3^- and the solutions of Tests 21b and 22b are 0.5 F in both HSO_3^- and $S_2O_3^=$. The data in Figure 13 are for 50° and 70° C. Comparable data for 60° are given in Tests 10a and 25c. In Figure 14 the specific first order rate constants obtained from taking slopes of Figures 13 and 8a and 11a are plotted against the reciprocal of the absolute temperature. From the slope of this so-called Arrhenius plot the apparent activation energy may be obtained. It is found to have a value of approximately 16.1 kcal/mol for solutions containing HSO_3^- and both HSO_3^- and $S_2O_3^=$. The specific first order rate constants are presented in Table XIV.

Atmospheric Oxidation of $Na_2S_2O_4$:- As seen in Figure 15, Tests 21cd, 22c, and 23a, and Table XV, Tests 21cd, 22cd, and 23a, the atmospheric oxidation of $Na_2S_2O_4$ given by the overall stoichiometry of equation (2) proceeds via an approximately first-order mechanism and the rate increases with temperature. A comparison of Test 21c and d at 50° C shows that with an increase in the flow rate of air, the decomposition rate is increased and thus the rates measured are partially dependent on diffusion rates. In the absence of NaOH in the solution or in the presence of 0.1 F $NaHSO_3$ the rate of oxidation is so extremely high that making measurements is very difficult, so basic solutions inhibit this oxidation. In the absence of buffering action, the $NaHSO_4$ formed during the oxidation may accelerate the decomposition of $Na_2S_2O_4$ since it is known that at concentrations of H^+ above 10^{-3} $Na_2S_2O_4$ rapidly decomposes. By a

comparison of Figure 15 with Figures 8a and 11a for decomposition it is evident that the former rates are much greater than the latter so that oxidation will overshadow thermal decomposition when air is not excluded.

SUMMARY AND CONCLUSIONS

The data presented here outline a reaction which appears to be extremely complex. Briefly, the decomposition of $Na_2S_2O_4$ is the chain branching type in pure aqueous solution but becomes first order with respect to the concentrations of $S_2O_4^{=}$ and HSO_3^-, when HSO_3^- is present in concentrations greater than that of the $Na_2S_2O_4$. Both the chain-branching reaction and the first-order reaction are catalyzed by the presence of HSO_3^- and $S_2O_3^{=}$. The first order reaction is but little affected by the concentration of H^+ in buffered solutions of $HSO_3^- - SO_3^{=}$, but in the presence of $S_2O_3^{=}$ a rise in the concentration of H^+ causes a more definite increase in the rate of decomposition. NaCl shows a positive salt effect by increasing the rate of decomposition. Colloidal sulfur increases the rate by a mechanism which has not been established. Neither $S^{=}$ nor $SO_3^{=}$ appear to affect either the chain-branching reaction or the first order reaction specifically, but both rates are greatly reduced when the concentration of H^+ becomes comparable to that in a solution of 0.1 F NaOH. The rate of atmospheric oxidation is also first order with respect to the concentration $S_2O_4^{=}$ in solutions 0.1 F in NaOH. The rate of oxidation in initially neutral solution is too high to measure with the present techniques.

The change in the reaction behavior with the accumulation of the products of the decomposition has discouraged the proposal of a specific reaction mechanism. The present practice in the industry of adding sodium hydroxide or carbonate as preservatives to sodium dithionite is seen to be a wise one, whereas the practice of adding sodium chloride is at best useless insofar as stabilizing the sodium dithionite is concerned.

REFERENCES

1. K. Jellinek, Z. phys. Chem., 93, 325 (1919).

2. K. Jellinek, Z. phys. Chem., 70, 93 (1911).

3. M. Nicloux, Compt. Rend., 196, 616 (1933).

4. E. Baatard, "Recherches sur la decomposition de l'hydrosulfite de sodium" Thesis Lausanne (1931).

5. D. Yost and H. Russel, Jr., "Systematic Inorganic Chemistry", Prentice-Hall, New York (1944).

6. K. Jellinek, "Das Hydrosulfit" 188 pg. F. Enke, Stuttgast (1911).

7. Bassett & Durant, J. Chem. Soc., 1401 (1927).

8. Knecht and Hibbert, Ber., 40, 3819 (1907).

9. J. L. Myers, Fainer, and Percy, Anal Chem., 24, 1384 (1952).

10. J. Rosin, "Reagent Chemicals", D. van Nostrand, New York (1937).

11. E. Swift, "Systematic Quantitative Analysis", Prentice-Hall, New York (1939).

12. S. Lynn and D. M. Mason, Anal. Chem., 24, 1844 (1952).

13. N. Semenoff, "Chemical Kinetics and Chain Reactions", Oxford Univ. Press, New York (1935) pp. 40-87, 454ff.

14. J. Murib and D. Ritter, J.A.C.S., 74, 3394 (1952).

15. W. Ramsey, Ph.D. Thesis, California Institute of Technology (1953).

16. Hedges and Myers, "The Problem of Physicochemical Periodicity", Arnold (1926).

17. M. Peard and C. Cullis, Trans. Faraday Soc., 47, 616 (1951).

18. V. LaMer, Chem. Rev., 10, 179 (1932).

19. R. Dinegar, R. Smellic and V. LaMer, J.A.C.S., 73, 2050 (1951).

LIST OF TABLES

LIST OF TABLES (cont.)

LIST OF FIGURES

LIST OF FIGURES (cont.)

TABLE I.

THERMAL DECOMPOSITION OF PURE $Na_2S_2O_4$ AT 60° C.

Test 1		Test 2		
Time	$(S_2O_4^{=})$	Time	$(S_2O_4^{=})$	(H^{+})
Min	Moles/lit x 10^{-3}	Min	Moles/lit x 10^{-3}	Moles/lit x 10^{-7}
1.0	<7.1	1.2	7.3	
3.0	6.4	4.0	6.7	
8.5	6.4	12.7	6.9	
13.2	6.4	18.0	7.0	
18.2	6.4	28.5	7.1	
27.0	6.6	34		2.88
36.5	6.6	38.5	6.8	
39.2	6.4	43		2.88
45.5	6.6	50.7	6.8	
51.5	6.6	61.5	6.2	
52.0	6.4	64		3.16
60.5	6.4	71.7	5.9	
72.5	6.3	73		3.55
82.0	6.2	81.7	5.6	
90.2	6.2			
106.5	5.8	86.0	5.2	
129.5	5.6	87		3.63
134.0	5.3	96.2	4.3	
185.5	3.0	98		5.12
189.5	2.0	102.7	2.2	
192.0	0.9	104		7.94
196.0	0.1	105.1	0.1	
		106		10.00
		106.1	<0.1	
		107		10.48

TABLE II.

DEGENERATE CHAIN BRANCHING NATURE OF DECOMPOSITION OF $Na_2S_2O_4$

Test 1			Test 2		
Time	$(S_2O_4^{=})^*$	$C_o - C$	Time	$(S_2O_4^{=})^*$	$C_o - C$
Min	Moles/lit x 10^{-3}	Moles/lit x 10^{-3}	Min	Moles/lit x 10^{-3}	Moles/lit x 10^{-3}
0	6.60	-	0	7.10	-
40	6.52	0.08	40	6.97	0.13
60	6.40	0.20	60	6.62	0.48
80	6.28	0.32	80	5.65	1.45
100	6.08	0.52	90	4.75	2.35
120	5.76	0.84	100	3.10	4.00
140	5.33	1.27			
160	4.70	1.90			
180	3.60	3.00			
190	2.35	4.25			

* Evaluated from smooth curves of Figure 1.

TABLE III.

PERIODIC FLUCTUATIONS IN THERMAL DECOMPOSITION OF $Na_2S_2O_4$

Test 3		Test 3		Test 4		
Time	$(S_2O_4^{=})$	Time	(H^{+})	Time	$(S_2O_4^{=})$	(H^{+})
Min	Moles/lit x 10^{-3}	Min	Moles/lit x 10^{-7}	Min	Moles/lit x 10^{-3}	Moles/lit x 10^{-7}
3.6	6.8	5.0	3.24	1.3	8.2	
9.5	6.8	22.0	3.47	3.0		2.19
12.5	6.4	37.0	3.63	4.5	7.7	
17.5	6.4	45.0	3.63	8.0	7.2	
23.5	6.4	59.0	3.71	14.7	7.2	
33.0	6.7	65.0	3.80	16.0		2.24
38.6	6.6	66.0	3.98	22.0		2.26
41.7	6.7	70.0	4.37	24.7	7.4	
50.5	6.4	74.0	4.46	35.2	7.1	
58.0	6.2	85.0	4.79	39.0		2.30
60.2	6.3	92.0	5.01	42.7	6.1	
64.0	6.1	98.0	5.01	49.0		2.40
69.7	5.8	109.0	5.25	54.0		2.46
75.5	5.0	122.0	5.37	55.0	6.9	
80.6	5.6	124.0	5.49	62.0		2.51
83.6	5.8	132.0	5.62	63.2	6.9	
88.5	5.3	138.0	5.75	69.0		2.57
96.0	5.8	145.0	6.31	73.2	7.0	
103.0	5.8	150.0	6.45	74.0		2.82
112.0	5.9	180.0	6.61	79.5	6.7	
122.0	5.3	190.0	6.92	80.0	6.8	
130.5	5.2	198.0	7.08	89.0		2.88
143.5	4.6	233.0	8.13	94.0		2.95
152.0	4.3	240.0	8.91	97.0	6.8	2.95
169.0	5.0	244.0	10.00	102.7	6.4	
191.7	4.3	250.0	10.48	104.0		3.16
235.2	2.9	252.0	11.23	110.0		3.39
246.7	2.2	256.0	13.80	122.7	5.4	
252.0	1.4	259.0	14.79	124.0		3.63
257.2	0.6	260.0	15.12	128.0	5.2	
260.2	0.4	263.0	15.49	130.0		4.26
263.7	< 0.1	266.0	15.84	132.2	4.4	
				135.0		5.01
				139.0	3.0	
				140.0		5.89
				143.0	1.7	
				144.0		7.08
				145.5	0.5	
				147.0		8.13
				150.0		8.91
				148.2	< 0.1	

TABLE IV.

EFFECT OF INITIAL CONCENTRATION IN THERMAL DECOMPOSITION OF $Na_2S_2O_4$ IN PRESENCE OF NaCl

Test 5 μ=1.00

a		b		c		d	
(NaCl) = 0.965F		(NaCl) = 0.915F		(NaCl) = 0.829F		(NaCl) = 0.654F	
Time	$(S_2O_4^{=})$	Time	$(S_2O_4^{=})$	Time	$(S_2O_4^{=})$	Time	$(S_2O_4^{=})$
Min	Moles/lit x 10^{-3}	Min	Moles/lit x 10^{-3}	Min	Moles/lit x 10^{-3}	Min	Moles/lit x 10^{-3}
6.5	8.1	7.5	20.6	7.5	40.2	6.5	81.8
16.0	8.5	17.0	20.5	16.0	40.2	16.0	79.8
19.0	8.0	20.5	19.8	30.0	4.9	33.0	31.3
46.0	7.8	47.0	0.4	36.0	4.5	35.0	28.5
64.2	7.0	65.5	0.3	46.0	4.2	46.2	28.0
72.5	5.3	83.5	0.3	65.5	3.7	64.5	24.7
79.5	0.2	125.0	0.3	93.0	3.1	72.5	24.1
81.5	0.2	161.0	0.3	124.0	2.4	93.0	20.2
124.0	0.1			161.0	1.9	125.0	16.4
160.0	<0.1			188.0	1.8	161.0	12.8
				312.2	0.8	188.0	10.4
						312.0	4.2

TABLE V.

EFFECT OF IONIC STRENGTH ON DECOMPOSITION OF $Na_2S_2O_4$

Test 6

a		b		c		d	
(NaCl) = 0		(NaCl) = 0.025 F μ = 0.025		(NaCl) = 0.10 F μ = 0.10		(NaCl) = 0.25 F μ = 0.25	
Time	$(S_2O_4^{=})$	Time	$(S_2O_4^{=})$	Time	$(S_2O_4^{=})$	Time	$(S_2O_4^{=})$
Min	Moles/lit x 10^{-3}	Min	Moles/lit x 10^{-3}	Min	Moles/lit x 10^{-3}	Min	Moles/lit x 10^{-3}
3.2	13.1	3.8	10.4	4.0	13.8	5.0	10.2
14.0	11.6	14.5	10.5	16.0	10.4	15.5	9.6
27.0	11.0	26.5	10.2	39.0	10.2	28.5	10.0
41.2	10.9	40.7	10.2	42.0	9.4	42.5	9.4
54.0	10.6	55.0	10.2	55.5	9.8	56.0	8.8
68.5	10.2	69.5	9.8	70.0	9.4	70.5	3.6
90.5	8.7	87.5	8.8	79.0	7.7	77.5	0.6
100.5	7.9	99.0	8.1	85.5	3.6	79.5	0.4
112.0	3.6	110.5	2.4	88.5	1.4	138.5	0.4
116.5	2.0	114.5	1.4	97.5	0.8	142.0	0.2
121.5	1.6	120.0	1.1	100.5	0.6	260.0	0.3
127.0	1.5	128.0	1.1	109.0	0.7		
140.5	1.4	141.5	1.0	138.0	0.7		
249.5	0.8	255.0	0.8	142.0	0.6		
				257.5	0.6		

TABLE VI.

THERMAL DECOMPOSITION OF $Na_2S_2O_4$ IN PRESENCE OF LOW CONCENTRATION OF $NaHSO_3$

Test 7 ($\mu = 0.02$)

a		b		c		d	
$(NaCl) = 0.02F$		$(NaCl) = 0.015F$ $(HSO_3^-) = 0.005F$		$(NaCl) = 0.01F$ $(HSO_3^-) = 0.01F$		$(HSO_3^-) = 0.02F$	
Time	$(S_2O_4^=)$	Time	$(S_2O_4^=)$	Time	$(S_2O_4^=)$	Time	$(S_2O_4^=)$
Min	Moles/lit x 10^{-3}	Min	Moles/lit x 10^{-3}	Min	Moles/lit x 10^{-3}	Min	Moles/lit x 10^{-3}
4.0	12.5	4.5	12.7	5.5	11.7	6.5	11.2
11.5	11.8	12.5	11.7	14.5	11.9	15.5	9.4
22.0	12.2	22.8	11.5	24.5	10.3	26.0	7.4
37.5	11.5	36.8	11.4	35.2	3.4	34.2	7.2
46.0	11.3	43.8	10.1	41.0	2.3	40.0	7.1
56.2	11.9	61.2	0.4	62.5	2.2	64.8	6.0
81.5	10.9	80.5	0.4	79.2	1.9	78.2	6.0
102.5	10.8	103.5	0.4	104.5	1.9	105.5	5.3
129.5	0.4	132.0	0.4	133.0	1.7	134.0	4.6
130.5	0.1	-	-	183.0	0.2	186.0	-
232.0	0.1	226.0	0.3	217.0	1.3	189.0	4.2
						221.0	3.8
						346.0	2.5

TABLE VI. (cont.)

Test 8 (μ = 0.02)

a		b		c		d	
		(NaCl) = 0.04F		(NaCl) = 0.05F (HSO_3^-) = 0.05F		(HSO_3^-) = 0.10F	
Time	($S_2O_4^=$)	Time	($S_2O_4^=$)	Time	($S_2O_4^=$)	Time	($S_2O_4^=$)
Min	Moles/lit x 10^{-3}	Min	Moles/lit x 10^{-3}	Min	Moles/lit x 10^{-3}	Min	Moles/lit x 10^{-3}
4.2	11.9	4.5	12.4	5.8	11.7	6.2	11.3
14.8	11.6	15.2	9.7	16.2	11.6	16.8	11.3
30.0	-	27.2	0.7	30.5	11.6	33.5	11.7
46.5	11.2	47.5	0.6	48.2	11.7	49.0	11.2
68.5	11.5			69.5	11.4	70.0	11.2
96.0	11.0			102.5	10.8	111.5	10.6
117.5	9.7			123.5	10.6	124.0	10.5
119.5	0.2			139.0	10.1	139.0	9.8
				155.5	9.9	162.5	9.2
				192.0	8.8	198.5	-

Test 24 (μ = 0.02)

(HCO_3^-) = 1.0F

Time	($S_2O_4^=$)
Min	Moles/lit x 10^{-3}
1.5	9.4
8.2	8.4
15.0	8.4
25.5	8.1
39.5	7.9
47.0	8.3
57.0	8.0
71.5	7.9
83.5	7.8
98.0	7.2
107.8	7.2
120.5	7.1
145.8	6.2
220.5	6.2

TABLE VII.

DECOMPOSITION OF $Na_2S_2O_4$ IN THE PRESENCE OF HIGH CONCENTRATIONS OF $NaHSO_3$

Test 9

a		b		c		d	
$(HSO_3^-) = 0.282F$		$(HSO_3^-) = 0.282F$ $(SO_3^=) = 0.50F$		$(HSO_3^-) = 0.141F$		$(HSO_3^-) = 0.141F$ $(SO_3^=) = 0.50F$	
Time	$(S_2O_4^=)$	Time	$(S_2O_4^=)$	Time	$(S_2O_4^=)$	Time	$(S_2O_4^=)$
Min	Moles/lit x 10^{-3}	Min	Moles/lit x 10^{-3}	Min	Moles/lit x 10^{-3}	Min	Moles/lit x 10^{-3}
3.8	11.4	5.0	11.4	5.8	11.5	6.8	11.2
12.8	10.4	13.5	10.8	14.8	10.3	17.2	10.8
22.8	10.0	24.2	10.2	27.5	10.1	29.5	10.4
43.0	8.7	44.2	9.8	45.5	9.9	46.5	10.0
58.0	8.0	58.2	8.6	59.2	9.4	60.2	9.4
74.2	6.6	78.2	7.4	81.2	7.8	84.0	8.3
89.2	5.9	94.8	6.6	97.0	7.3	99.8	7.8
104.2	4.9	107.5	5.8	111.5	6.6	114.5	7.4
125.0	4.5	126.0	5.7	127.0	6.6	128.0	7.4
140.0	4.0	141.8	5.0	142.5	6.0	143.5	6.6
158.2	3.4	159.2	4.3	160.2	5.0	160.8	5.7
175.8	2.9	180.8	3.7	185.2	4.6	188.2	5.7
210.5	2.1	216.0	2.9	217.2	3.8	218.0	4.6
237.2	1.4	238.2	2.3	238.8	3.1	239.8	3.9
259.0	1.1	259.8	1.9	260.5	2.8	261.2	3.6
286.8	0.9	287.8	1.5	288.5	2.3	289.5	3.0

TABLE VII. (cont.)

Test 10

a		b		c		d	
$(HSO_3^-) = 0.50F$		$(HSO_3^-) = 0.50F$ $(SO_3^=) = 0.50F$		$(HSO_3^-) = 0.10F$		$(HSO_3^-) = 0.10F$ $(SO_3^=) = 0.10F$	
Time	$(S_2O_4^=)$	Time	$(S_2O_4^=)$	Time	$(S_2O_4^=)$	Time	$(S_2O_4^=)$
Min	Moles/lit x 10^{-3}	Min	Moles/lit x 10^{-3}	Min	Moles/lit x 10^{-3}	Min	Moles/lit x 10^{-3}
1.8	11.5	2.8	12.1	4.8	12.0	5.8	11.8
9.0	11.2	10.0	11.2	10.5	11.2	11.5	10.6
18.0	9.9	19.0	10.4	20.0	10.8	20.8	10.2
25.0	8.9	26.0	9.3	29.5	10.6	30.5	10.6
38.0	7.9	39.0	8.4	39.5	10.3	40.2	9.9
48.8	6.8	49.5	7.6	50.5	9.6	51.5	9.1
62.5	5.5	63.5	6.3	64.5	9.4	65.2	9.1
77.0	4.6	78.5	5.6	79.5	9.4	80.5	9.1
94.5	3.8	95.5	4.6	96.5	8.6	97.2	8.8
116.2	2.2	117.0	2.9	118.0	6.5	101.8	8.8
135.8	1.9	136.8	2.6	137.8	7.2	107.0	8.6
148.8	1.4	149.5	2.1	150.8	7.0	110.8	8.7
						112.2	8.7
						119.0	6.9
						131.0	7.8
						138.8	6.9
						151.5	7.2
						159.5	7.0
						162.5	7.0

TABLE VII. (cont.)

Test 11

Dichromate Analysis

$(HSO_3^-) = 0.452F$

Time Min	$(S_2O_4^{=})$ Moles/lit x 10^{-3}
2.1	10.7
8.4	9.9
12.3	9.4
38.2	8.5
51.2	8.4
67.0	7.4
82.0	6.7
97.0	6.2
112.0	6.0
127.5	4.8
142.5	3.9
159.5	3.3
106.0	2.6

Test 12

a

$(HSO_3^-) = 0.50F$

Time Min	$(S_2O_4^{=})$ Moles/lit x 10^{-3}
7.5	6.0
17.5	5.3
26.5	4.6
34.5	3.8
44.0	3.2
52.2	2.7
61.8	2.3
72.5	2.1
87.2	1.5
101.0	1.0
119.8	0.7
142.0	0.4
176.0	0.2

b

$(HSO_3^-) = 0.50F$

Time Min	$(S_2O_4^{=})$ Moles/lit x 10^{-3}
8.8	11.8
19.2	9.8
27.8	8.4
35.5	6.8
45.0	6.0
53.2	5.0
62.8	4.0
73.2	3.1
88.0	2.1
102.0	1.3
122.5	0.8
144.0	0.4
178.0	0.1

Test 25

a

$\mu = 0.4$

$(NaOH) = 0.1F$

Time Min	$(S_2O_4^{=})$ Moles/lit x 10^{-3}
4.0	11.8
12.0	11.2
27.0	12.3
41.0	11.4
53.0	13.0
90.0	12.6
125.0	12.4
170.0	12.4
238.0	11.6
288.0	12.2
393.0	12.4
478.0	12.8
1180.0	12.1
1833.0	11.9
2705.0	11.2
2998.0	9.7
4090.0	7.4

b

$\mu = 2.0$

$(SO_3^{=}) = 0.5F$

Time Min	$(S_2O_4^{=})$ Moles/lit x 10^{-3}
6.0	11.0
13.0	11.7
31.0	11.8
43.0	9.6
55.0	11.6
91.0	11.2
104.0	11.7
132.0	11.0
180.0	10.6
246.0	10.0
294.0	9.3
397.0	8.4
482.0	7.5
1187.0	2.4
1837.0	0.9
2710.0	0.2

c

$\mu = 0.4$

$(S^{=}) = 0.1F$

Time Min	$(S_2O_4^{=})$ Moles/lit x 10^{-3}
18.0	9.6
26.0	10.4
40.0	10.6
88.0	10.5
388.0	9.6
1176.0	8.2
1831.0	8.3
2701.0	6.3

TABLE VIII.

FIRST ORDER NATURE OF THE THERMAL DECOMPOSITION OF $Na_2S_2O_4$ IN THE PRESENCE OF HIGH CONCENTRATIONS OF $NaHSO_3$

Test No.	Initial $(S_2O_4^{=})$ Moles/lit x 10^{-3}	(HSO_3^{-}) Moles/lit	$(SO_3^{=})$ Moles/lit	k (Min^{-1}) x 10^{-3}	(H^{+}) Moles/lit x 10^{-7}
9 a	10	0.282	-	3.90	117.5
b	10	0.282	0.50	3.10	1.55
c	10	0.141	-	2.50	120.1
d	10	0.141	0.25	2.00	1.95
10 a	10	0.50	-	6.42	117.5
b	10	0.50	0.50	5.64	2.88
c	10	0.10	-	1.61	132.0
d	10	0.10	0.10	1.28	3.72
12 a	50	0.50	-	8.41	79.5
b	100	0.50	-	9.19	83.2

TABLE IX.

THERMAL DECOMPOSITION OF $Na_2S_2O_4$ IN THE PRESENCE OF SULFUR AND LOW CONCENTRATIONS OF NaCl AND $Na_2S_2O_3$

Test 13

a		b		c		d	
(NaCl) = 0.02F		(NaCl) = 0.02F		$(S_2O_3^{=})$ = 0.01F		Colloidal S	
Time	$(S_2O_4^{=})$	Time	$(S_2O_4^{=})$	Time	$(S_2O_4^{=})$	Time	$(S_2O_4^{=})$
Min	Moles/lit x 10^{-3}	Min	Moles/lit x 10^{-3}	Min	Moles/lit x 10^{-3}	Min	Moles/lit x 10^{-3}
4.2	13.0	4.2	12.3	5.8	12.5	6.5	11.0
11.0	11.8	12.0	11.4	13.2	11.4	14.0	10.6
22.5	11.8	23.5	11.3	24.5	11.6	25.0	11.1
35.5	11.7	36.5	11.1	37.5	11.2	38.5	10.6
47.5	11.6	48.5	10.8	49.0	11.1	51.0	10.4
63.0	11.2	71.0	10.8	76.0	9.4	79.0	8.8
75.0	11.0	89.0	10.6				
108.5	10.2	111.5	9.9	97.5	0.2	95.5	0.1
120.5	9.3	121.5	8.8				
130.5	3.4	131.5	6.4				
132.5	0.5	133.5	5.1				
135.5	0.1	136.5	0.9				
		139.5	0.1				
149.0	0.1	150.0	0.1				

TABLE X.

THERMAL DECOMPOSITION OF $Na_2S_2O_4$ IN THE PRESENCE OF HIGH CONCENTRATIONS OF $Na_2S_2O_3$ AND $NaHSO_3$ COMPARED TO A RUN WITH NO ADDITIVES

Test 12

c

$(S_2O_3^{=}) = 0.4F$
$(HSO_3^{-}) = 0.5F$

Time	$(S_2O_4^{=})$
Min	Moles/lit x 10^{-3}
10.0	4.3
20.2	3.5
29.0	2.7
37.2	1.7
46.0	1.3
54.5	1.0
64.0	0.7
74.0	0.5
89.0	0.1
103.0	0.1

d

$(S_2O_3^{=}) = 0.40F$
$(HSO_3^{-}) = 0.50F$

Time	$(S_2O_4^{=})$
Min	Moles/lit x 10^{-3}
12.0	9.7
21.5	7.3
30.5	5.0
38.8	3.0
47.2	2.5
55.5	1.2
65.5	0.7
77.0	0.7
90.5	0.2
104.0	0.04

Test 14

a

$(S_2O_3^{=}) = 0.10F$
$(HSO_3^{-}) = 0.10F$

Time	$(S_2O_4^{=})$
Min	Moles/lit x 10^{-3}
4.2	11.2
10.0	8.8
17.0	8.4
26.0	7.4
38.0	5.7
51.5	4.9
71.8	4.6
104.8	3.0
136.0	2.2
166.0	1.4
203.0	0.8
248.0	0.5

b

$(S_2O_3^{=})$ 0.10F

Time	$(S_2O_4^{=})$
Min	Moles/lit x 10^{-3}
5.0	12.4
10.5	7.4
18.0	2.2
21.5	1.5
32.0	1.6
38.8	1.4
52.0	1.3
73.0	1.0
109.0	0.8
139.5	0.5
169.5	0.2

TABLE X. (cont.)

Test 15

a		b		c		d	
				$(HSO_3^-) = 0.50\,F$ $(SO_3^=) = 0.25\,F$ $(S_2O_3^=) = 0.25\,F$		$(HSO_3^-) = 0.50\,F$ $(SO_3^=) = 0.25\,F$ $(S_2O_3^=) = 0.25\,F$	
Time	$(S_2O_4^=)$	Time	$(S_2O_4^=)$	Time	$(S_2O_4^=)$	Time	$(S_2O_4^=)$
Min	Moles/lit x 10^{-3}	Min	Moles/lit x 10^{-3}	Min	Moles/lit x 10^{-3}	Min	Moles/lit x 10^{-3}
3.0	11.5	4.0	10.9	4.5	4.0	5.0	9.9
10.7	11.2	11.2	10.0	12.5	9.0	13.2	8.9
20.2	10.7	21.0	9.7	22.0	8.2	23.0	7.8
30.3	10.6	31.2	9.6	32.0	6.9	33.0	6.7
42.7	10.4	42.5	10.0	44.0	6.3	45.2	5.6
53.7	11.4	54.7	10.8	55.7	5.4	56.5	5.4
60.5	6.6	61.5	7.2	62.2	3.7	68.5	5.4
68.0	8.1	69.2	8.9	70.0	3.9	70.7	3.3
80.2	9.4	81.0	6.9	81.0	2.4	82.2	2.5
90.0	7.9	91.0	7.5	92.0	3.0	93.5	2.5
100.7	5.9	101.5	4.6	102.2	2.2	103.0	2.0
117.7	0.2	112.5	0.1	113.0	2.4	113.7	2.4
				122.5	2.4	123.2	2.1
				137.2	1.8	138.2	1.8
				194.0	0.8	196.0	0.6

TABLE X. (cont)

Test 16

a		b		c		d	
$(HSO_3^-) = 0.25F$		$(HSO_3^-) = 0.25F$		$(HSO_3^-) = 0.25F$		$(HSO_3^-) = 0.50F$	
$(S_2O_3^=) = 0.10F$		$(S_2O_3^=) = 0.25F$		$(S_2O_3^=) = 0.50F$		$(S_2O_3^=) = 0.50F$	
Time	$(S_2O_4^=)$	Time	$(S_2O_4^=)$	Time	$(S_2O_4^=)$	Time	$(S_2O_4^=)$
Min	Moles/lit x 10^{-3}	Min	Moles/lit x 10^{-3}	Min	Moles/lit x 10^{-3}	Min	Moles/lit x 10^{-3}
2.8	10.3	4.0	11.6	4.8	13.2	5.5	9.2
10.0	10.2	11.0	9.2	12.0	7.9	13.2	7.2
16.2	10.2	17.0	8.5	17.8	7.0	19.2	6.3
23.5	8.2	24.2	6.6	25.0	5.1	26.0	3.0
30.2	7.6	31.2	5.7	32.0	4.2	33.0	3.3
38.2	6.7	39.2	4.8	40.8	3.4	41.5	2.7
48.0	5.6	49.5	3.7	50.0	2.5	50.8	1.7
57.5	4.6	58.5	3.0	59.0	1.6	60.0	1.1
68.3	4.1	69.3	2.4	70.0	1.1	71.0	0.8
87.5	3.1	88.5	1.6	89.0	0.7	90.2	0.3
103.0	2.0	103.8	1.0	104.8	0.3		
121.0	1.3	123.5	0.5				
146.0	1.0	148.5	0.2				
172.0	0.7						

TABLE X. (cont.)

Test 17

a		b	
$(HSO_3^-) = 0.10F$		$(HSO_3^-) = 0.25F$	
$(S_2O_3^=) = 0.25F$		$(S_2O_3^=) = 0.25F$	
$(SO_3^=) = 0.40F$		$(SO_3^=) = 0.25F$	
Time	$(S_2O_4^=)$	Time	$(S_2O_4^=)$
Min	Moles/lit x 10^{-3}	Min	Moles/lit x 10^{-3}
1.8	11.0	3.5	8.9
8.5	10.4	9.5	8.6
25.8	4.5	22.0	8.9
31.5	8.7	32.8	8.3
45.0	8.3	46.0	7.2
57.8	8.9	58.5	6.6
77.0	9.0	80.0	6.7
98.0	4.9	103.0	5.0
118.0	5.9	119.0	3.7
146.0	6.4	150.5	3.6
146.5	6.2	151.0	3.3
179.0	5.3	190.5	2.4
204.0	4.6	207.2	1.9
251.0	3.4	253.5	1.2
292.5	2.9	294.5	0.8

TABLE X. (cont.)

Test 18

a		b		c	
(HSO_3^-) = 0.25F		(HSO_3^-) = 0.25F		(HSO_3^-) = 0.25F	
$(SO_3^=)$ = 0.01F		$(SO_3^=)$ = 0.05F		$(SO_3^=)$ = 0.15F	
$(S_2O_3^=)$ = 0.25F		$(S_2O_3^=)$ = 0.25F		$(S_2O_3^=)$ = 0.25F	
Time	$(S_2O_4^=)$	Time	$(S_2O_4^=)$	Time	$(S_2O_4^=)$
Min	Moles/lit x 10^{-3}	Min	Moles/lit x 10^{-3}	Min	Moles/lit x 10^{-3}
5.0	8.9	4.5	9.1	4.0	9.9
12.5	8.4	11.5	8.5	10.5	9.2
19.5	8.6	20.5	7.9	21.0	7.9
31.0	6.4	30.0	8.9	29.5	8.9
				35.5	5.9
				38.2	8.6
				40.8	8.2
43.0	5.9	43.5	6.7	44.2	6.9
				49.5	7.4
56.2	5.0	57.2	6.5	58.0	7.3
68.5	3.5	69.0	4.9	69.5	5.7
76.5	3.5	77.5	5.2	78.0	5.9
87.5	3.0	83.5	4.1	89.5	5.2
91.8	2.4				
100.0	2.3	100.5	3.4	101.5	4.5
113.8	1.9	114.8	3.1	115.8	4.1
133.5	1.3	134.0	2.5	135.0	3.6
168.0	0.6	170.0	1.6	173.0	2.3

TABLE XI.

FIRST ORDER NATURE OF THE THERMAL DECOMPOSITION OF $Na_2S_2O_4$ IN THE PRESENCE OF MIXTURES OF HIGH CONCENTRATIONS OF $NaHSO_3$ AND $Na_2S_2O_3$

Test No.	Initial $(S_2O_4^{=})$ Moles/lit x 10^{-3}	(HSO_3^{-}) Moles/lit	$(S_2O_3^{=})$ Moles/lit	$(SO_3^{=})$ Moles/lit	k (Min^{-1}) x 10^{-3}	(H^{+}) Moles/lit x 10^{-7}
12 c	50	0.50	0.40	-	18.7	79.5
d	100	0.50	0.40	-	23.12	79.5
14 a	10	0.10	0.10	-	5.66	117.3
16 a	10	0.25	0.10	-	7.56	120.1
b	10	0.25	0.25	-	11.20	123.0
c	10	0.25	0.50	-	15.33	117.3
d	10	0.50	0.50	-	17.69	117.3
17 a	10	0.10	0.25	0.40	15.8	0.83
b	10	0.25	0.25	0.25	12.7	3.24
18 a	10	0.25	0.25	0.01	6.61	49.0
b	10	0.25	0.25	0.05	4.33	18.2
c	10	0.25	0.25	0.15	3.35	6.02

TABLE XII.

FIRST ORDER NATURE OF THE ABSORBANCE-TIME RELATIONSHIP FOR THE THERMAL DECOMPOSITION OF $Na_2S_2O_4$

Test 19

a		b		c		d	
$(HSO_3^-) = 0.50F$							
$(SO_3^=) = 0.25F$		$(S_2O_3^=) = 0.25F$		$(S_2O_3^=) = 0.63F$		$(S_2O_3^=) = 0.63F$	
Time	$(S_2O_4^=)$	Time	Absorbance	Time	$(S_2O_4^=)$	Time	Absorbance
Min	Moles/lit x 10^{-3}	Min	@ 400 mμ	Min	Moles/lit x 10^{-3}	Min	@ 400 mμ
3.8	10.6	3.0	0.550	1.5	8.7	2.0	0.493
6.5	10.1	8.0	0.538	3.5	6.9	4.0	0.450
10.0	7.7	10.0	0.515	5.5	5.6	5.0	0.428
13.5	8.9	12.0	0.498	7.8	5.4	5.5	0.412
17.2	8.4	14.0	0.482	11.8	3.4	6.0	0.400
21.0	7.7	17.0	0.463	15.8	2.9	6.5	0.386
25.2	7.1	19.0	0.443	18.2	2.5	7.0	0.362
30.3	6.4	21.0	0.431	21.2	2.1	7.5	0.347
35.8	6.4	24.0	0.417	23.7	1.8	8.0	0.330
40.0	5.5	26.0	0.401	27.0	1.6	8.5	0.315
43.2	4.7	29.0	0.381	31.2	1.2	9.0	0.300
46.8	4.7	31.0	0.370	37.0	0.9	9.5	0.288
49.5	3.9	34.0	0.354	42.0	0.7	10.0	0.275
55.5	4.1	36.0	0.343	52.0	0.5	10.5	0.266
60.0	3.8	38.0	0.330			11.0	0.257
64.0	3.4	40.0	0.320			12.0	0.240
68.8	3.1	42.0	0.310			13.0	0.225
72.0	2.9	45.0	0.295			14.0	0.210
83.5	2.0	48.0	0.280			15.0	0.198
89.8	1.9	51.0	0.268			16.0	0.186
106.0	1.4	54.0	0.254			17.0	0.176
116.0	1.1	58.0	0.240			18.0	0.169
		62.0	0.225			19.0	0.160
		66.0	0.210			20.0	0.151
		70.0	0.197			21.0	0.145
		75.0	0.185			22.0	0.132
		81.0	0.169			26.0	0.112
		85.0	0.158			28.0	0.106
		89.0	0.146			32.0	0.089
		94.0	0.137			37.0	0.075
		99.0	0.126			42.0	0.065
		104.0	0.116			48.0	0.055
		109.0	0.108			59.0	0.051

TABLE XII. (cont).

Test 20

a		b	
(HSO_3^-) = 1.0F		(HSO_3^-) = 1.0F	
Time	$(S_2O_4^{=})$	Time	Absorbance
Min	Moles/lit x 10^{-3}	Min	@ 400 mμ
2.2	12.4	0	0.801
6.2	11.4	1.0	0.791
9.8	10.8	2.0	0.757
14.5	10.1	3.0	0.732
18.0	9.1	4.0	0.717
22.0	7.8	5.0	0.697
27.8	7.1	6.0	0.678
32.8	6.1	7.0	0.660
36.0	5.5	8.0	0.653
42.5	4.5	9.0	0.630
47.5	3.7	10.0	0.616
51.5	3.2	12.0	0.590
57.2	2.7	14.0	0.564
64.0	2.1	16.0	0.534
66.2	1.8	18.0	0.510
70.8	1.6	20.0	0.484
76.2	1.1	22.0	0.459
82.2	1.0	24.0	0.430
87.5	0.8	26.0	0.410
92.2	0.6	28.0	0.388
97.2	0.4	30.0	0.368
111.0	0.2	32.0	0.351
196.0	0.1	35.0	0.326
		39.0	0.295
		43.0	0.268
		47.0	0.241
		51.0	0.219
		59.0	0.177
		66.0	0.149
		72.0	0.131
		76.0	0.117
		83.0	0.102
		88.0	0.092
		93.0	0.083
		100.0	0.073
		107.0	0.063
		137.0	0.042
		164.0	0.046
		194.0	0.047
		288.0	0.025

TABLE XIII.

FIRST ORDER RELATIONSHIP FOR THERMAL DECOMPOSITION OF $Na_2S_2O_4$ IN PRESENCE OF $NaHSO_3$ AND $Na_2S_2O_3$ AT VARIOUS TEMPERATURES

Test 21 t = 50°C

a

$(HSO_3^-) = 0.50F$

Time Min	$(S_2O_4^=)$ Moles/lit x 10^{-3}
2.5	10.9
6.0	10.8
12.5	9.6
17.5	9.7
24.0	9.6
30.0	9.5
37.0	9.2
46.0	8.5
57.0	8.1
69.8	7.6
82.2	6.9
99.0	6.4
113.8	5.3
125.5	5.0
131.5	4.4
156.5	4.1
179.5	3.5
221.0	2.8
279.0	1.1

b

$(HSO_3^-) = 0.50F$
$(S_2O_3^=) = 0.50F$

Time Min	$(S_2O_4^=)$ Moles/lit x 10^{-3}
3.2	10.5
7.0	9.7
13.2	8.6
18.5	7.8
24.8	7.0
30.8	6.4
37.5	5.6
46.8	4.9
57.8	4.0
70.2	3.2
82.8	2.6
100.8	2.0
114.2	1.3
126.5	1.1
132.0	0.9
156.5	0.6
180.5	0.4

Test 22 t = 70°C

a

$(HSO_3^-) = 0.50F$

Time Min	$(S_2O_4^=)$ Moles/lit x 10^{-3}
1.8	6.6
3.8	6.3
7.0	7.7
11.8	7.4
16.8	6.8
21.2	5.9
26.5	5.4
33.8	4.4
41.0	3.5
51.2	2.7
63.0	2.0
73.0	1.4
86.0	0.9
118.5	0.4
145.2	0.1

b

$(HSO_3^-) = 0.50F$
$(S_2O_3^=) = 0.50F$

Time Min	$(S_2O_4^=)$ Moles/lit x 10^{-3}
2.5	9.0
4.5	7.0
7.8	5.3
12.5	3.7
17.2	2.7
22.0	2.2
27.2	1.1
34.5	0.5
41.3	0.2
73.8	0.1

TABLE XIV.

FIRST ORDER RATE CONSTANTS AS A FUNCTION OF TEMPERATURE

Temperature	k Min^{-1} x 10^{-3}	Test No.	k Min^{-1} x 10^{-3}	Test No.
70° C	12.3	22a	40.0	22b
60° C	6.12	10a	17.2	16d
50° C	2.77	21a	8.06	21b

TABLE XV

FIRST ORDER NATURE OF ATMOSPHERIC OXIDATION OF AQUEOUS SOLUTIONS OF $Na_2S_2O_4$ AT VARIOUS TEMPERATURES

Test 21 t = 50°C		Test 22 t = 70°C		Test 23 t = 60°C	
c		d		c	a
(NAOH) = 0.10F		(NaOH) = 0.10F		(NaOH) = 0.10F	(NaOH) = 0.10F
Time Min	$(S_2O_4^{=})$ Moles/lit x 10^{-3}	Time Min	$(S_2O_4^{=})$ Moles/lit x 10^{-3}	Time Min	$(S_2O_4^{=})$ Moles/lit x 10^{-3}	Time Min	$(S_2O_4^{=})$ Moles/lit x 10^{-3}
0	12.1	0	12.0	0	11.2	1.5	12.6
8.0	11.9	1.8	11.0	2.5	10.9	8.5	12.6
8.2	10.3	2.0	10.1	3.0	7.8	46.0	-
8.8	8.0	2.8	8.7	3.2	5.8	46.2	12.5
9.8	5.5	3.2	7.2	3.8	2.8	47.0	10.8
10.8	5.4	3.8	5.6	4.0	1.7	47.8	8.2
11.5	4.1	4.5	4.6	4.9	0.5	48.5	6.0
13.0	1.7	5.0	2.3	5.7	0.1	49.8	4.0
14.0	2.1	6.5	1.0	6.8	-	50.8	3.0
15.5	1.1	8.5	5.0			51.8	1.6
17.0	0.8	9.5	0.1			53.0	1.0
18.0	0.4	10.5	-			54.0	0.5
19.8	0.1					55.2	0.2
20.8	-					56.5	0.8

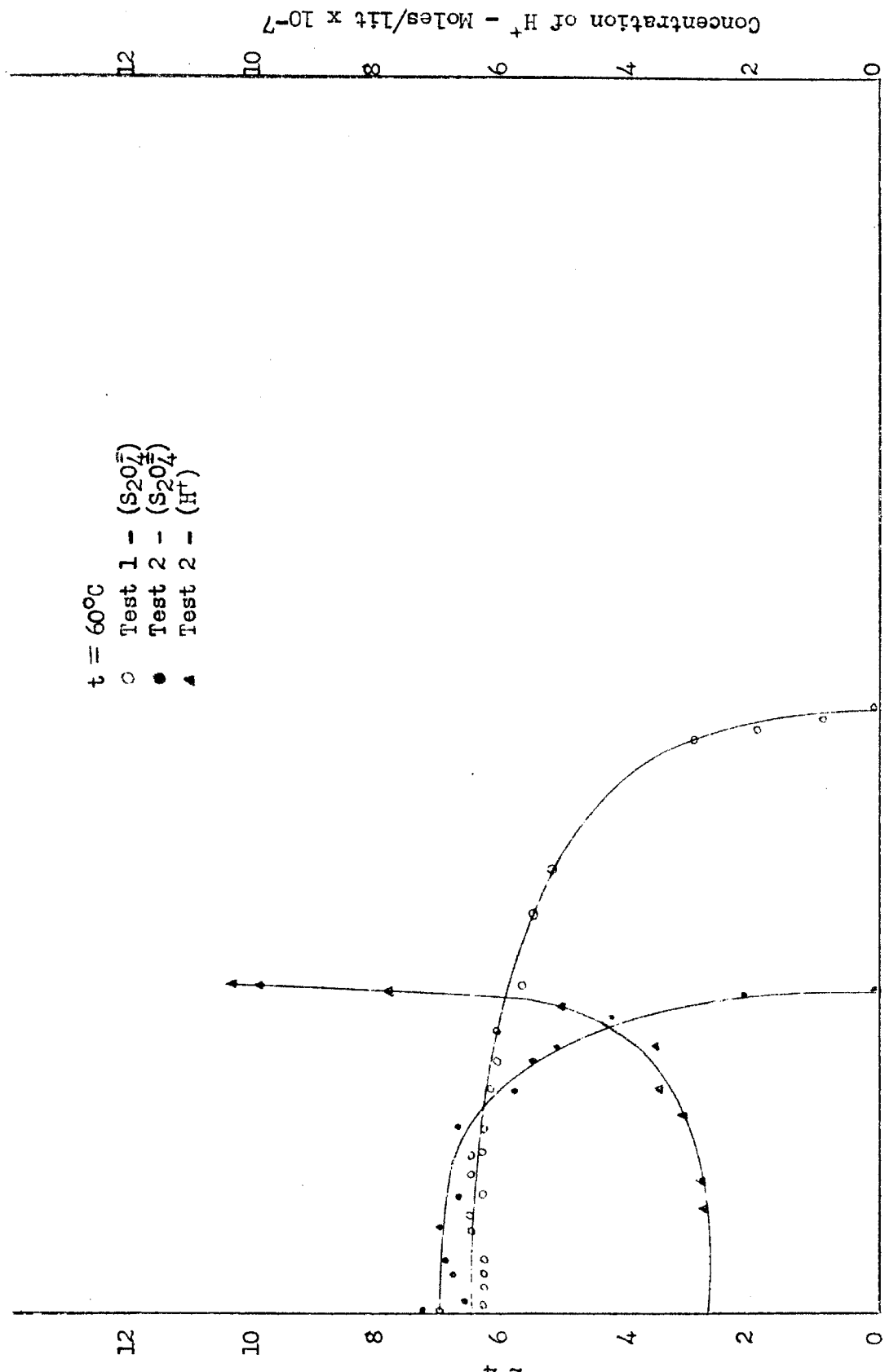

Figure 1 - Thermal Decomposition of $Na_2S_2O_4$

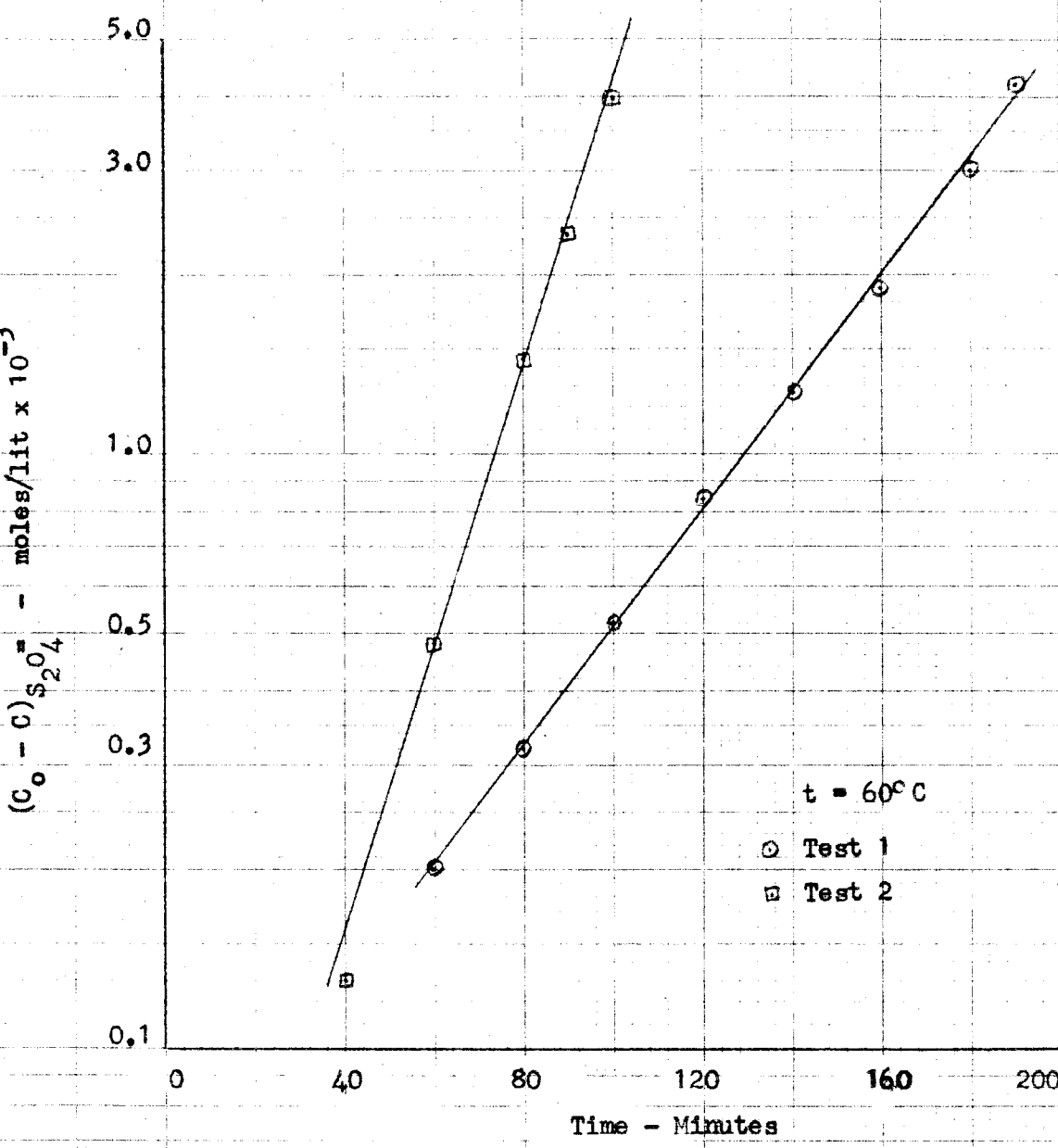

Figure 2 - Degenerate Chain Branching Nature of Decomposition of $Na_2S_2O_4$

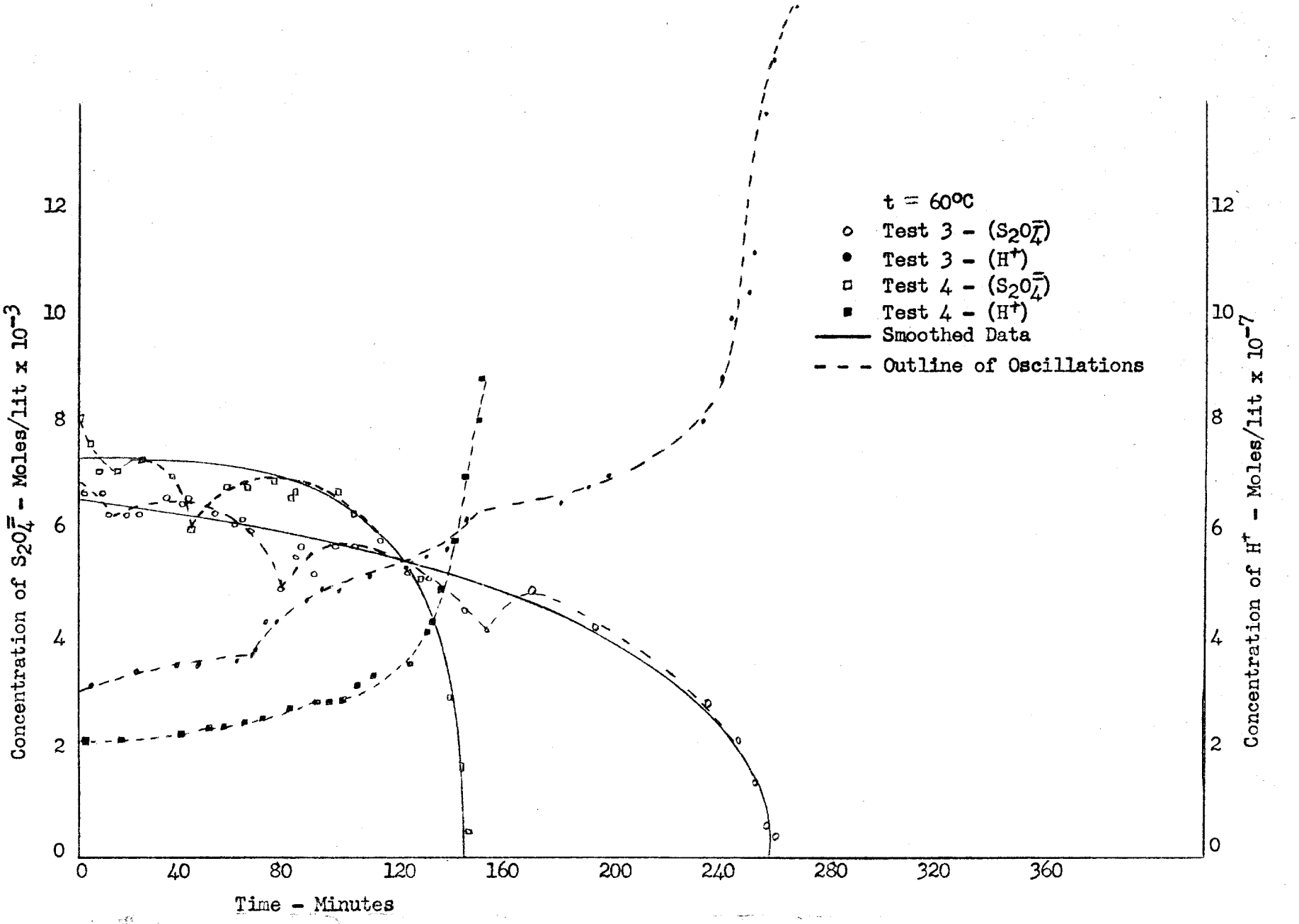

Figure 3 - Periodic Fluctuations in Thermal Decomposition of $Na_2S_2O_4$

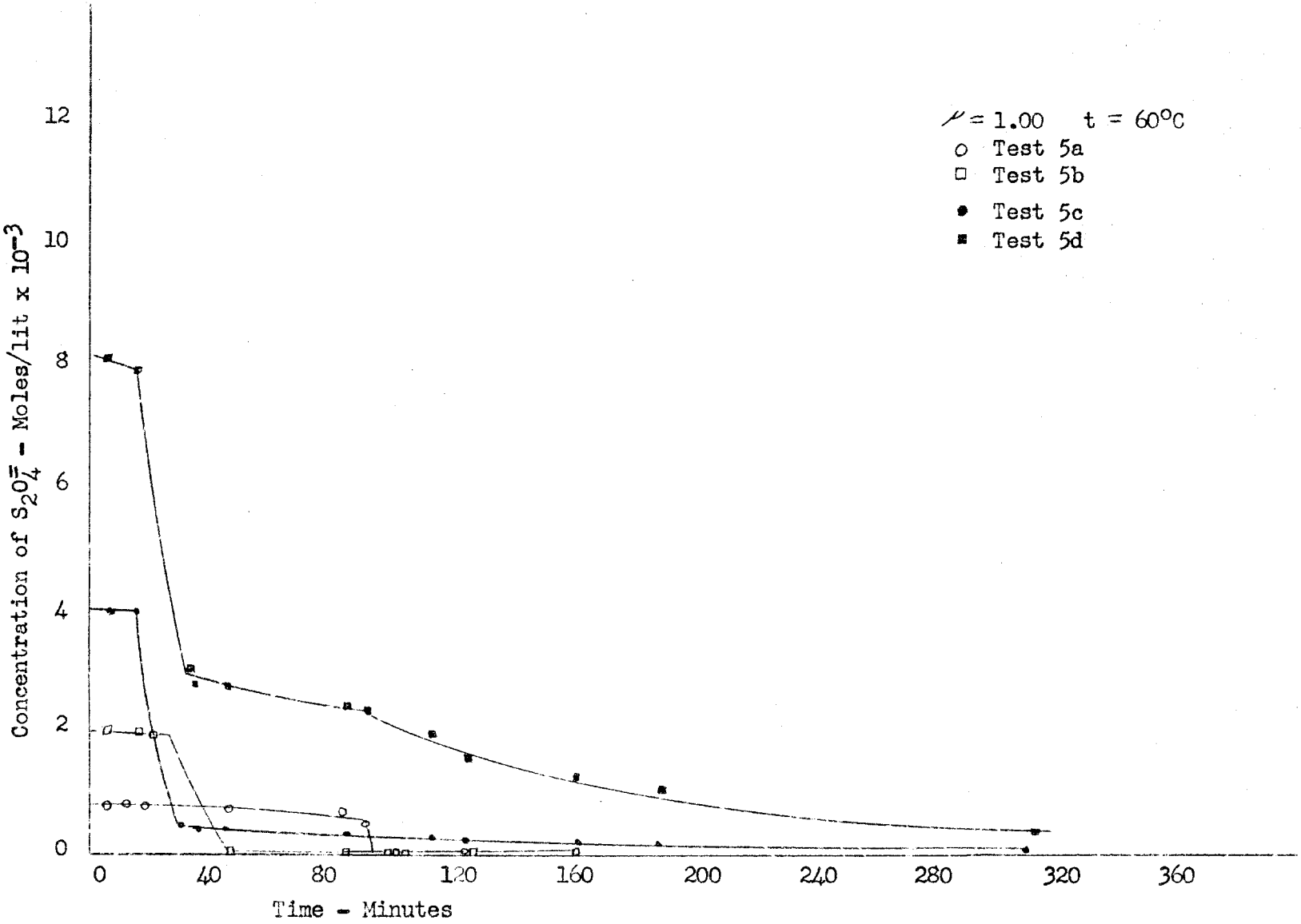

Figure 4 - Effect of Initial ($S_2O_4^{=}$) on Thermal Decomposition in the Presence of NaCl

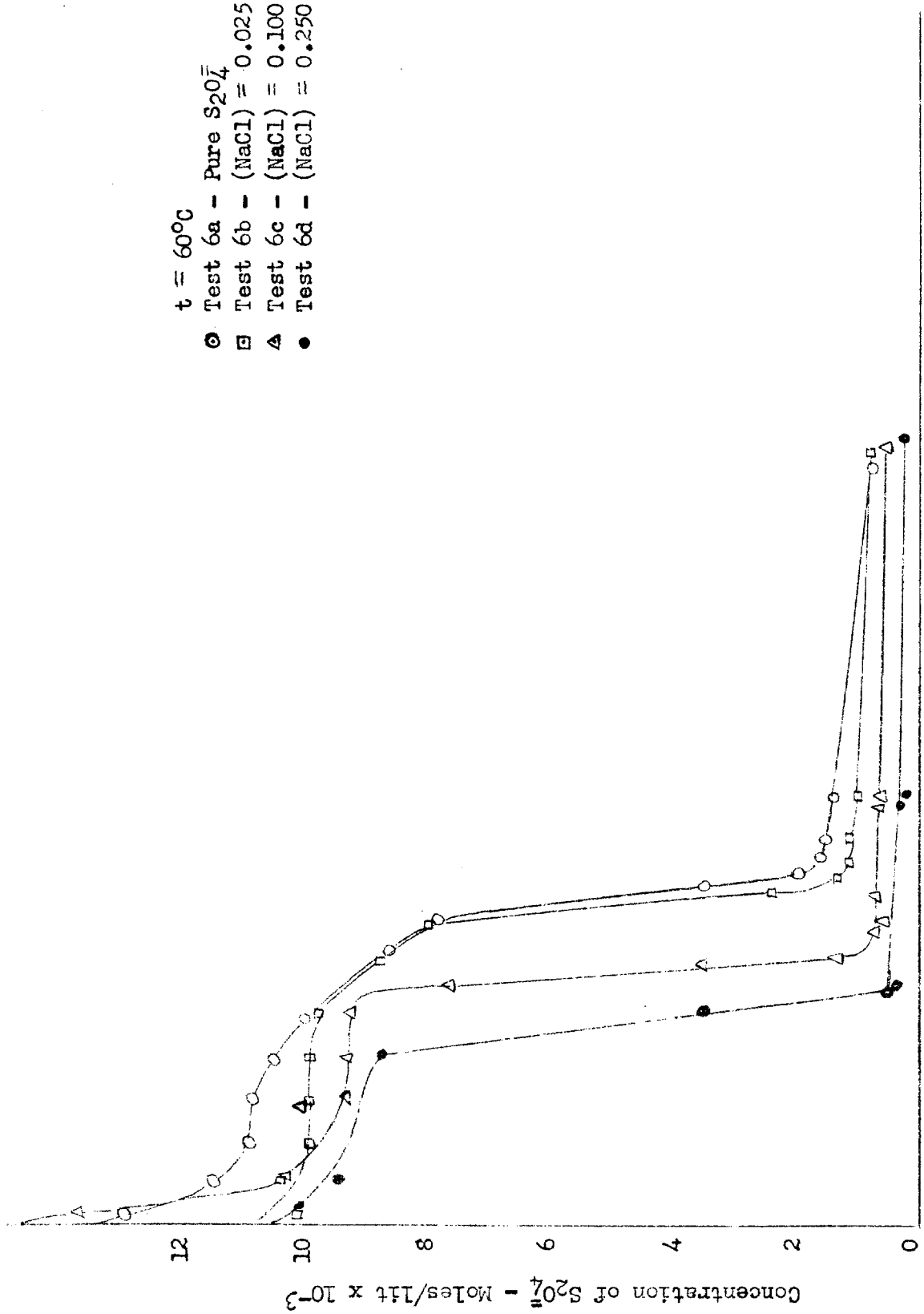

Figure 5 - Effect of Ionic Strength on Thermal Decomposition of $Na_2S_2O_4$

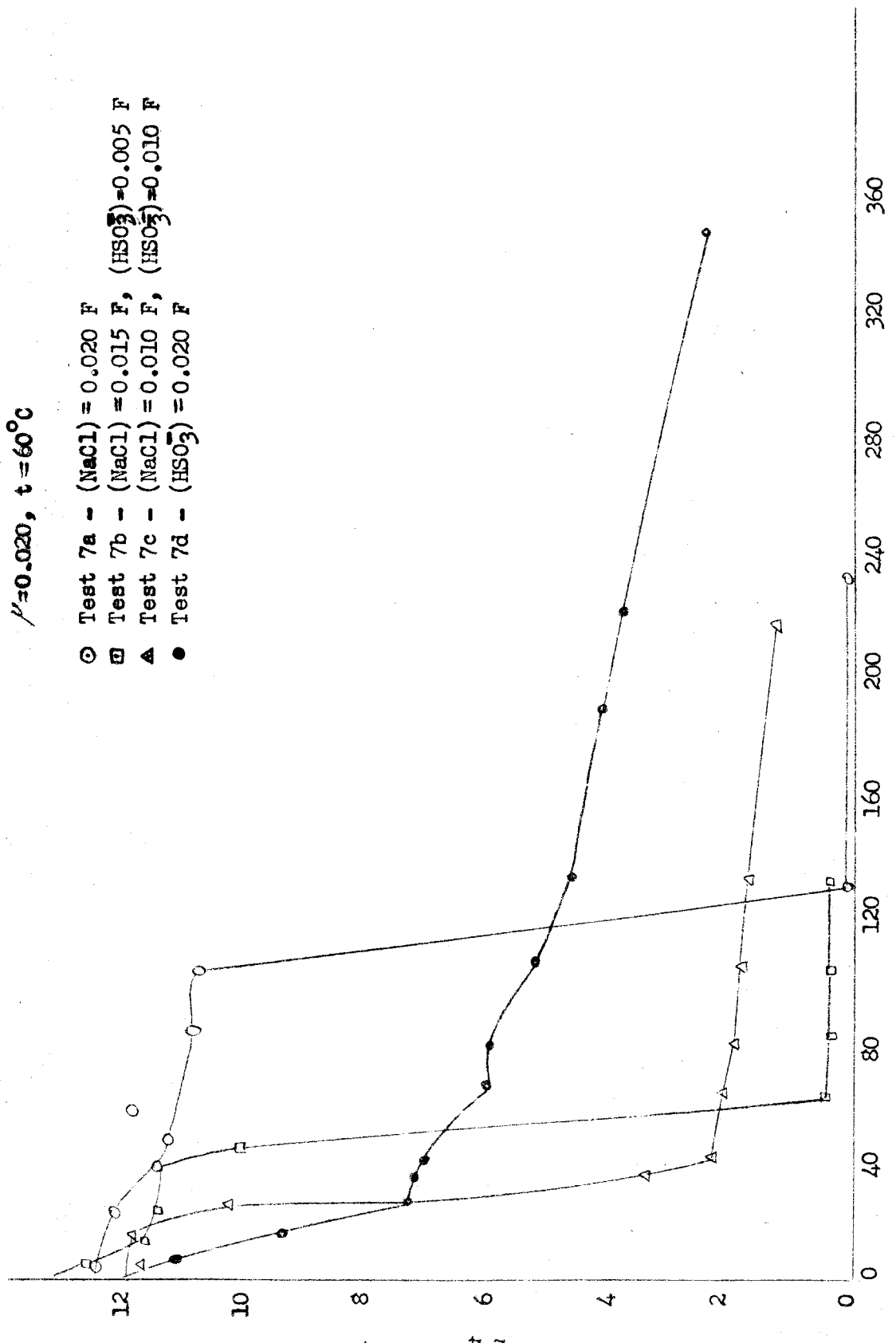

Figure 6 - Thermal Decomposition of $Na_2S_2O_4$ in the Presence of Low Concentrations of $NaHSO_3$

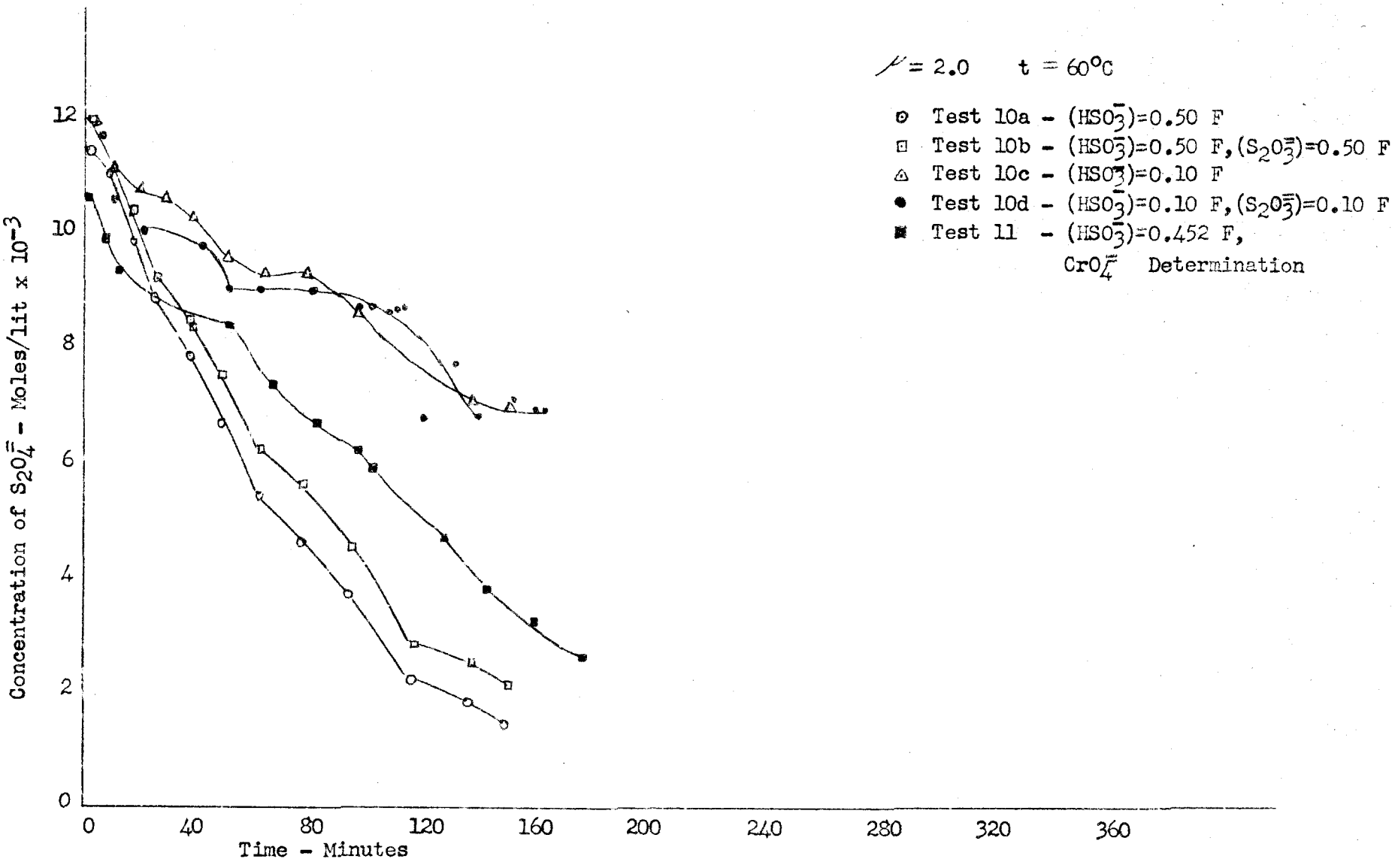

Figure 7a - Thermal Decomposition of $Na_2S_2O_4$ in Presence of High Concentrations of $NaHSO_3$

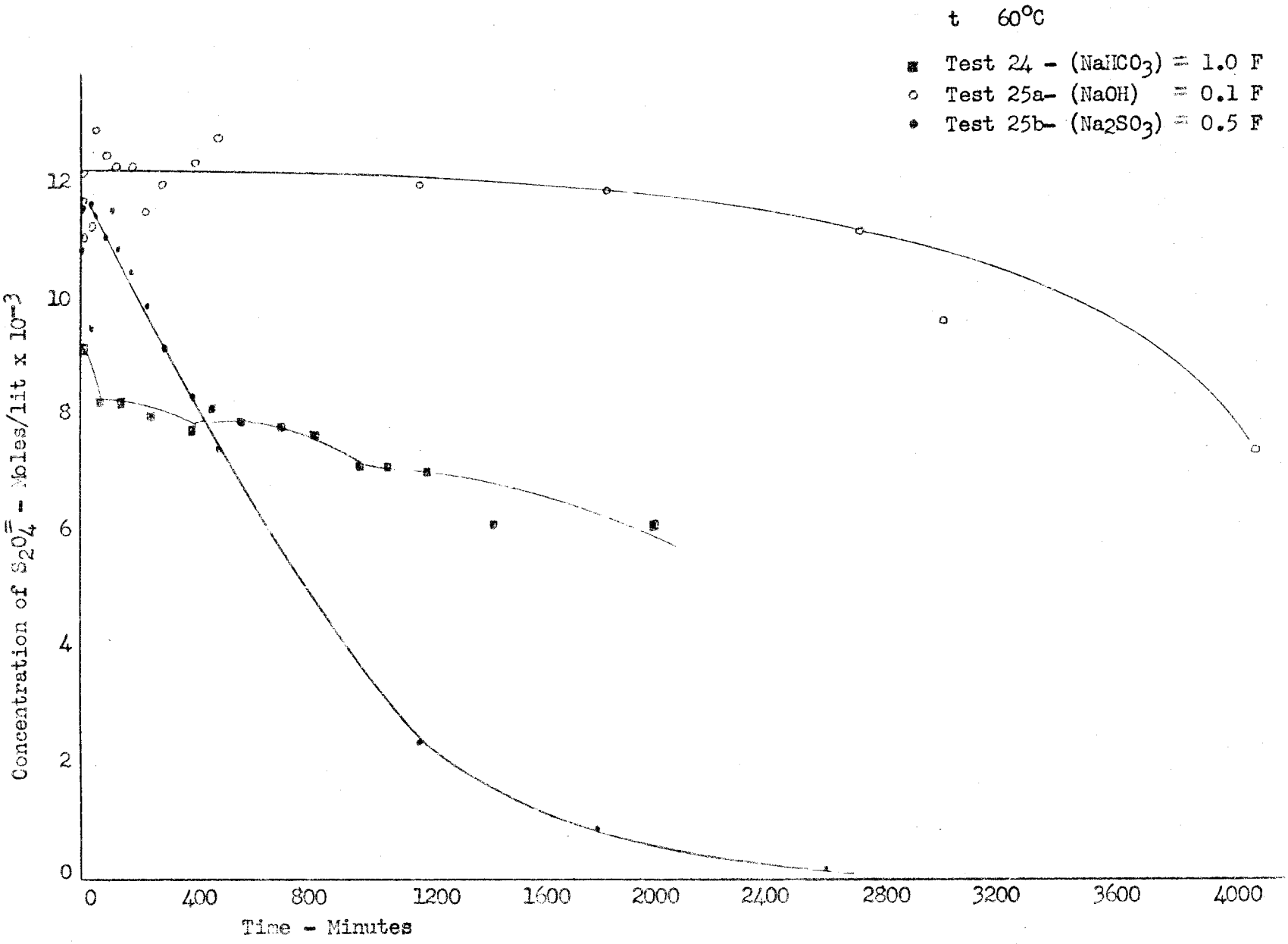

Figure 7b - Decomposition of $Na_2S_2O_4$ over a Range of Concentrations of H^+

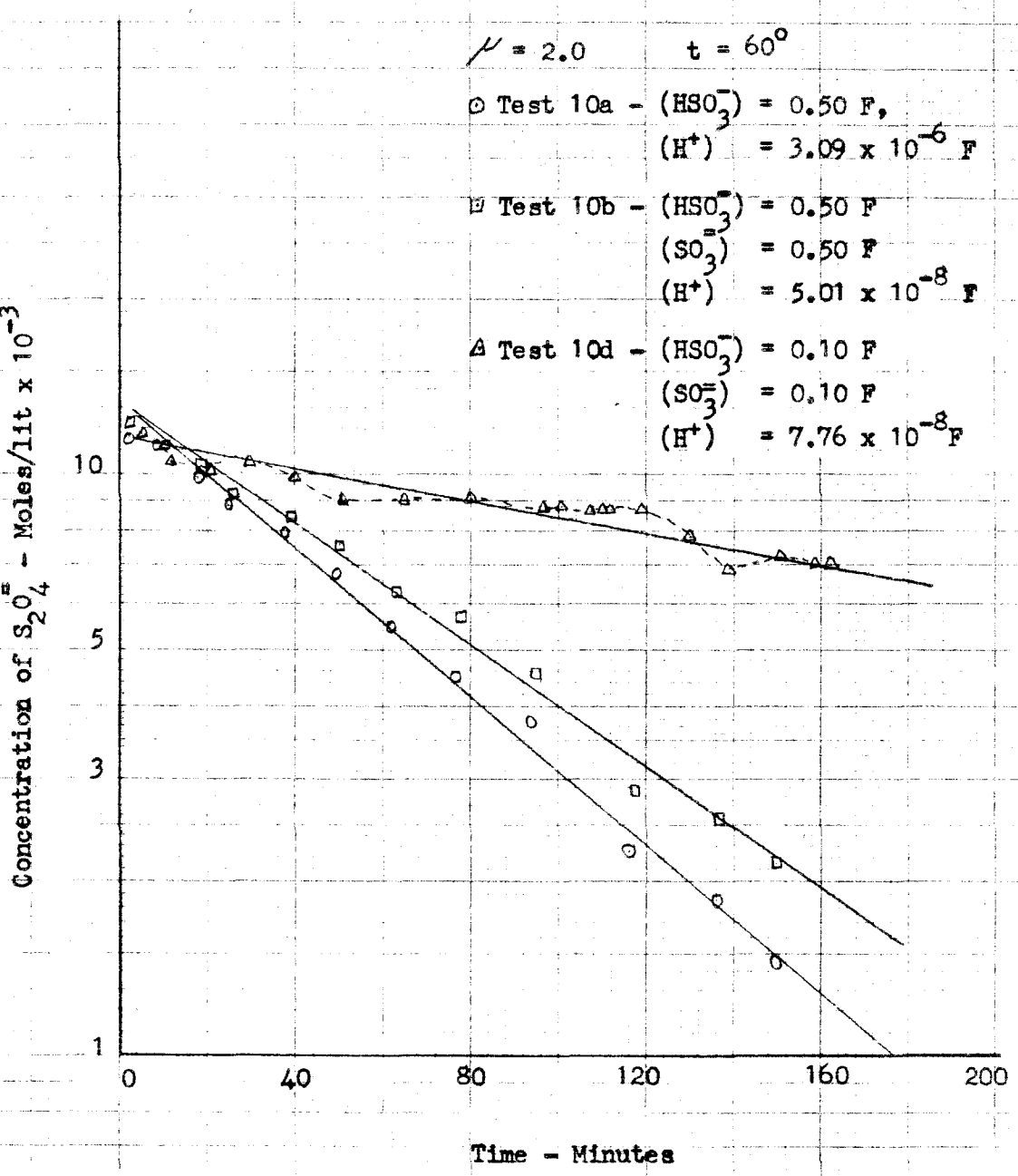

Figure 8a - First Order Nature of the Thermal Decomposition of $Na_2S_2O_4$ in the Presence High Concentrations of $NaHSO_3$

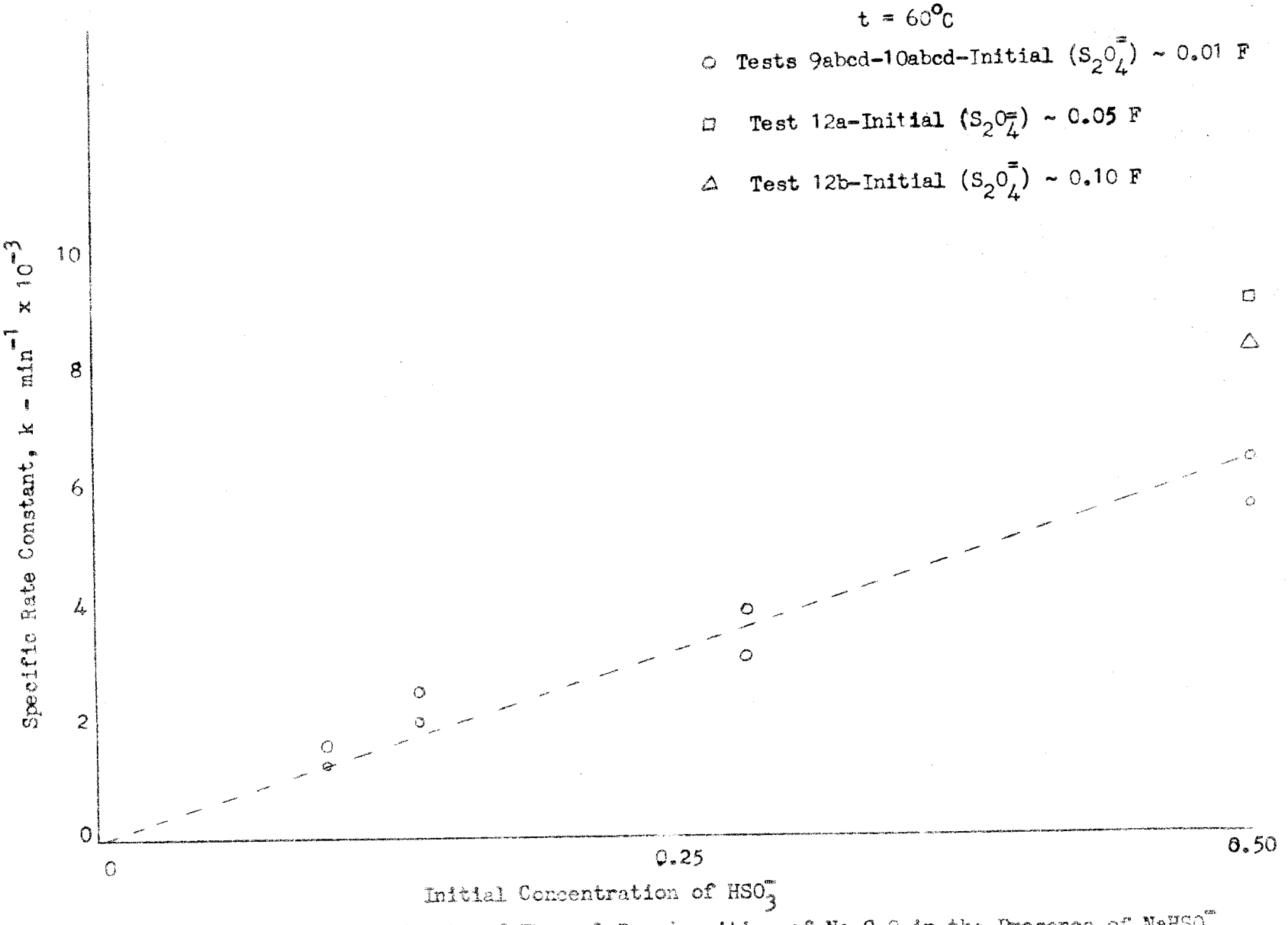

Figure 8b - Dependence of Rate of Thermal Decomposition of $Na_2S_2O_4$ in the Presence of $NaHSO_3^-$ at Various (H^+) and ($SO_3^=$)

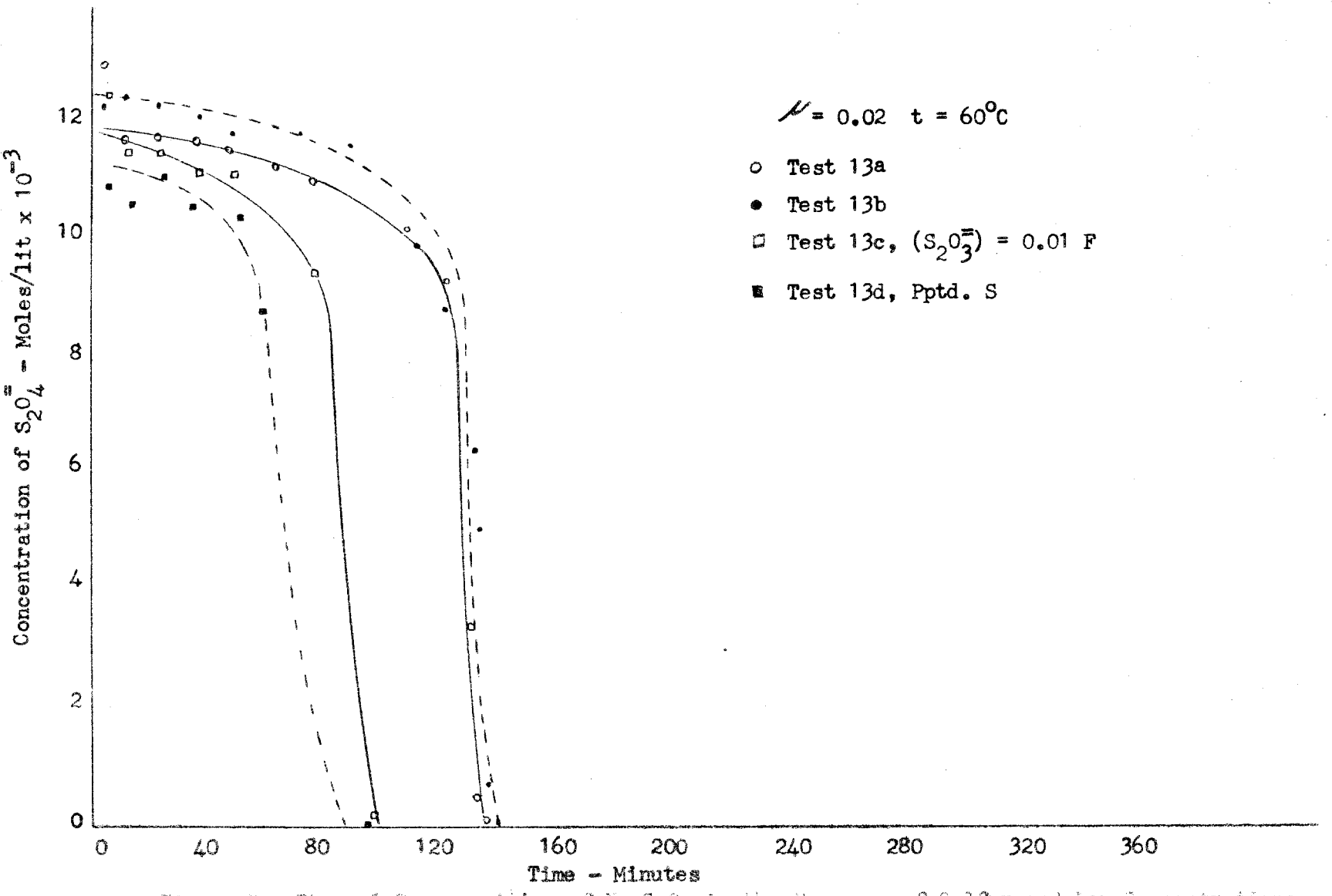

Figure 9 - Thermal Decomposition of $Na_2S_2O_4$ in the Presence of Sulfur and Low Concentrations of NaCl and $Na_2S_2O_3$

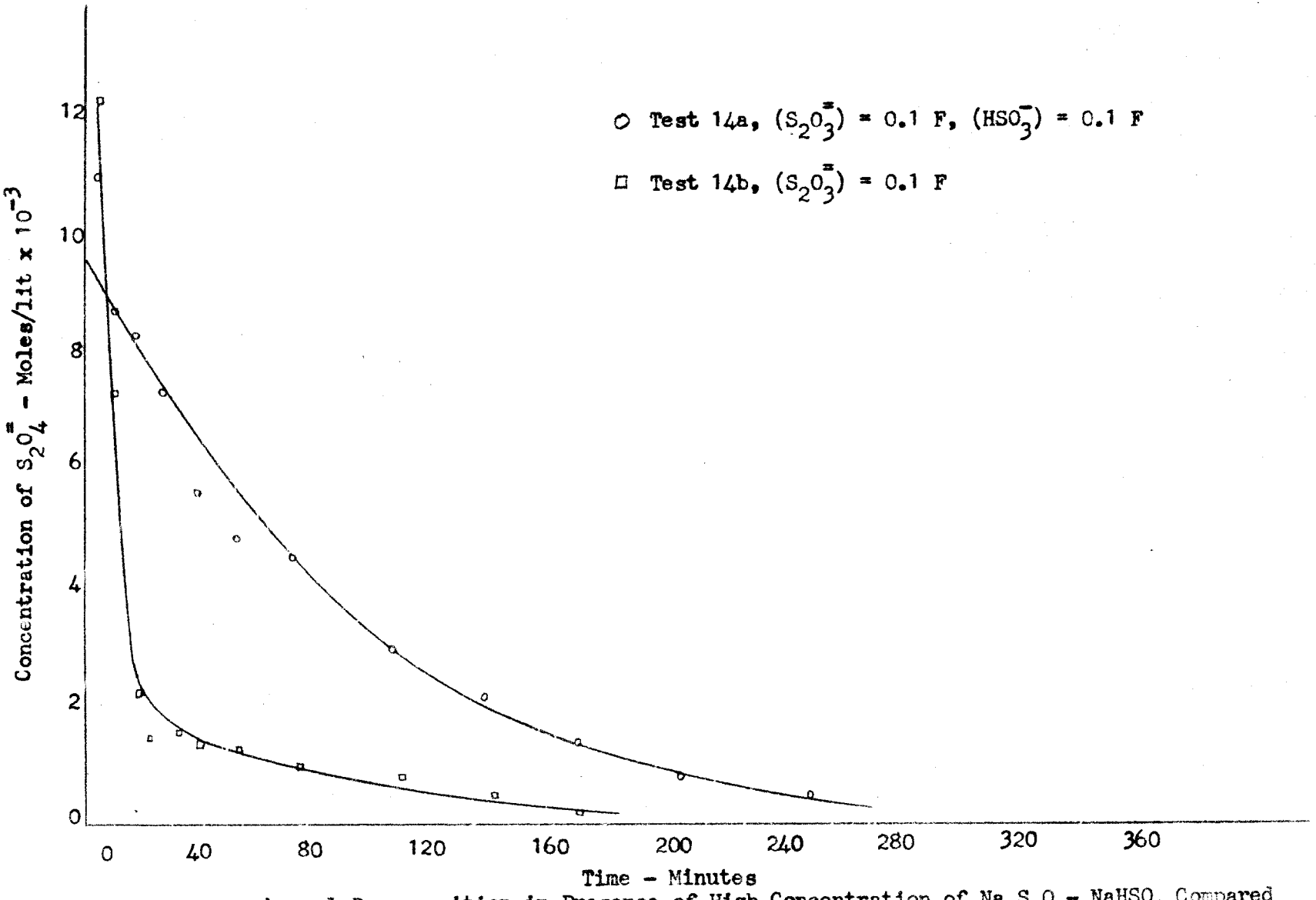

Figure 10a - Thermal Decomposition in Presence of High Concentration of $Na_2S_2O_3$- $NaHSO_3$ Compared with Run with no Additives

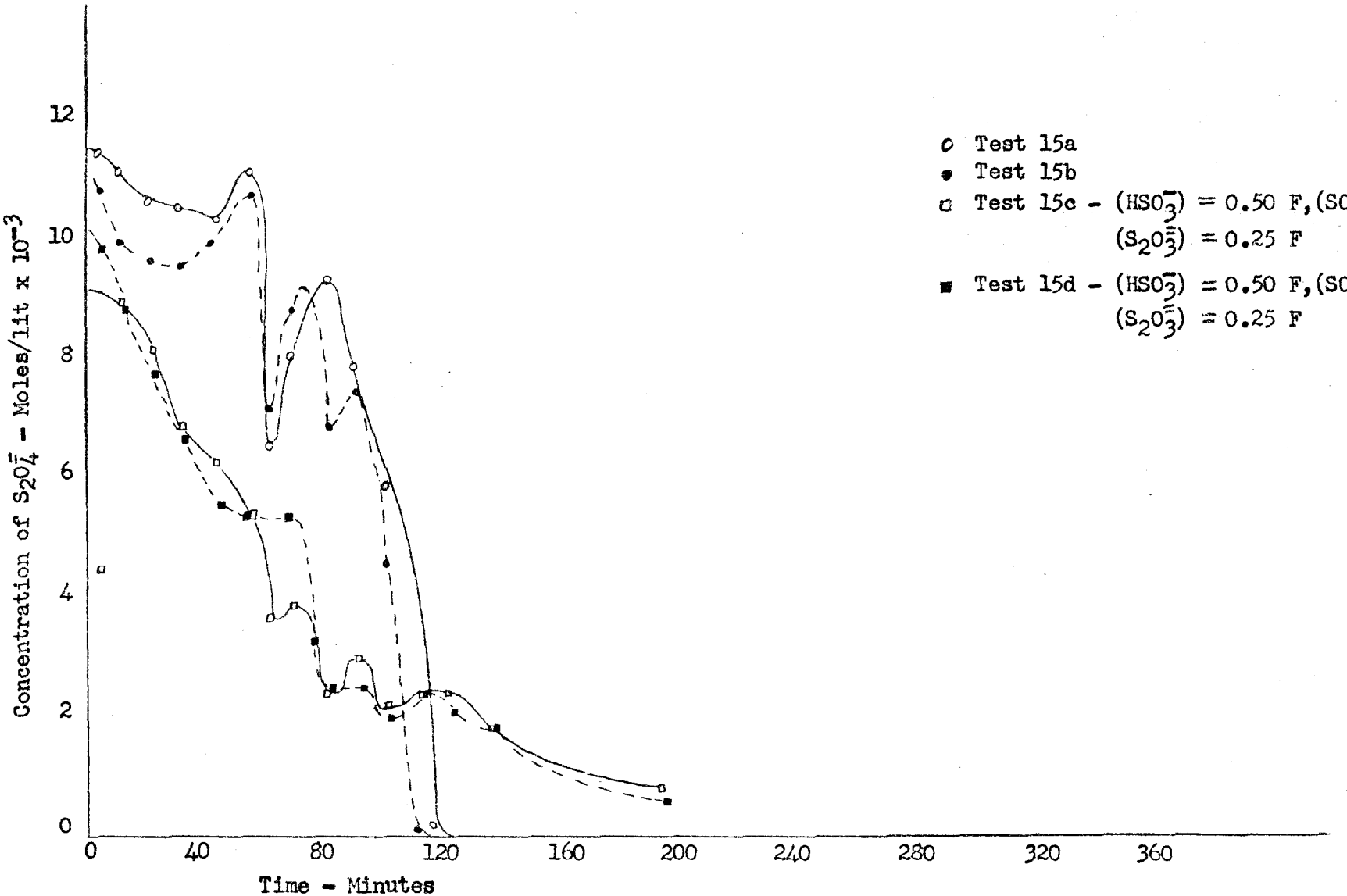

Figure 10b - Thermal Decomposition in Presence of High Concentrations of [illegible] Compared with Run with No Additives

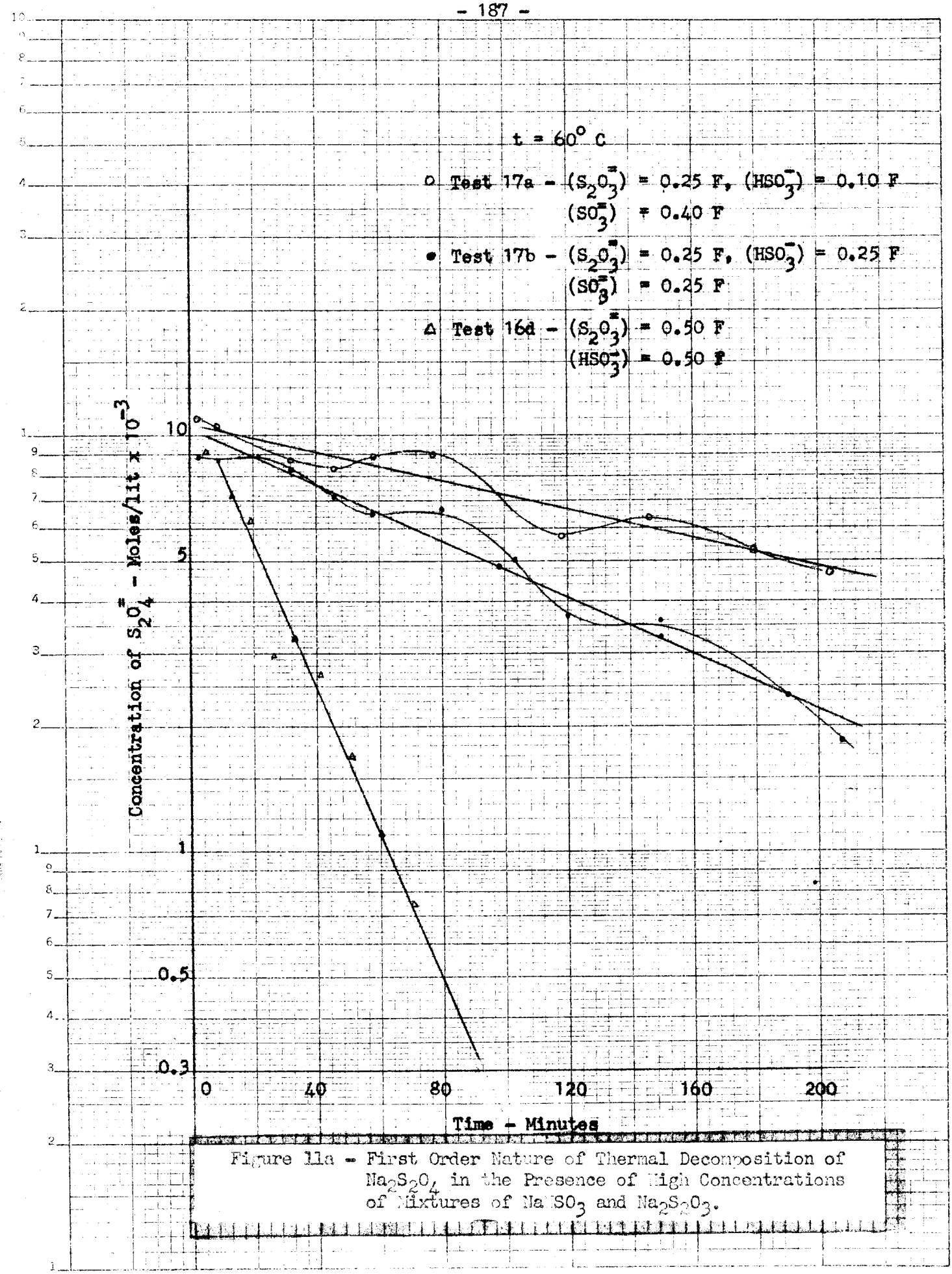

Figure 11a - First Order Nature of Thermal Decomposition of $Na_2S_2O_4$ in the Presence of High Concentrations of Mixtures of $NaHSO_3$ and $Na_2S_2O_3$.

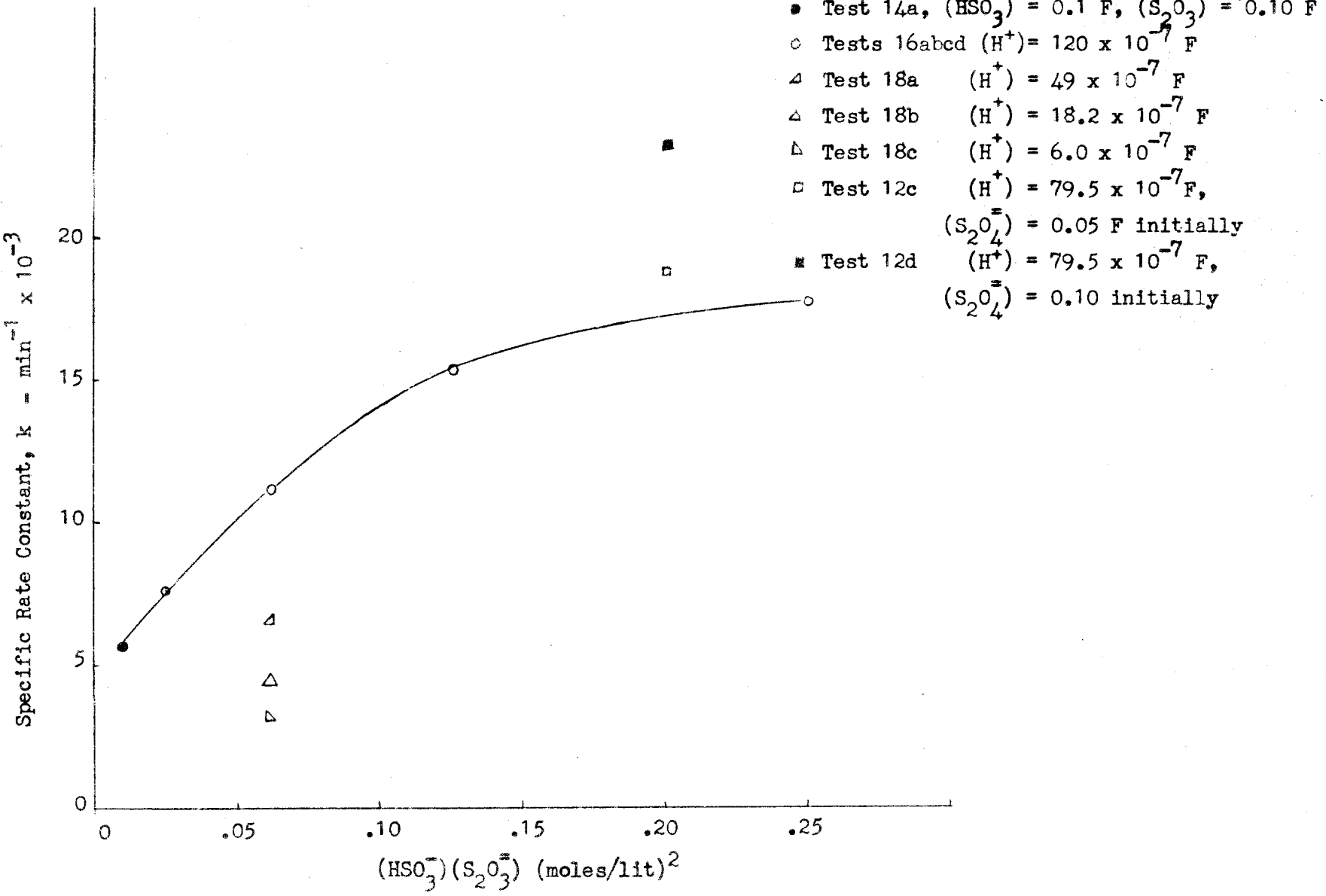

Figure 11b - Dependence of the Rate of Thermal Decomposition of $Na_2S_2O_4$ in the Presence of $NaHSO_3$ and $Na_2S_2O_3$ on Various Ionic Species.

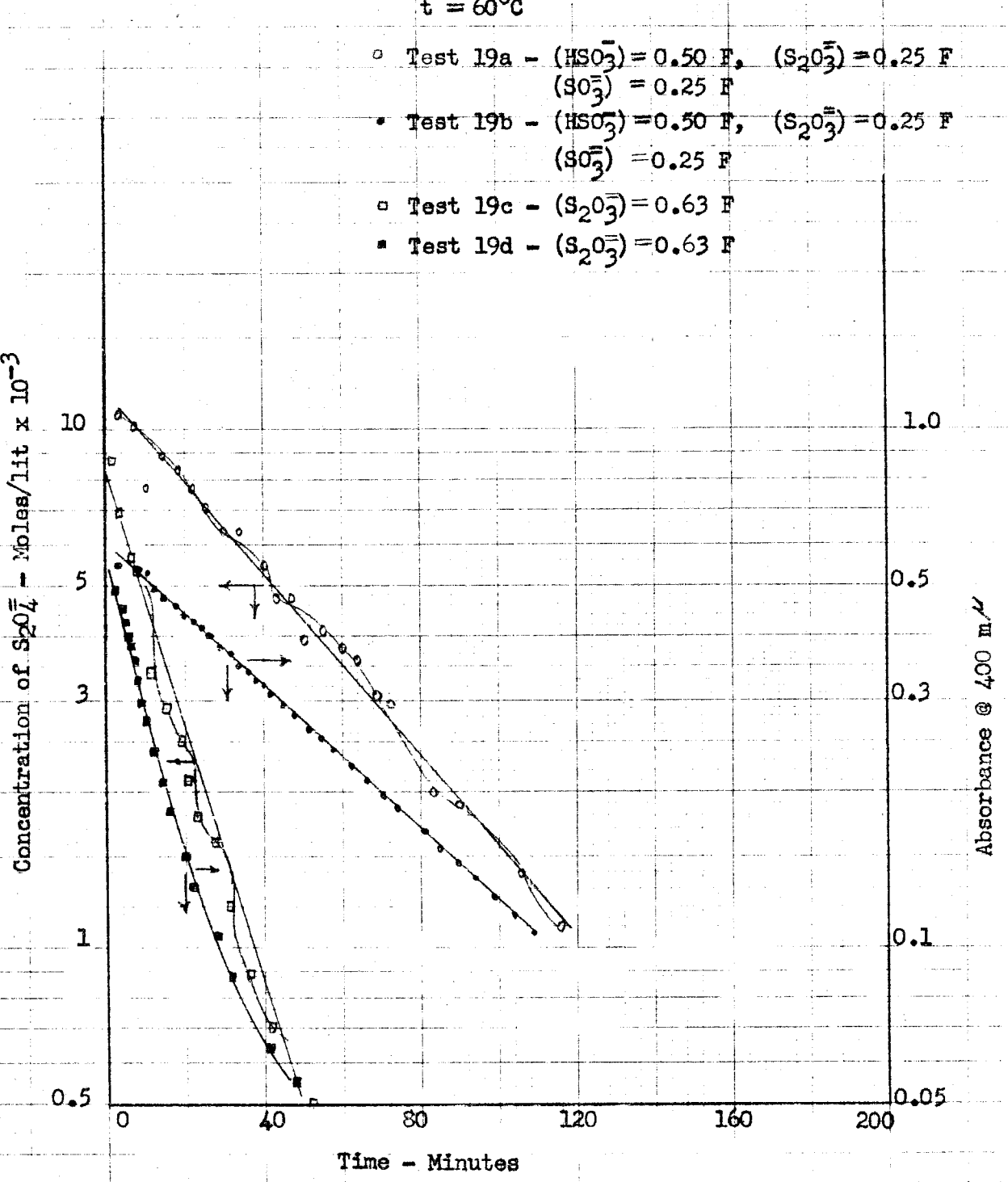

Figure 12 - First Order Nature of the Absorbance-Time Relationship for the Thermal Decomposition of $Na_2S_2O_4$

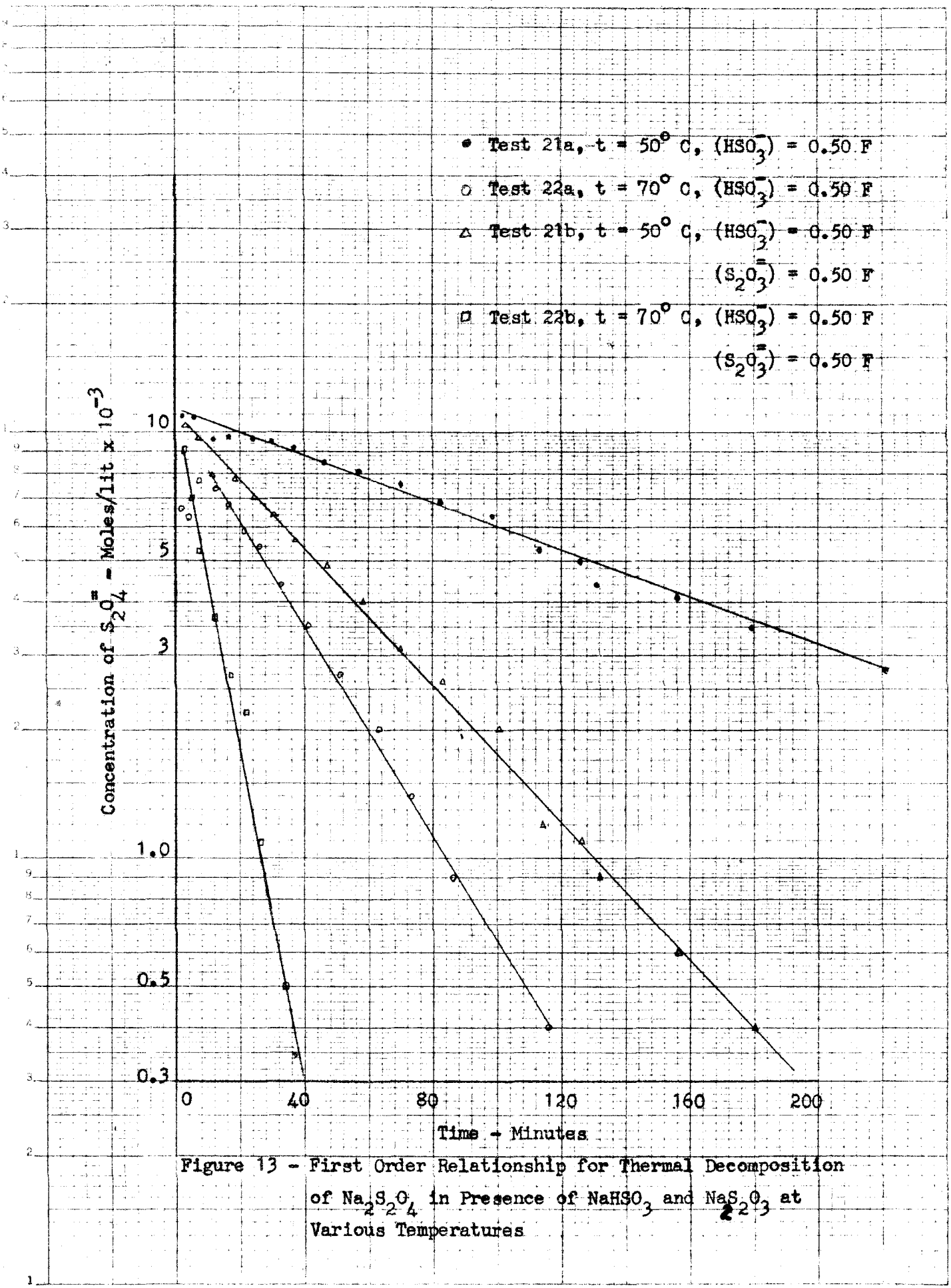

Figure 13 - First Order Relationship for Thermal Decomposition of $Na_2S_2O_4$ in Presence of $NaHSO_3$ and $Na_2S_2O_3$ at Various Temperatures

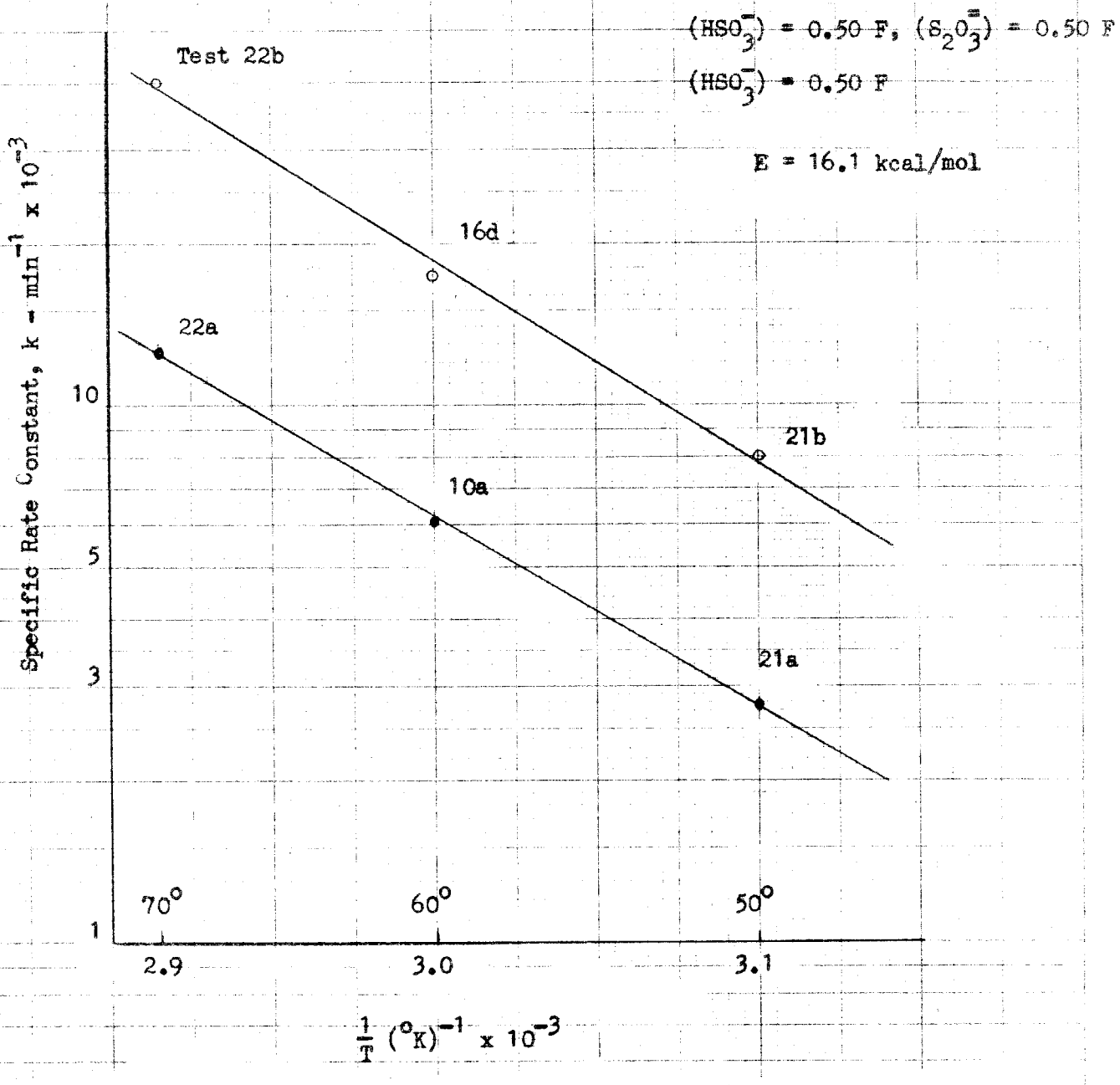

Figure 14 - Arrhenius Plot of First Order Rate Constant a Function of Temperature

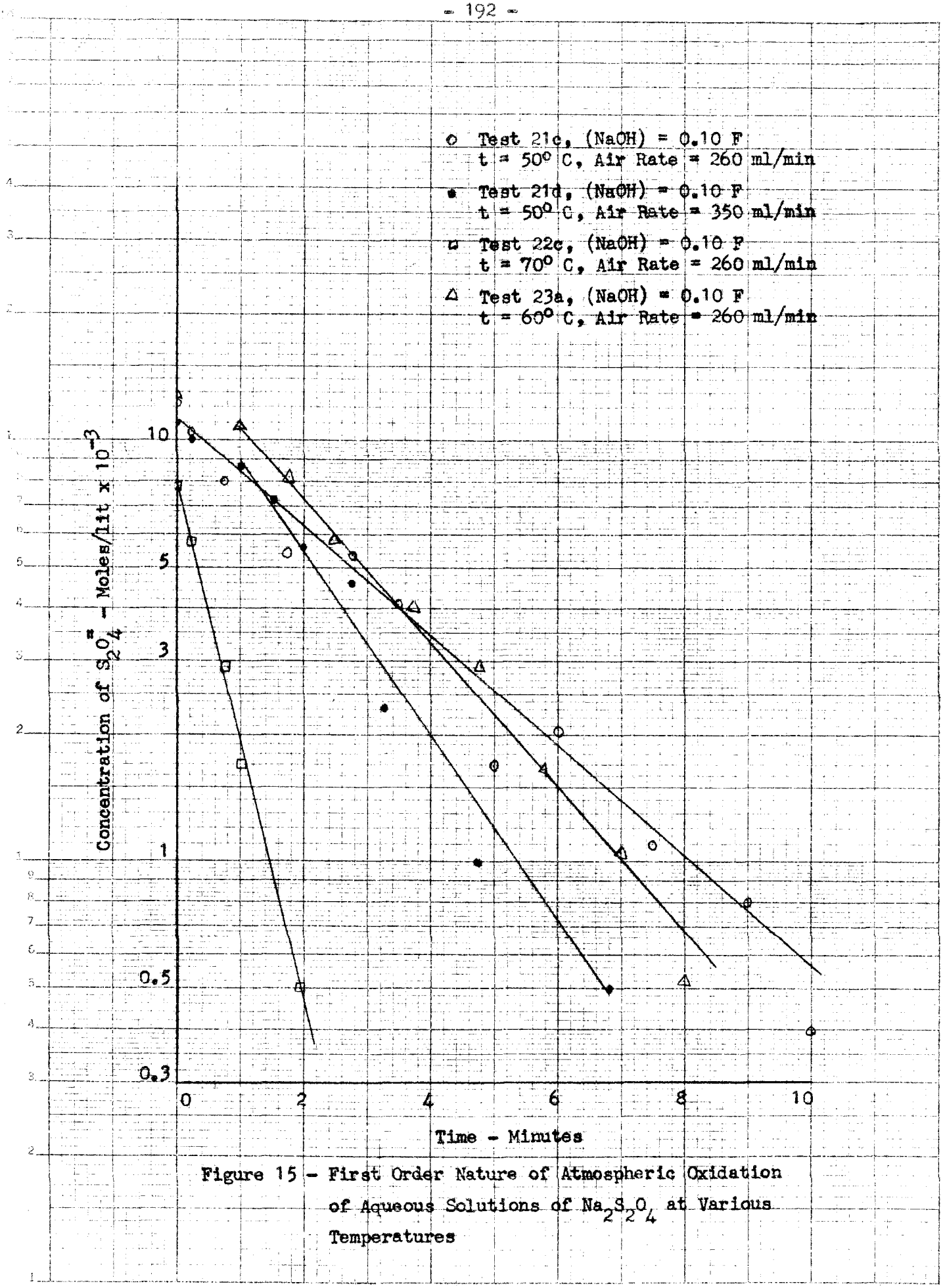

Figure 15 - First Order Nature of Atmospheric Oxidation of Aqueous Solutions of $Na_2S_2O_4$ at Various Temperatures

PART IV

THE DETERMINATION OF CHROMIUM BY OXIDATION IN THE PRESENCE OF SILVER NITRATE.

Reprinted from ANALYTICAL CHEMISTRY, Vol. 24, Page 1855, November 1952

Determination of Chromium by Oxidation in the Presence of Silver Nitrate

SCOTT LYNN AND DAVID M. MASON

California Institute of Technology, Pasadena, Calif.

A VOLUMETRIC method of quantitative analysis was desired for determining amounts of chromium less than 10 mg. A widely used method for the quantitative estimation of chromium in ores and various industrial products such as leather and steel involves complete oxidation of chromium from the tripositive to the hexapositive state. When in the hexapositive state chromium can be determined by some conventional means such as the iodometric method described by Swift (*10*). It was found difficult to get quantitative results using hydrogen peroxide in a basic aqueous solution to oxidize chromium. The oxidizing property of hot, fuming perchloric acid has been utilized by previous investigators (*2–9, 11*) to oxidize chromium. The methods used, however, are rather elaborate, and for small quantities of chromium neither fuming perchloric acid alone nor a mixture of perchloric acid and other acids gave quantitative results. It was the purpose of the present investigation to modify a procedure using mixed perchloric and sulfuric acids (*9*) in order to get quantitative results in the determination of small quantities of chromium. The chief modification proposed is the addition of silver nitrate to the fuming mixture.

Smith and his coworkers (*3–9*) digest chromium with a fuming mixture of perchloric and sulfuric acids in an Erlenmeyer flask under carefully controlled conditions. The procedure recommended demands that the temperature of the reactants and the period of time of the digestion be maintained within relatively narrow limits. It is necessary to use a reflux condenser to prevent loss of vapors from the reaction flask (*6*). The contents of the flask are cooled rapidly with water, and, after the removal of dissolved chlorine by boiling, the resulting solution is ready for titration of the chromate. One suggested modification (*6*) of this procedure requires that another oxidizing agent such as potassium permanganate or ammonium persulfate be added to the solution after the digestion process to ensure complete oxidation.

PROCEDURE

The following method is recommended for the quantitative oxidation of 10 mg. or less of tripositive chromium. Initially the chromic salt is present in approximately 5 ml. of an aqueous solution which is made acidic with nitric acid. To this solution in a 125-ml. Erlenmeyer flask equipped with a heavy ground-glass stopper is added 1 ml. of a reagent made from 2 volumes of 72 weight % perchloric acid, 1 volume of 98 weight % sulfuric acid, and 1 volume of 0.2 formal silver nitrate. The flask and its contents are placed in a liquid bath of orthophosphoric and metaphosphoric acids maintained at a temperature in the range of 200° to 220° C. Volatile constituents consisting chiefly of water are distilled from the mixture in the flask until the volume is reduced to about 1 ml., and then upon the first appearance of dense white fumes of perchloric acid the ground-glass stopper is wet with distilled water and placed in the flask. After the volatile constituents are distilled off by forcing the heavy glass stopper up enough to leak through the resulting annular space the glass stopper settles into position. This treatment prevents the loss of chromium by volatilization which has been observed by the authors and by other investigators (*1*). Only the lower part of the flask is submerged in the bath; the upper portion is exposed to the air to permit condensation of the fuming acid, which refluxes down the side to the bottom of the flask. The oxidation of greenish tripositive chromium to the reddish hexapositive state takes place rapidly at temperatures in the range 200° to 220° C. Reddish droplets condense on the inside of the flask during fuming. Digestion for 1 minute after the change in color from green to red suffices for complete oxidation. The flask is taken out of the bath and cooled externally with cold water. The stopper is removed, and the contents of the flask are diluted with 70 ml. of water at approximately 25° C. Silver chloride is precipitated upon dilution. The resulting solution is boiled until the volume is reduced to 20 ml. It is found that chlorine is completely removed, during the boiling, as evidenced by a negative starch-iodide paper test. The volume of the cool solution is increased to 50 ml., which gives a hydrogen ion concentration within the range 0.2 to 0.4 formal recommended for the subsequent iodometric titration (*10*). Potassium iodide is added to the solution, and the iodine formed is determined by titrating with a standard solution of sodium thiosulfate. It is found that the silver iodide precipitated does not materially mask the starch-iodine end point.

RESULTS

In the series of tests of the procedure equal amounts of a standard potassium dichromate solution were made 0.1 formal in nitric acid and reduced with 2 drops of 30 weight % hydrogen peroxide. The resulting solution containing trivalent chromium was evaporated to dryness to decompose the peroxide thoroughly. One milliliter of the perchloric acid reagent was added, and the oxidation procedure described above was carried out. Sample tests are shown in Table I.

Table I. Results of Oxidation of Tripositive Chromium

(Chromium taken, 2.751 mg.)

Chromium Found	
Mg.	Deviation, %
2.745	−0.2
2.728	−0.8
2.745	−0.2
2.753	0.1

The procedure was further tested over a range of amounts of chromium from 10 to 0.1 mg., and the results were of comparable accuracy to the data of Table I. For 2.751 mg. of chromium the method described by Smith *et al.* (*9*) without the presence of silver nitrate during digestion gave results which were on the average 5.2% low.

CONCLUSIONS

It appears that the addition of silver nitrate to a mixture of fuming perchloric and sulfuric acids at 200° to 220° C. as outlined results in a more quantitative oxidation of small amounts of tripositive chromium than has been obtained by the methods mentioned above. The mechanism by which the silver nitrate aids in effecting the quantitative oxidation of trivalent chromium has not been established.

LITERATURE CITED

(1) Hoffman, J. I., and Lundell, G. E. F., *J. Research Natl. Bur. Standards*, **22**, 465–70 (1939).
(2) Lichin, J. J., IND. ENG. CHEM., ANAL. ED., **2**, 126–7 (1930).
(3) Smith, G. F., *Chem. Products*, **12**, 158–61 (1949).
(4) Smith, G. F., IND. ENG. CHEM., ANAL. ED., **6**, 229–30 (1934).
(5) Smith, G. F., "Mixed Perchloric, Sulfuric, and Phosphoric Acids and Their Application in Analysis," Columbus, Ohio, G. Frederick Smith Chemical Co., 1934.
(6) Smith, G. F., and Getz, C. A., IND. ENG. CHEM., ANAL. ED., **9**, 378–81 (1937).
(7) *Ibid.*, pp. 518–19.
(8) Smith, G. F., McVickers, L. D., and Sullivan, V. R., *J. Soc. Chem. Ind. London*, **54**, 369–72T (1935).
(9) Smith, G. F., and Smith, G. P., *Ibid.*, **54**, 185–9T.
(10) Swift, E. H., "A System of Chemical Analysis," 1st ed., p. 197, New York, Prentice Hall, Inc., 1950.
(11) Willard, H. H., and Gibson, R. C., IND. ENG. CHEM., ANAL. ED., **3**, 88–93 (1931).

RECEIVED for review November 13, 1951. Accepted August 18, 1952.

PRINTED IN U. S. A.

PROPOSITIONS

Submitted by Scott Lynn for Ph. D. Oral Examination, July 7, 1953, 9:00 A.M., Crellin Conference Roon.

Committee: Professor Sage (Chairman), Professors Buchman, Corcoran, Lacey, Plesset, and Yost.

Chemical Engineering:

1. Plotting temperature, velocity, and composition vs. the square of the distance from the center of the channel is a convenient tool in determining the values of the eddy properties at the center when the center line is an axis of symmetry.

2. Acetylene and ethylene are produced commercially by the Wulff process, in which propane or other light hydrocarbons are pyrolized in a non-equilibrium reaction. Dichloroacetylene and/or trichloroethylene might be produced from tetrachloroethane in a similar process at a lower cost than is now possible.

3. Specifying the temperature and entropy of a one phase, one component system is not always sufficient to fix the state of the system.

4. The eddy diffusivity appears to be a marked function of the rate of change of composition with distance along a flow channel.

5. The distance required to return to the normal level of turbulence

characteristic of a given flow rate in a channel is much greater after the introduction of large scale turbulence than after the introduction of small scale turbulence.

6. The variation of the eddy diffusivity with x, the axial distance, in a non-uniform stream is to a certain extent independent of the variation of the eddy viscosity with x.

Chemistry:

7. The presence of a small amount of silver ion facilitates the quantitative oxidation of chromium by perchloric acid.

8. The determination of the absolute concentration of nitrogen dioxide in nitric acid solution by measuring the magnetic susceptibility would be a valuable addition to the work done on the absorption of light by these solutions.

9. Fibers which do not conduct electricity tend to build up charges of static electricity. This reduces their desirability as fabrics because of the resulting tendency to cling to the wearer and to produce sparks and shocks. A coating to reduce this tendency could be made from hydroxy substituted polysiloxanes, which would tend to adsorb water molecules and hence produce a semi-conducting layer. Polysiloxanes are widely used at present to produce a water repellant layer on glass and synthetic fabrics. (Warrick, E.L., Huner, M.J. and Barry, A.J., Ind. Eng. Chem., 44:2196 (1952).)

10. The addition of an excess of $KHSO_4$ to a solution of NO_2 in HNO_3 markedly reduces the optical absorbance of the solution. This might indicate that $NOHSO_4$ is partially but not completely ionized in nitric acid solution.

11. A.R.Ubbelohde, Disc. of Far. Soc., 8, 203 (1950), states that metal hydrides of the type $M-H_n$ tend to have the properties of the elements n places to the right in the periodic table. In support of this he describes the properties of PdH, comparing them to those of silver, and goes on to point out that iron charged cathodically with atomic hydrogen is wet by mercury. Since cobalt is not wet easily by mercury, and since an iron surface formed when a bar of iron is broken under mercury is wet, the phenomenon described by Ubbelohde would seem to indicate that it is a surface oxide which ordinarily prevents iron from being wet by mercury.

Mechanical Engineering:

12. Corcoran (Ph. D. Thesis, California Institute, 1948) has proposed that Cr_2O_3 dissolved in metallic chromium might be removed by introducing a second liquid phase in which the oxide was more soluble. An alternative method, which has the advantage of greater ease of recovery of the Cr_2O_3, would be the addition of a calcium chloride-lime mixture. Chromic chloride would be distilled off and recovered. The function of the lime would be to reduce the vapor pressure of the calcium chloride, if this proved to be necessary.

13. A cutting torch attaining very high temperatures might be made by using a nozzle in which a chemical reaction is taking place to get a rather high (~ 3000°K) temperature and a velocity of about 6000 ft/sec. The stagnation temperature of such a stream would be about 5000°K.

Pedagogy:

14. Insufficient attention is paid to developing in the student the ability to present and defend subjects of a controversial nature in a formal lecture.